UNIVERSITA' DEGLI STUDI DI MILANO

Dottorato di Ricerca in Scienze Farmacologiche

XXVIII CICLO

The activity dependent cleavage and nuclear function of female limited epilepsy protein PCDH19

Coordinatore: Prof. Alberto Corsini

Relatore: Prof.ssa Monica Maria Grazia DiLuca

Correlatore: Dott.ssa Maria Passafaro

Tesi di Dottorato di Ricerca di:

Laura Gerosa

Matricola R10143

Anno accademico 2014/2015

CONTENT

1. INTRODUCTION

1.1 Early-onset epileptic encephalopathies

Early-onset epileptic encephalopathies (EIEE) are a heterogeneous group of rare and severe neurological disorders, characterized by intractable epilepsy within the first period of life, which results in devastating global developmental delay and intellectual disability. Patients have impaired cognitive, sensory and motor development, leading to lack of motor, language and social development (Duszyc, Terczynska et al. 2015).

EIEEs are genetically and phenotipically heterogeneous and, recently, 25 genes have been identified as causative for these pathologies (*Tab.1*). Further, different kind of mutations within each gene gives rise to a broad spectrum of phenotypes.

Table 1 Molecular background of 25 types of early infantile epileptic encephalopathy (EIEE) [according to OMIM (08-08-14)]

	OMIM number	Gene	Locus	Inheritance	Protein
EIEE 1	308350	*ARX*	Xp22.13	XR	Aristaless-related homeobox protein
EIEE 2	300672	*CDKL5*	Xp22.13	XD	Cyclin-dependent kinase-like 5
EIEE 3	609304	*SLC25A22*	11p15.5	AR	Mitochondrial glutamate carrier 1
EIEE 4	612164	*STXBP1*	9q34.1	AD	Syntaxin-binding protein 1
EIEE 5	613477	*SPTAN1*	9q33-q34	AD	Non-erythrocytic alpha-spectrin-1
EIEE 6	607208	*SCN1A*	2q24.3	AD (de novo)	Alpha 1 subunit of voltage-gated sodium channel
EIEE 7	613720	*KCNQ2*	20q13.3	AD	Voltage-gated potassium channel
EIEE 8	300607	*ARHGEF9*	Xq22.1	XR	Rho guanine nucleotide exchange factor 9
EIEE 9	300088	*PCDH19*	Xq22.1	XD limited to females	Protocadherin-19
EIEE 10	613402	*PNKP*	19q13.4	AR	Polynucleotide kinase
EIEE 11	613721	*SCN2A*	2q24.3	AD	Alpha 2 subunit of voltage-gated sodium channel
EIEE 12	613722	*PLCB1*	20p12.3	AR	Phospholipase C-beta
EIEE 13	614558	*SCN8A*	12q13.13	AD	Alpha 6 subunit of voltage-gated sodium channel
EIEE 14	614959	*KCNT1*	9q34.3	AD	Sodium-activated potassium channel
EIEE 15	615006	*ST3GAL3*	1p34.1	AR	Beta-galactoside-alpha-2,3-sialyltransferase-III
EIEE 16	615338	*TBC1D24*	16p13.3	AR	Member 24 of TBC1 domain family
EIEE 17	615473	*GNAO1*	16q12.2	AD (de novo)	Alpha subunit of the heterotrimeric guanine nucleotide-binding proteins
EIEE 18	615476	*SZT2*	1p34.2	AR	Seizure threshold 2
EIEE 19	615744	*GABRA1*	5q34	AR	Alpha 1 subunit of gamma-aminobutyric acid receptor
EIEE 20	300868	*PIGA*	Xp22.2	XR	Phosphatidylinositol glycan, class A
EIEE 21	615833	*NECAP1*	12p13.31	AR	Endocytosis-associated protein 1
EIEE 22	300896	*SLC35A2*	Xp11.23	XD	UDP-galactose transporter, isoform 1
EIEE 23	615859	*DOCK7*	1p31.3	AR	Dedicator of cytokinesis 7
EIEE 24	615871	*HCN1*	5p12	AR	Hyperpolarisation-activated cyclic nucleotide-gated potassium channel 1
EIEE 25	615905	*SLC13A5*	17p13.1	AR	Solute carrier family 13

Table 1 Summary of 25 genes involved in early infantile epileptic encephalopathies (Duszyc, Terczynska et al. 2015).

For these reasons, unfortunately, there are not specific treatments for the patients. However, some patients respond to common anti-epileptic drugs (AED). For other

patients, hormonal treatments have been used, such as corticosteroids. Some are resistant to pharmacotherapy and have been used surgery and neurostimulation. Since an early diagnosis of EIEE is difficult given the variety and heterogeneity of clinical features, there are several studies directed to unravel the etiopathogenesis and genetical basis of these pathologies in order to detect responsible genes and assign specific therapies.

1.2 PCDH19-female limited epilepsy, EIEE9

The following section will provide a brief explanation of the main features of the pathology caused by PCDH19 mutations, to give some elucidation and discuss about the possible mechanism of action and involvement of this protein in the pathology.

PCDH19-female limited epilepsy (PCDH19-FLE) is classified as early infantile epileptic encephalopathy type 9 (EIEE9) and is characterized by seizure onset in infancy or early childhood (6-36 months) and cognitive impairment (Dibbens, Tarpey et al. 2008).

1.2.1 Clinical features

Affected infants appear normal until 4-18 months, then they begin to have partial and generalized febrile convulsions that gradually increase in frequency and are accompained by developmental regression. Patients experience a variety of generalized and focal seizure types: these mostly consist in generalized tonic, clonic or tonic-clonic, and/or focal seizures with or without secondary generalization. In most cases seizures are resistant to treatment, especially to the AEDs. In most females, the frequency of seizures decline dramatically by the age of 2-3 years and stop in some cases in adolescence, but intellectual disability generally persists after seizure remission (Depienne and LeGuern 2012).

Moreover, behavioral disturbances are frequent and essentially manifest as autistic, obsessive, or aggressive features. Intellectual outcome ranges from normal intellect to mild, moderate, or severe cognitive impairment (Depienne and LeGuern 2012).

In conclusion, this pathology is characterized by heterogeneous phenotypic spectrum that range from severe generalized or multifocal epilepsy, resembling Dravet syndrome, to more benign focal epilepsies with normal intelligence.

1.2.2 Causative gene and mutations

The disorder was first described in 1971 by Juberg and Hellman in 15 related females with early onset grand mal seizures and mental retardation. It was mapped more than 20 years later on chromosome X: in particular, linkage analysis narrowed the FLE locus to an approximately 34-megabase region of the X chromosome (Ryan, Chance et al. 1997).

Only in 2008 the gene encoding protocadherin-19 (*PCDH19*) was identified as the gene mutated in FLE. Recently, several studies showed that PCDH19-FLE is more frequent than expected; in particular it represents the 16% of cases in the SCN1A-negative Dravet syndrome-like patients. *PCDH19* is now considered the second gene, after SCN1A, most clinically relevant in epilepsy.

The same authors that found *PCDH19* as causative gene of FLE, identified different *PCDH19* gene mutations in all the seven families with PCDH19-FLE analyzed: five mutations resulted in the introduction of a premature termination codon (Dibbens, Tarpey et al. 2008).

Over time, during the last years, several studies identified more than 100 pathogenic point mutations (missense, nonsense, splicing, small deletion/insertion, whole gene deletion) in the *PCDH19* gene (*Figure 1*).

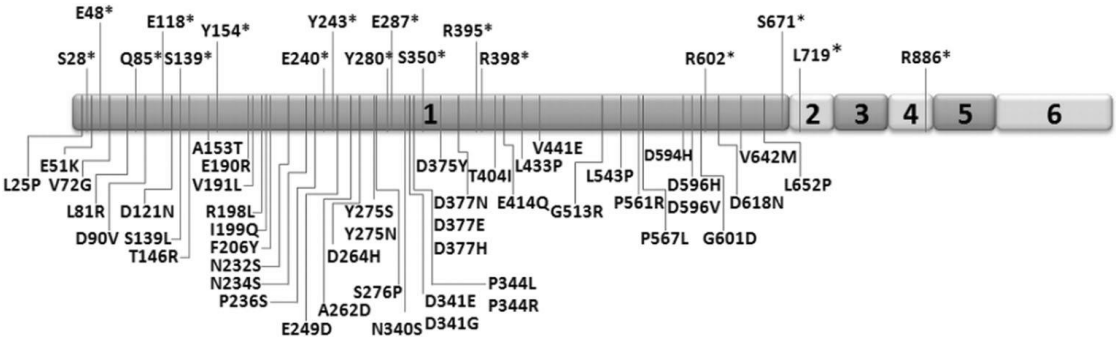

Figure 1 Schematic representation of *PCDH19* sequence and the most common point mutations that cause PCDH19-FLE. Above the mRNA there are nonsense mutations, while below are reported the missense mutations. The number from 1 to 6 represent the exons of PCDH19 protein (Duszyc, Terczynska et al. 2015).

In particular, the most frequently FLE causative mutations are point mutations, even if there are rare cases in which also gross whole-gene or intragenic deletions have been reported. In any case, these mutations lead to degradation of mRNA and loss of PCDH19 protein expression. Indeed, half of the missense pathologic allelic variants result in the appearance of premature termination codons that result in a truncated form of the mRNA, degradated by non-mediated decay (NMD) process. Interestingly, there are also evidences of *PCDH19* gene duplication in at least two cases: a male with only cognitive impairment and a female with focal epilepsy (van Harssel, Weckhuysen et al. 2013).

As indicated in *Figure1*, the majority of the mutations identified are located in the large PCDH19 extracellular domain containing the cadherin repeats and residues that are thought to be involved in calcium binding, damaging therefore adhesiveness of the protein (Dibbens, Tarpey et al. 2008, Jamal, Basran et al. 2010). Mutations in the cytoplasmic tail seem to be more tolerated as indicated by the numerous non pathological polymorphisms identified (Hynes, Stone et al. 2011).

1.2.3 PCDH19-FLE mode of inheritance and pathogenic mechanism

A peculiar feature of PCDH19-FLE is its unusual inheritance pattern. Indeed, even if the causative gene is located on the X-chromosome, mutations are not transmitted in the common way, neither as X-linked dominant nor X-linked recessive mode (*Figure*

2). In particular, it spares hemizygous males carring PCDH19 mutations and affects heterozygous females (Dibbens, Tarpey et al. 2008, Marini, Mei et al. 2010, Specchio, Marini et al. 2011).

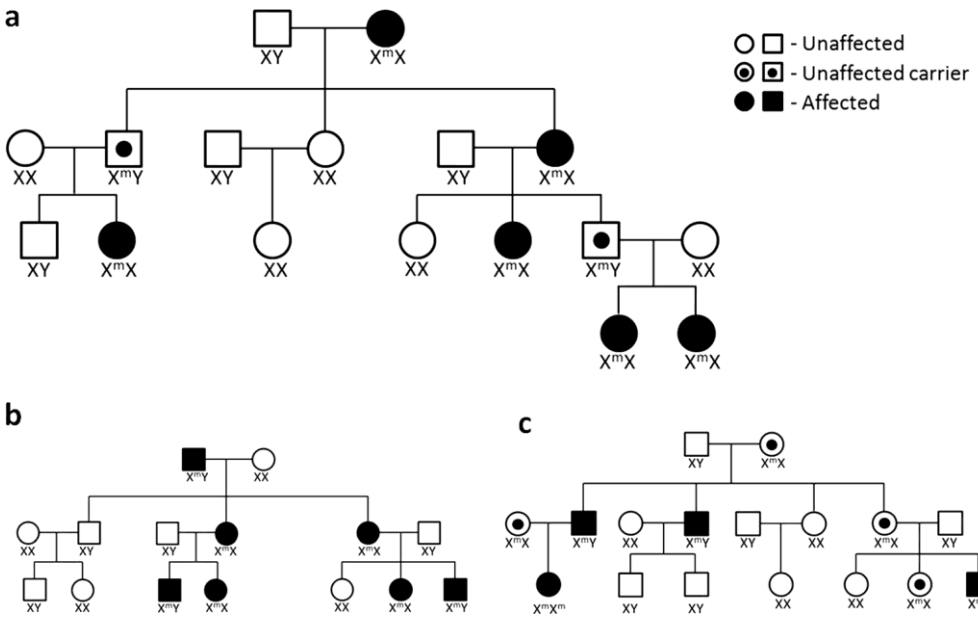

Figure 2 Schematic representation of unusual X-linked female restricted inheritance, resembling that of PCDH19-FLE (a) in comparison to X-linked dominant (b) and X-linked recessive (c) patterns. (a) Only heterozygous females are affected, while hemizygous males transmit mutations, but remain unaffected. (b) Males and females carrying mutations are affected. Affected males never transmit the disease to their sons. (c) Hemizygous males carrying a mutation and homozygous females for a mutation exhibit the symptoms of the disease. Usually, transmitting heterozygous females are unaffected (Duszyc, Terczynska et al. 2015).

Further, despite the unique inheritance pattern of PCDH19-FLE, there are rare cases of females carring PCDH19 mutations that are asymptomatic. Furthermore, even for the same mutations, the clinical manifestations vary from mild to severe (Dibbens, Tarpey et al. 2008, Dimova, Kirov et al. 2012). Till now there are no cases of females carring the homozygous PCDH19 mutation, while in very rare cases mosaic males affected have been identified (Depienne, Bouteiller et al. 2009).

Given the peculiarity regarding the inheritance pattern of the pathology, three models have been hypothesized three models that try to give an explanation to PCDH19-FLE transmission mode.

The first and second models try to explain the presence of healthy hemizygous males. The first hypothesis suggests that there is an homologous gene in males on the Y chromosome expressed in each cell that can compensate for the loss of function of the mutated PCDH19.

The second model assumes that *PCDH19* gene produces a protein that is not essential for brain development since this protein belongs to a family composed by more than 70 elements that have overlapping expression in brain and, for this, maybe their expression can compensate the loss of function of mutated form of PCDH19 (Ryan, Chance et al. 1997, Dibbens, Tarpey et al. 2008).

The last hypothesis gives an explanation for females and mosaic males affected by PCDH19-FLE. It contemplates the random X-inactivation, since the PCDH19 gene is located in a region submitted to X inactivation in females. In particular, this model considers the idea that heterozygous females manifest a tissue mosaicism with random ratio between cells that have inactivated the mutated PCDH19 allele and express the normal protein, and PCDH19-negative cells that have inactivated the normal allele. This mosaicism could account for the pathogenesis by scrambling the cell-cell communication. The loss of function of PCDH19 at the level of the cell would thus result in a gain of function at the tissue level because of abnormal interactions between “mutated” and “normal” cells. A mechanism of this type is termed “cellular interference” (*Figure 3*) (Ryan, Chance et al. 1997, Dibbens, Tarpey et al. 2008, Depienne, Bouteiller et al. 2009, Depienne and LeGuern 2012). This model is supported by the identification of an affected male that is a mosaic for mutated and wild type PCDH19 (Depienne, Bouteiller et al. 2009).

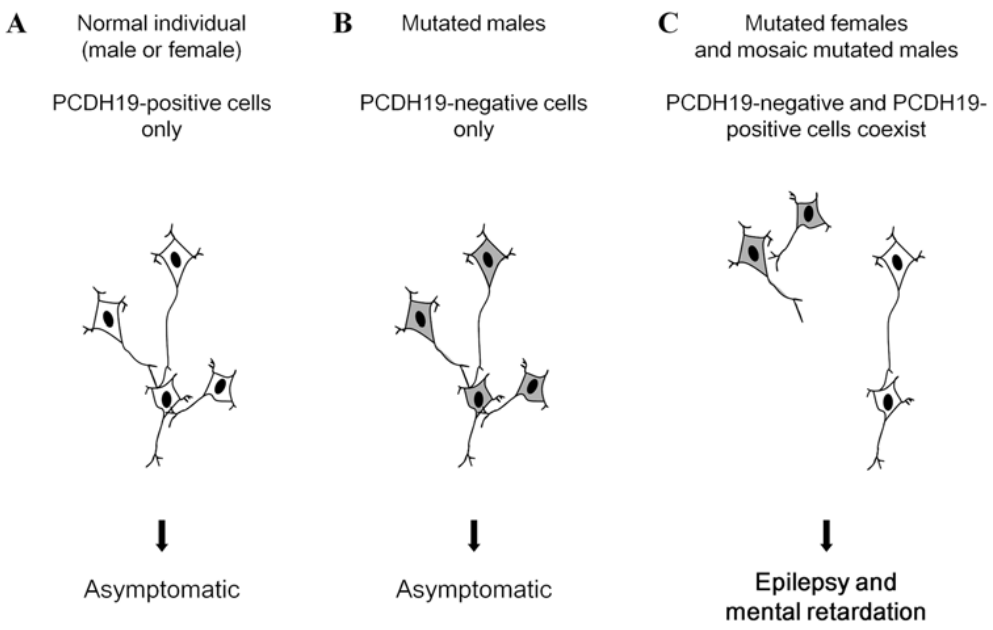

Figure 3 Schematic illustration of "cellular interference" mechanism proposed for PCDH19 mutations. (A) Absence of PCDH19 mutations, in which all cells are phenotipically homogeneous, express PCDH19 wt protein and are able to form normal neuronal networks; (B) Mutated males in which all the cells are PCDH19-negative, so, also in this case, are phenotipically homogeneous and able to form normal neuronal connections that do not affect normal development of these individuals; (C) Heterozygous mutated females in which random X-inactivation leads to the co-existence of two PCDH19-positive and PCDH19-negative cell populations. These two different kind of cells are no more able to form normal neuronal network since there are attractive or repulsive interactions that lead to divergent cell sorting and migration. Somatic mosaicism in mutated males is proposed to generate the same pathological situation (Depienne, Bouteiller et al. 2009).

Anyway, all of phenotypes heterogeneity supports the fact that there are different factors that act concomitantly to produce the heterogeneous and various phenotypes in patients carring *PCDH19* gene mutations. The genotype and the presence of different genes, that can act as modifier of phenotype, may play an important role in the clinical outcome of mutations. Further, the extent of mosaicism, so the percentage of mutated cells, could has a relevant influence on the manifestation of different phenotypes, leading to several degrees of heterogeneity in cell population that reflect various clinical outcome (Depienne, Trouillard et al. 2010).

However, a clear explanation of the pathological mechanism that leads to a variety of clinical outcomes is still lacking. So, it is important to analyze PCDH19 function in brain to better define this pathology.

1.3 PCDH19 and protocadherin family proteins

The following section will describe protocadherins family and mainly PCDH19 protein, in order to highlight what is known about this protein and what is still missing.

1.3.1 The protocadherin family proteins

Cadherins are cell adhesion molecules encoded by genes classified into several subfamilies: the classical cadherin (Type I and II), the protocadherins and desmosomal cadherins. This enormous superfamily contains a large number of transmembrane proteins with extracellular domains that mediate calcium-dependent intercellular interactions.

The protocadherin (Pcdh) family represents the widest subgroup within the cadherin superfamily. It is composed by almost 80 members of type I integral membrane proteins. Interestingly, a common feature of these family members is the presence of a single large exon that codes for the entire extracellular and transmembrane domains and also for a small portion of the C-terminal tail (Nollet, Kools et al. 2000, Wu, Zhang et al. 2001). Another characteristic that distinguishes these proteins from other cadherins is the frequent occurrence of alternative splice variants.

Based on structural differences between the different protocadherin genes, these family members are classified into several subgroups: α-, β- and γ-protocadherins, which are clustered in a small genomic region; CELRS protocadherins, that contain seven-pass transmembrane domains; Fat-like protocadherins, that contain more than seven extracellular domains; the novel subgroup of non clustered δ-protocadherins and other protocadherins with different origins but still sharing similar structure domains with other cadherin members.

The δ-protocadherin subgroup has been recently identified and it comprises nine protocadherins. δ-protocadherins are divided into two subgroups: δ1- and δ2-protocadherins. δ1 group comprises protocadherin-1, -7, -9 and -11, which are the only protocadherins with seven extracellular cadherin domains and, beside the common motif 1 and 2 (CM1 and CM2) contain one more common motif 3 (CM3). The δ2-protocadherins comprise protocadherin-8, -10, -17, -18 and -19, are composed by

six extracellular cadherin domains and do not have the CM3 motif in their cytoplasmic domain (Wolverton and Lalande 2001, Redies, Vanhalst et al. 2005, Vanhalst, Kools et al. 2005).

1.3.2 Protocadherins functions

There are very few studies about the functional role of protocadherins. Since they belong to the cadherin superfamily, the first function that was analyzed is their capability to mediate cell adhesion. The results demonstrated that they are able to interact in trans to form intercellular connections but the binding seems to be weaker compared to that of classical cadherins. Interestingly, it was also demonstrated that protocadherins are able to mediate adhesion at synaptic junctions. Indeed they are predominantly expressed in the brain, and are though to play significant roles in neurodevelopment during neuronal migration and in synaptic plasticity. Even if there are few works about their neuronal role, protocadherins appear to be important for circuit and synapses formation and, interestingly, there are new investigations that are focusing more in protocadherins intracellular signalling than in cell-cell adhesion (Depienne, Gourfinkel-An et al. 2012).
Indeed, there are evidences that pcdhs play an important role at intracellular level both by their binding partners and by nuclear regulations following proteolytic processing.
Concerning the first point, several works demonstrated that C-terminal domains of some protocadherins can interact with various common partners, such as protein phosphatase-1α (PP1α) for δ1-protocadherin members, the tyrosine kinase Fyn for α-protocadherin proteins, and the microtubule-destabilizing protein SCG10 for γ-protocadherin members (Kohmura, Senzaki et al. 1998, Gayet, Labella et al. 2004).

Regarding the proteolytic processing, recently it has been shown that protocadherins such as γ-protocadherin and Fat-1 can be cleaved releasing their C-terminal domains that to go into the nucleus (Hambsch, Grinevich et al. 2005, Magg, Schreiner et al. 2005, Smalley, Brafford et al. 2005).

Altogether these findings highlight the important role of protocadherins in linking extracellular with intracellular signalling trough interacting proteins or gene-expression regulation in the nucleus.

1.3.3 Protocadherin-19 gene and protein

PCDH19 gene is located in Xq22.1 and is orientated in a telomere to centromere direction (Depienne, Gourfinkel-An et al. 2012).

PCDH19 is conserved in dog, cow, mouse, rat, chicken and zebrafish (Entrez Gene) species, and has been found to be moderately expressed in all regions of the human brain (Dibbens, Tarpey et al. 2008).

The complete 3,447-bp ORF of *PCDH19* consists of six exons, with a large first exon encompassing over half of the mRNA length. The transcript is subject to alternative splicing that gives rise to three different isoforms: the first isoform (isoform 1) is without the exon 2; the second isoform (isoform 2) lacks the second exons and the amino acid 893; the third isoform (isoform 3) maintains the second exon and the amino acid 893.

The gene encodes a 1,148 amino acids (aa) transmembrane protein belonging to the δ2-subclass of non-clustered pcdhs (Dibbens, Tarpey et al. 2008).
PCDH19 contains a signal peptide of 23 aa, six calcium-dependent extracellular cadherin (EC) repeats that mediate cell-cell interactions and are homologous to those of classical cadherins, a short transmembrane domain and a cytoplasmic region with two conserved and characteristic δ-protocadherins CM1 and CM2 domains *(Figure 4), (Dibbens, Tarpey et al. 2008)*.
The first exon encodes for the entire extracellular and transmembrane domain and for a small initial part of the C-terminal tail. The rest of the cytoplasmic domain is encoded by exons 2-6 and, in particular, exons 5 and 6 encode CM1 and CM2 respectively (*Figure 4*).

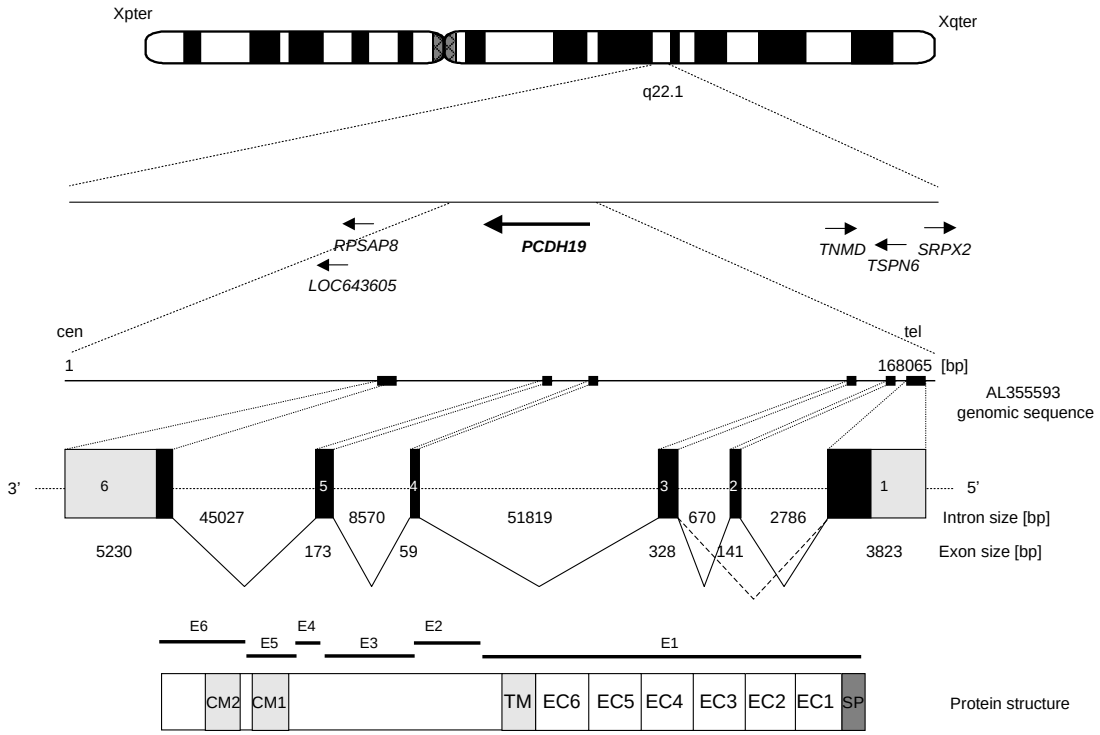

Figure 4 Scheme of PCDH19 gene and protein structure. Human X-chromosome and genomic of the *PCDH19* gene. Closest flanking genes with their orientations are indicated by arrows. The lower part of the figure represents PCDH19 protein structure. Exons (E1-6), signal peptide (SP), extracellular domains (EC1-6) and the two common regions (CM1 and CM2) are shown (Dibbens, Tarpey et al. 2008).

1.3.4 PCDH19 gene expression

As mentioned above, PCDH19 gene is widely expressed in the human brain, but it was also detected in primary skin fibroblasts, kidney and other tissues (Gaitan and Bouchard 2006).

However, *in situ* hybridization analysis in the developing mouse and human central nervous system revealed that pcdh19 is expressed predominantly in neural tissues at different developmental stages.

In mice *PCDH19* mRNA has widespread expression in both the embryonic and adult brain, including the developing cortex and hippocampus. Interestingly, in embryos, as many other protocadherins, pcdh19 shows an elaborate expression profile in neural

tissues, meaning that its region-specific expression depends on the embryonic stage (*Figure 5*), (Gaitan and Bouchard 2006).

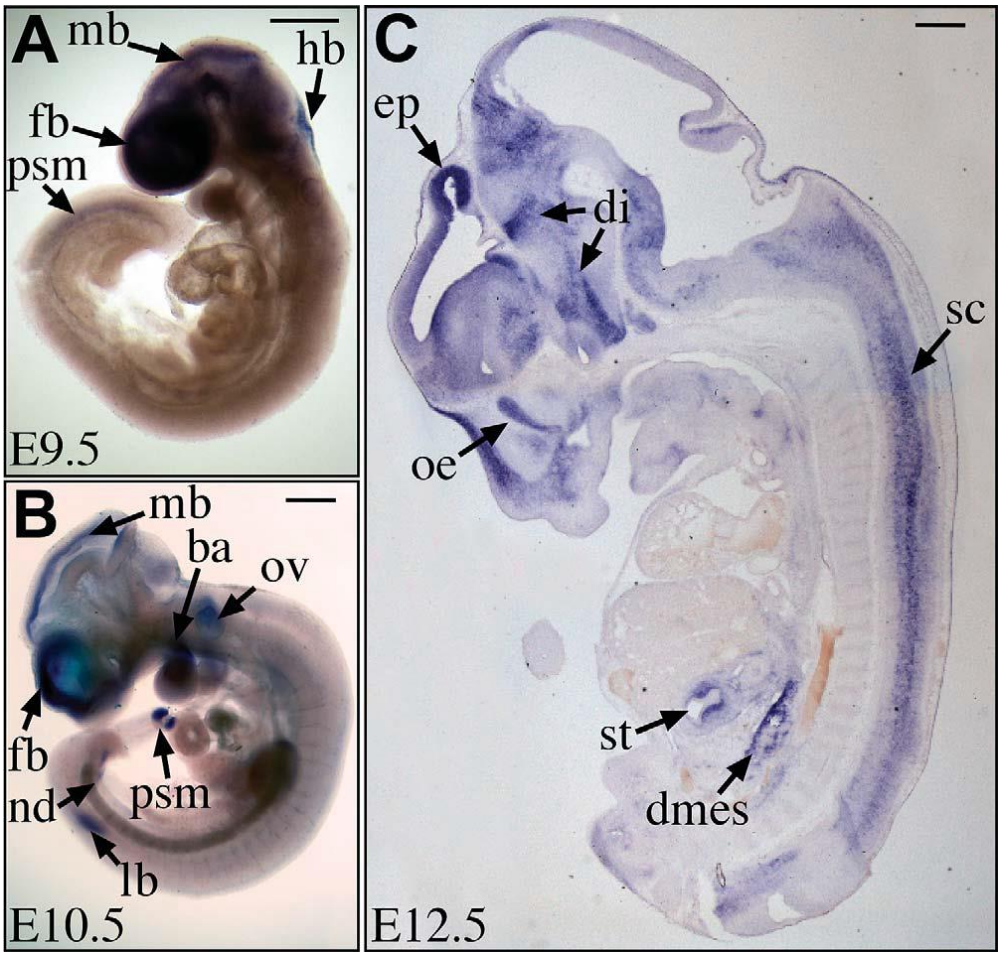

Figure 5 Early expression of *PCDH19* gene investigated in mice embryos by in situ hybridization. A and B represent the whole mount, C is a sagittal cryosection. (A) At E9.5, Pcdh19 transcript is detected in the brain and presomitic mesoderm. (B) At E10.5, brain expression is maintained and additional expression is detected in the brachial arches, otic vesicles, limb buds and caudal nephric duct. (C) In E12.5 embryos, high mRNA levels were observed in specific regions of the brain, in the epithelium lining the nasal cavity, spinal cord, stomach region and dorsal mesenteries. Ba=branchial arch; di=diencephalons; dmes=dorsal mesentery; ep=epiphysis; fb=forebrain; hb=hindbrain; lb=limb bud; mb=midbrain; nd=nephric duct; oe=olfactory epithelium; ov=otic vesicle; psm=presomitic mesoderm; sc=spinal cord; st=stomach (Gaitan and Bouchard 2006).

Regarding the human *PCDH19* gene expression, RT-PCR approaches showed its expression in various adult human tissues, such as brain, kidney, lung and trachea. In

neural tissues, *PCDH19* gene was shown to be expressed in developing cortical plate, amygdala and subcortical regions and in the ganglionic eminence (Dibbens, Tarpey et al. 2008, Depienne and LeGuern 2012).

Further, a recent study on *PCDH19* expression in adult rat brain, in particular in hippocampal formation, revealed that this gene is expressed with a specific pattern showing temporal preferences, suggesting that PCDH19 may have a role in the formation and maintenance of hippocampal circuits. This consideration is supported by the investigation of *PCDH19* hippocampal expression changes after electroconvulsive shock (ECS). Results show that *PCDH19* mRNA levels are influenced by direct electrical brain stimulation suggesting a PCDH19 role in structural rearrangements of the hippocampus (Kim, Mo et al. 2010).

Altogether these findings about *PCDH19* gene expression are in accordance with the clinical features of FLE, especially cognitive impairment, epilepsy, autism and behavioral disturbances.

1.3.5 PCDH19 protein functional role

The biological role of the PCDH19 protein is not known. There are very few studies which revealed that other δ2-pcdhs mediate calcium-dependent cell-cell adhesion in vitro and cell sorting in vivo and could regulate the establishment of neuronal connections during brain development and/or remodeling of selective synaptic connections during the early postnatal stage (Dibbens, Tarpey et al. 2008).

However, in contrast to cadherins, which associate through strong homophilic interactions, the extracellular domain of PCDH19 exhibits specific but weak homophilic adhesive properties (Depienne, Gourfinkel-An et al. 2012).

Recently, two studies performed on zebrafish, demonstrated that PCDH19 and N-cadherin are able to interact through their extracellular domains to form a complex and acting together to regulate cell movements during anterior neurulation in embryos. These evidences demonstrate that physically and functional interactions between PCDH19 and N-cadherin are essential for brain morphogenesis suggesting that protocadherins may act as cofactors for cadherin function at least during vertebrate development (Biswas, Emond et al. 2010, Emond, Biswas et al. 2011).

1.4 Proteolytic cleavage

The following section will provide a brief explanation of proteolytic cleavage, since our results demonstrate that PCDH19 protein is cleaved in response to neuronal activity.

In these last years, an increasing number of studies describe a new picture in which cells can rely signals from the extracellular space to their interior through presenilin-dependent proteolysis within the membrane-spanning regions of type I integral membrane proteins to generate potential transcriptionally active intracellular fragments.

Presenilin carries the active site of γ-secretase enzyme, which is responsible for this kind of cleavage. In particular, γ-secretase complex is a multisubunit aspartyl protease composed by four proteins: presenilin (PS), nicastrin, anterior pharynx-defective 1 (Aph1) and presenilin enhancer 2 (Pen2) (McCarthy, Twomey et al. 2009).

Initially, the γ-secretase complex was discovered as an essential element for the cleavage of β-amiloid precursor protein to generate Aβ peptides and, for this reason there are a lot of works that are interested in PS1/γ-secretase complex activity in Alzheimer disease (De Strooper, Saftig et al. 1998).

Recently, new findings reveal that the same proteolytic process occurs in an increasing growing number of integral membrane proteins, providing unexpected insights into general basic mechanisms of cell signaling functions (Schroeter, Kisslinger et al. 1998, Gu, Misonou et al. 2001, Okamoto, Kawano et al. 2001, Marambaud, Shioi et al. 2002).

In particular, this new general method for cellular communication between extracellular and intracellular environment is called regulated intramembrane proteolysis (RIP) and is characterized by two sequential cleavages. The first process is mediated by extracellular metalloproteases that usually shed the extracellular domain of the protein releasing it in the extracellular environment, thus leaving the intracellular domain tethered to the membrane. This fragment is sequentially cleaved by γ-secretase complex that releases a soluble intracellular domain (usually called as

ICD) that either acts as second messengers in the cytoplasm or enters the nucleus and regulates gene expression (*Figure 6*).

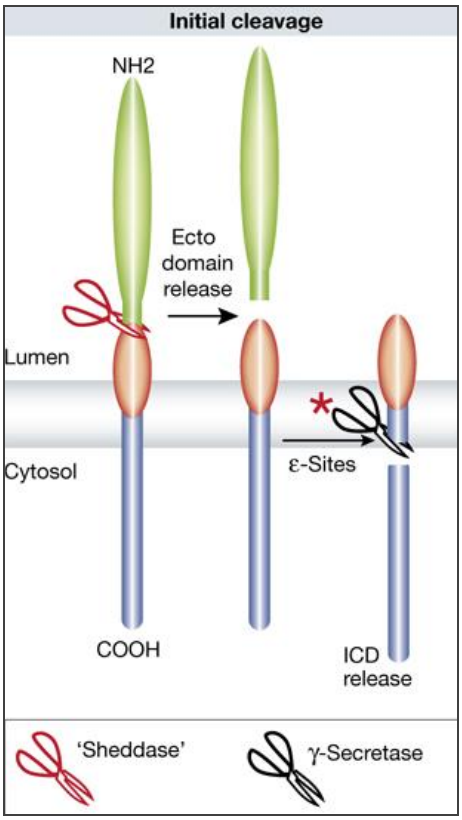

Figure 6 Schematic representation of proteolytic process RIP. Extracellular domain is first cleaved by metalloproteases and is exctracellularly released. Subsequently intracellular domain (ICD) is released in the cytoplasm by a second cleavage mediated by γ-secretase enzyme (Golde, Ran et al. 2012).

Within the new substrate that undergo to this proteolytic cleavage there are proteins implicated in synapse remodeling and maintenance, including EphRs, ephrins and cadherins (Dalva, McClelland et al. 2007, McCarthy, Twomey et al. 2009). Interestingly, PS1 has been shown to bind classical cadherins such as E-cadherin and N-cadherin (Georgakopoulos, Marambaud et al. 1999, Baki, Marambaud et al. 2001). Remarkably, E-cadherin also seems to be proteolytical processed by two sequential cleavage steps, even if its second cleavage site, differently from those of the other known γ-secretase substrates, does not seems to reside within the transmembrane but rather right at the membrane-cytosol interface (Marambaud, Shioi et al. 2002).

Further, in this case, γ-secretase enzyme could act also on the full-length E-cadherin, suggesting that a first cleavage by metalloproteases is not always necessary for γ-secretase action (Marambaud, Shioi et al. 2002).

Indeed, a recent study evidenced that the site of proteolysis varies among the different substrates, even if it remains close to the membrane-cytosol interface within the transmembrane sequence. Moreover there is not a unique consensus sequence for γ-secretase enzyme, although a Valine residue right after the cleavage site is present in most cases.

The precise location of γ-secretase proteolytic machinery is still unclear. In particular, the γ-secretase localizes in neurons mainly in membranes of endosomes, even if recent works demonstrate that it could be present also at the plasma membrane, in particular in synaptic complexes together with its substrates (Georgakopoulos, Marambaud et al. 2000, Kaether, Haass et al. 2006). These finding suggest a new role for this proteolytic machinery, in particular it could modulate synaptic function.

As a confirm of the newly discovered role for γ-secretase proteolytic machinery at synapses, recent works demonstrate that cadherin substrate for this enzyme undergo to proteolytic cleavage after neuronal activity, in particular mediated by NMDA receptors activation, such as for N-cadherin and γ-protocadherin (Reiss, Maretzky et al. 2006, Uemura, Kihara et al. 2006, Restituito, Khatri et al. 2011).

1.5 Synapse-to-nucleus signaling

We demonstrated that C-terminal domain of PCDH19 is able to shuttle between cytoplasm to nucleus in hippocampal neuronal cells. For this reason, this section will provide a brief overview on synapse to nucleus communications, highlighting recent discovery on protein messengers.

For neuronal cells it is fundamental to converge and integrate in the nucleus synaptic signals to determine a genomic response that regulates gene expression in response to neuronal activity. This process is critical for proper neuronal functions, such as

neuronal development, plasticity and survival. For these reasons, synapse-to-nucleus communication plays an important role.

The classical view of this process involves calcium ions as principal messenger, but recently there are substantial evidences, that for this type of signaling it is necessary also the nuclear import of cytosolic proteins.

Supporting this concept, recent studies showed that proteins enriched at neuronal synapses can accumulate in the nucleus in response to synaptic activity (Jordan, Fernholz et al. 2007, Proepper, Johannsen et al. 2007, Dieterich, Karpova et al. 2008, Lai, Zhao et al. 2008). Indeed, proteomic experiments identified many proteins in purified synaptosomes that contain a nuclear localization sequence (NLS), indicating a dual nuclear and synaptic localization of these synaptic junction proteins(Husi, Ward et al. 2000, Jordan, Fernholz et al. 2004).
Further, components of the classical nuclear import machinery (α-importin and β-importin) are also present at synapse and translocate to the nucleus in response to neuronal activity, specifically after N-methyl-D-aspartate receptor (NMDA) stimulation (Thompson, Otis et al. 2004).
All of these indications suggest that classical nuclear import mechanisms facilitate synapse-to-nucleus transport (Jordan, Fernholz et al. 2004).

However, it is unclear how synaptic nuclear messengers dissociate from synapses and by which mechanisms they are translocating to the nucleus.

1.5.1 Types of retrograde synapse-to-nucleus communications

Neurons utilize multiple mechanisms for signaling between distal subcellular compartments and the nucleus. These methods can be divided into two major classes: the first one is a rapid communication involving calcium ions, while the second is slower than calcium propagation and requires physical translocation of signaling molecules.

Rapid communications

Rapid communications are mediated by calcium ions flux and could be due to electrochemical signaling or to regenerative calcium waves in the ER.

In particular, the first mechanism allows extremely rapid communication to the cell body and nucleus. Action potentials lead to rapid influx of calcium ions at the soma activating calcium-sensitive signaling cascades that in turn activate transcription factors, thereby coupling neuronal activity to changes in gene expression within minutes (*Figure 7*) (Adams and Dudek 2005, Bengtson, Freitag et al. 2010, Hardingham and Bading 2010).

The second calcium-dependent nuclear signaling method in neurons involves regenerative calcium waves propagated along endoplasmic reticulum (ER). Besides its functions in the secretory pathway, the ER is an internal calcium store that is continuous with the nuclear membrane and extends into distal axons and dendrites. In this way, through the activation of two calcium receptors present on ER surface (the inositol triphosphate receptor and ryanodine receptor) the calcium influx is regenerated and propagates toward the nucleus through voltage gated channels activated at cell surface (*Figure 7*).

Physical translocation of signaling molecules

The physical transport of signaling molecules from their starting site to the nucleus is slower than calcium propagation and can persists over greater lengths of time. It comprises different mechanisms: in particular, this type of signaling includes passive diffusion or active transport of soluble signaling molecules and transport of signaling endosomes.

A difficult point of synapse-to-nucleus trafficking is the distance of messenger proteins that have to communicate from distal synapse to the nucleus. It is unlikely that diffusion-mediated signaling is efficient enough to allow distally generated signals to reach the nucleus in adequate concentration to alter transcription. Indeed, differently from the active transport, long distance travels without directionality don't permit the signal molecules to reach the nucleus with information enough to modulate transcriptional events, since the signal is degradate during the travel. This kind of diffuse transport is efficient only for small molecules and short distances (Howe 2005, Kholodenko, Hancock et al. 2010). Thereby, diffusion along a define axis could provide a fast and efficient mechanism for transport across large distances.

It could be along axis either without energy consume or active transport energy-dependent. In the first case messenger proteins moves along microtubule by Brownian motion or by facilitated diffusion interacting with guide molecules. In energy-dependent transport, molecules are shuttled along dendrites to nucleus by association with motor proteins, such as dynein, that allow long distance trafficking along microtubules. An important advantage of active transport in compare with passive diffusion is that motor proteins have directionality and processivity.

An example of this kind of transport is the internalization of signaling molecules into signaling endosomes. Once they arrives in the soma, the active complex interacts with a range of kinases or second messenger molecules. These secondary elements activate transcription factors to trigger gene expression in the nucleus (*Figure 7*) (Delcroix, Valletta et al. 2003, Ye, Kuruvilla et al. 2003, Cosker, Courchesne et al. 2008). Further, supporting the evidence that classic import nuclear machinery could be involved in long distance transport of synaptic messengers in the nucleus, it was observed that importins associate with the dynein motor complex, suggesting that this transport might require microtubules.

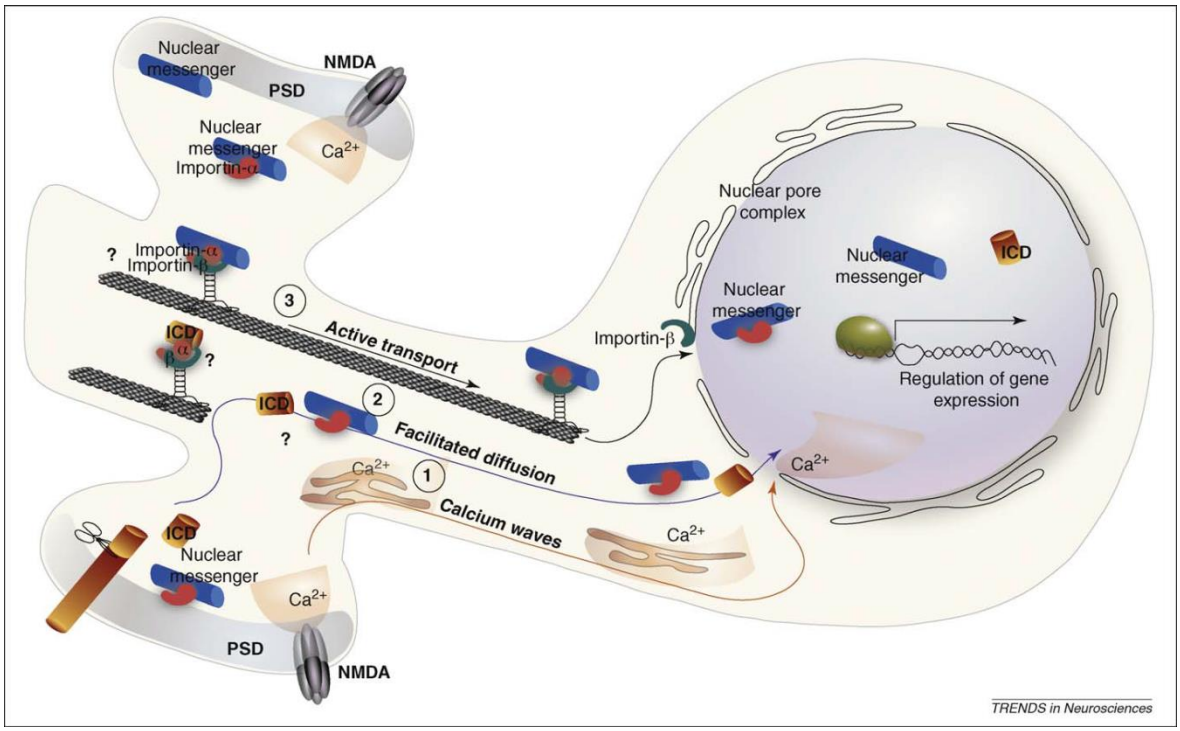

Figure 7 Representation of major synapse-to-nucleus communication pathways in neuronal cells after neuronal activity. Influx of calcium ions from the soma to the nucleus by activated receptors or by regenerative ER calcium waves. Diffusion of soluble molecules by simply Brownian motion or by

facilitated diffusion. Active retrograde transport mediated by molecular motors protein, such as dynein (Jordan and Kreutz 2009).

1.5.2 The role of NMDA receptor in synapse-to-nucleus communications

Recent studies identified synaptic proteins that shuttle from cytoplasm or synaptic sites into the nucleus in response to NMDA receptors (NMDARs) activation (Jordan, Fernholz et al. 2007, Proepper, Johannsen et al. 2007, Dieterich, Karpova et al. 2008, Lai, Zhao et al. 2008).

NMDARs play a central role in activity-dependent gene expression, in particular their activation is crucial for the control of plasticity-related gene expression and long-term memory formation.

NMDAR itself might function as nuclear signaling platform. Indeed this receptor complex is a particularly rich source of proteins that are capable to translocate into the nucleus (Husi, Ward et al. 2000, Pocklington, Cumiskey et al. 2006). Further, one of NMDAR subunit, the GluN1, in particular the -1a splice isoform, contains a classical NLS to which α-importin is docked and regulate its association and disponibility to signaling molecules through phosphorylation of serine adjacent the NLS (Jeffrey, Ch'ng et al. 2009). In fact, changes in the phosphorylation state induced by NMDARs activity play a role in the association of proteins messenger with importins, regulating their localization in neuronal cells, leading them to be transported into the nucleus after NMDARs activation.

Finally, recent studies showed that NMDAR-induced proteolytical cleavage of the protein messenger is a prerequisite for their nuclear transport. Indeed, in support to the hypothesis that proteolysis has a role in activity-dependent nuclear signaling, it has been demonstrated that soluble intracellular domains generated after proteolytic process of cellular adhesion molecules (CAMs) can accumulate in the nucleus and regulate gene expression (this was observed for N-cadherin, Notch, APP, γ-protocadherin etc..) (Marambaud, Wen et al. 2003, Uemura, Kihara et al. 2006).

1.6 Epigenetic modifications and histone lysine demethylation

The following section will provide a brief overview of histone lysine demethylase action on chromatin to explain the role of this enzyme in regulation of gene expression, since we observed that PCDH19 is able to interact with one of this histone lysine demethylase.

Several epigenetic modifications of DNA and histones, such as acetylation, methylation, phosphorylation and ubiquitination modulate chromatin structure and dynamics, playing important role in multiple biological processes, including neurogenesis.

Histones methylation is a fundamental posttranslational event that modulates chromatin state of condensation, regulating also transcriptional activity of different genes. Indeed, histones H3 and H4 can have different methylated lysines and, depending on the location and degree (mono-, di- or tri-methylation) of these modifications, the consequences could be either the repression or the activation of gene transcription (Martin and Zhang 2005, Mosammaparast and Shi 2010). In particular, H3 lysine 4 (H3-K4) di-methylation/tri-methylation (H3K4-me2/3) is usually associated with activation of gene transcription, whereas H3-K9 di-methylation/tri-methylation (H3K9-me2/3) is associated with a high level of chromatin condensation, corresponding to gene transcription repress state.

Interestingly, it has always been thought that histones lysine methylation was an irreversible chromatin modification, but recent studies demonstrate the existence of enzymes able to reverse this state. In particular, these enzymes can be divided at least into two classes of histone lysine demethylases: the Jumonji C-terminal domain (JmjC)-containing enzymes and the amine oxidase-related enzymes. Subsequently, other members of histone demethylase were discovered through sequence homology (Martin and Zhang 2005, Mosammaparast and Shi 2010).

These discoveries evidence the reversible state of histone lysine methylation like all other histone modifications, highlighting the crucial involvement of histone lysine demethylases for many chromatin-based cellular processes.

1.6.1 Lysine-specific demethylase 1 (LSD1)

The first histone demethylase that was identified is lysine-specific demethylase-1 (LSD1, also known as KDM1) that belongs to the superfamily of the flavin adenine dinucleotide (FAD)-dependent amine oxidases (Shi, Matson et al. 2005). Initially it was identified as a member of an HDAC-containing, transcriptional repressor complex (Ballas, Battaglioli et al. 2001, Shi, Matson et al. 2005). In particular, the first evidence showed that it is capable to remove mono- and di-methylation of histone H3 at lysine 4 (H3K4-me1/2) repressing, as a consequence, gene transcription. Subsequently, it was demonstrated that it is able to aggregate with other complexes, beyond Co-REST, and to be recruited to other gene promoters to demethylate H3K4-me1/2 and to repress transcription (Saleque, Kim et al. 2007, Wang, Scully et al. 2007, Wang, Hevi et al. 2009). LSD1 capability to be regulated by target gene recruitment and substrate specificity link its functions to a variety of biological events, such as development, differentiation, cancer and neurological disorders (Forneris, Binda et al. 2008, Nottke, Colaiacovo et al. 2009).

In particular, there are evidences that suggest an important role for LSD1 in neural differentiation. Further, inhibition of LSD1 activity leads to a dramatically reduced proliferation of mouse neural stem cells (Sun, Alzayady et al. 2010, Sun, Ye et al. 2011), while LSD1/CoREST complex control radial migration of cortical neurons being essential for their correct development (Fuentes, Canovas et al. 2012).

LSD1 structure and function is conserved from yeast to human (Dallman, Allopenna et al. 2004, Lakowski, Roelens et al. 2006). The lsd1 gene contains 19 exons and the human protein consists of 852 amino acids and comprises three major parts: the N-terminal SWIRM domain, involved in protein interactions, the C-terminal amine oxidase domain (AOD), consisting of two lobes which contains an insertion that forms the CoREST interacting site, and a long stalk formed by the insert between the two halves of AOD (Chen, Yang et al. 2006, Stavropoulos, Blobel et al. 2006).

An important characteristic of lsd1 gene is that through RNA alternative splicing, two additional exons can be included in the mature mRNA (exon E2a and exon E8a), generating, in this way, four possible LSD1 isoforms: the conventional LSD1, LSD1 with exon E2a (LSD1 +2a), LSD1 with exon E8a (LSD1 +8a) and LSD1 with both exons (LSD1 +2a+8a). Interestingly, LSD1+2a is present in all tissues, while the inclusion of

the 12-nt-long exon E8a limited the expression of the two isoforms (LSD+8a and LSD+2a+8a) in neuronal tissues.

1.6.2 NeuroLSD1 isoform

In mouse neurons, neuroLSD1 isoforms (LSD1+8a and LSD1+2a+8a) represent an important proportion of the total LSD1 transcripts pool (30%-40%) and during the perinatal period LSD1+8a is the predominantly expressed isoform (Zibetti, Adamo et al. 2010, Rusconi, Paganini et al. 2015). Indeed, during mouse brain development the expression of LSD1+8a isoforms is regulated (Zibetti, Adamo et al. 2010).

The characteristic of LSD1+8a isoform is the gene transcription activation, differently from the repressor action of LSD1. In fact, LSD1+8a demethylases the lysine 9 on histone H3, acting on the di-methylated form of this lysine (H3K9-me2) and, further, compromise LSD1 abilities to demethylate H3K4. LSD1+8a isoform is able to solve this action only through the collaboration with different factors, such as supervillin protein (SVIL), depending also by developmental mouse brain stage (Laurent, Ruitu et al. 2015) (*Figure 8*).

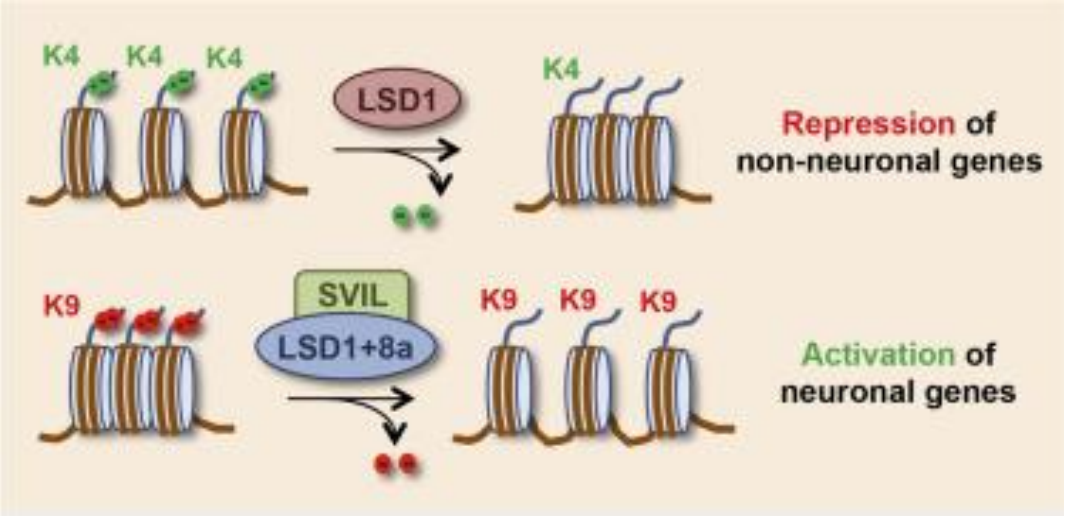

Figure 8 Schematic representation of LSD1 and neuroLSD1 action on gene expression regulation. LSD1 demethylases histone lysine 4 leading to a repression of non-neuronal gene transcription. LSD1+8a isoform demethylases histone lysine 9 usually by aggregation with cofactors such as SVIL, activating neuronal gene transcription (Laurent, Ruitu et al. 2015).

Besides the several roles of LSD1 in neuronal migration and development, its neuronal isoforms, which activate gene transcription, solve other important neuronal functions. In particular, the preponderant expression of neuroLSD1 during perinatal period suggests that it plays an important role for neuronal development. Indeed, some works demonstrate that LSD1+8a is involved in neurite morphogenesis and neuronal development by upregulating, during neuronal maturation, those set of genes involved in mitosis or microtubule cytoskeleton organization pathways, which are important for neurogenesis (Zibetti, Adamo et al. 2010, Laurent, Ruitu et al. 2015).

Further, neuroLSD1 plays important role in adult mouse brain contributing to maintain a correct balance between neuronal excitation/inhibition (Rusconi, Paganini et al. 2015). Indeed, neuroLSD1-null mice display a modified threshold of excitability, with a reduced susceptibility to Pilocarpine-induced status epilepticus (PISE), while mouse model of Rett Syndrome is characterized by an elevate seizures susceptibility have neuroLSD1 overexpression (Guy, Hendrich et al. 2001, Nan and Bird 2001, Rusconi, Paganini et al. 2015).

For these reasons, it is fundamental to maintain a correct ratio between LSD1 and neuroLSD1 during the entire life period of brain, in order to have specific chromatin modifications that regulate transcription of genes involved in neuronal development and excitatory/inhibitory balance.

1.6.3 NOVA1 and the importance of LSD1 alternative splicing

RNA binding proteins (RNABPs) regulate neuronal development and activity, playing a critical role in the brain.

NOVA proteins are RNBPs that are present in mammals in two paralogs: NOVA1 and NOVA2, which are largely expressed in the central nervous system (Buckanovich, Posner et al. 1993, Yang, Yin et al. 1998). These proteins regulate splicing, are able to shuttle between nucleus and cytoplasm and co-localize with target transcripts in dendrites. It was demonstrated that NOVA translocates into cytoplasm after neuronal activity and that mediates large changes in synaptic proteins, including proteins implicated in familial epilepsy. Further, mice that have haploinsufficient NOVA protein, manifest spontaneous epilepsy. These evidences linked NOVA to neuronal

activity, in particular it became important in mediated homeostatic excitation/inhibition in neuronal cells.

One of the NOVA target is LSD1, in particular this RNABP positively modulate exon E8a splicing inclusion generating neuroLSD1 isoform. In this way, neuronal activity modulates changes in LSD1/neuroLSD1 ratio by NOVA action, highlighting the crucial role of neuroLSD1 in modulation of neuronal excitability (*Figure 9*) (Rusconi, Paganini et al. 2015).

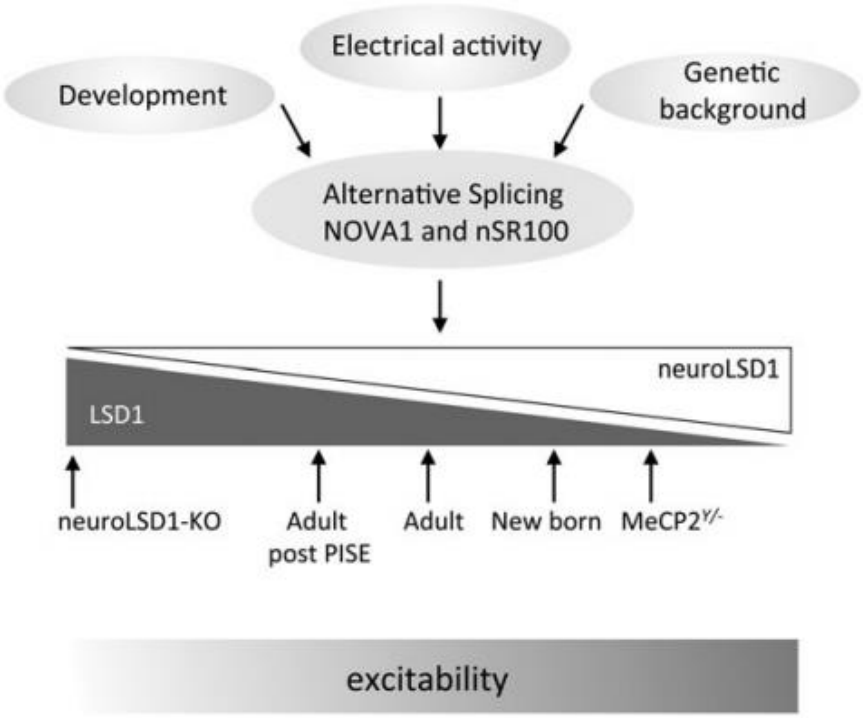

Figure 9 Model that link development, genetic background and electrical activity to excitability. Different LSD1/neuroLSD1 ratio is regulated by alternative splicing mediated by NOVA1 and nSR100 protein. Various balance between LSD1 and its neuronal isoform are associated with different degrees of neuronal excitability (Rusconi, Paganini et al. 2015).

These findings open to new clinical perspectives, in particular give rise to possibility to treat hyperexcitability-associated neurological disorders modulating neurospecific splicing of LSD1.

2. AIM OF THE PROJECT

PCDH19-female limited epilepsy, also known as early infantile epileptic encephalopathy type 9, is characterized by seizures onset in infancy or early childhood, cognitive impairment and behavioral disturbances. PCDH19 gene, located at the X-chromosome, is the causative gene and till now have been identified more than 100 different pathogenic point mutations which lead to degradation of mRNA and loss of PCDH19 protein expression (Duszyc, Terczynska et al. 2015).
A peculiar feature of PCDH19-FLE is the unusual inheritance pattern. Indeed, differently from the common X-linked pathology, FLE spares hemizygous males carring PCDH19 mutations and affects heterozygous females (Dibbens, Tarpey et al. 2008, Marini, Mei et al. 2010, Specchio, Marini et al. 2011). Further, there are various phenotypic degrees, even between patients carrying the same mutation. There are several hypothesis that try to explain the pathogenic mechanism. However a clear and precise explanation is still lacking.
Further, little is known about the expression and functions of PCDH19 protein encoded by the FLE causative gene.

Thus, the principal aim of our work is to go deeper into PCDH19 physiological functions in order to understand which kind of pathways could be impaired in patients and highlight crucial points altered in pathological conditions that could represent new therapeutic targets.

The first part of our work aimed to define PCDH19 expression in rat brain and in neuronal cells. In particular we investigated PCDH19 expression level in different adult rat brain regions and we analyzed the subcellular localization of PCDH19 in cultured hippocampal neurons.

In the second part of the work we investigated PCDH19 neuronal functions, in particular we examined a new molecular mechanism by which PCDH19 could link external stimuli with intracellular compartment focusing more on its putative intracellular functions than the extracellular.

The third part of the work aimed to go deeper into nuclear function of PCDH19-CTF. Firstly we investigated the effect of PCDH19 loss in cultured hippocampal neurons. We used a shRNA strategy that induces loss of expression of PCDH19 resembling PCDH19-FLE condition and analyzes which targets are impaired by PCDH19 knockdown.

Then, once we obtained putative targets, we went deeper into the molecular and functional mechanism that links PCDH19 protein to these targets in order to clarify the pathways in which PCDH19 plays an important role and that could be impaired by the loss of PCDH19 expression.

3. MATERIALS AND METHODS

3.1 cDNA constructs, shRNAs

The full-length PCDH19 isoform4 coding sequence was subcloned from pcDNA/V5 construct (gift from Joseph Gecz) cFUW (Addgene) vector using AscI/BamHI restriction enzymes in order to obtain PCDH19-V5 and for production of lentivirus.

CT-HA construct was obtained by PCR from PCDH19 sequence in pcDNA/V5 construct using these primers: 5' cgggatccatggcaatcaagtgcaagcgagac 3' and 5' gaagatctcatgagaacgatatccttcagacg 3'. The PCR product was inserted pCMV vector with the hemagglutinin (HA)- tag at C-terminal.

In order to produce PCDH19 shRNAs, the sequences 5' agaaccactcgtacctttaat 3' (shRNA 1873), 5' acaaagagatccggacctaca 3' (shRNA 2120), 5' gagcagcatgaccagtacaat 3' (shRNA 1240) were used and inserted into the pLL3.7 vector (Rubinson, Dillon et al. 2003); the same sequences were inserted into pLVTHM for production of lentivirus. The shRNAs were specific only for rat sequences. The scramble constructs were generated using these sequences: 5' gacagtattcatcccacatta 3' for sh1873, 5' gagcacactgcgaatcacaaa 3' for sh2120, 5' gaacagcatcccgaagtgtaa 3' for sh1240.

GST-PCDH19 construct, made with C-terminus (wt, aa 700-1148) was cloned into the E.Coli plasma vector pGEX-4T-1.

NOVA1, LSD1 and neuroLSD1 cDNAs with hemagglutinin (HA)-tag at C-terminal were a gift from Battaglioli's laboratory.

CT-V5 construct was obtained by PCR from PCDH19 sequence in pcDNA/V5 construct using these primers: 5' cgggatccatggcaatcaagtgcaagcgagac 3' and 5' aggcgcgccctaaccggtacgcgtagaatc 3'. The PCR product was inserted into cFUW/RFP vector using BamHI/AscI restriction enzymes. CT-V5 and cFUW/RFP vector were used for production in lentivirus.

The truncated form of PCDH19 isoform4 (aa 1-844) was amplified by PCR from PCDH19-pcDNA/V5 using this primer for C-terminal 5' aggcgcgccgtcaaaagaatagttttcagt 3'. The truncated form was cloned in lentiviral vector cFUW/RFP using BamHI/AscI restriction enzymes.

PCDH9 coding sequence was inserted into pIRES2 vector (gift from Fengmin Lu).

3.2 Cell cultures, transfection and infection

Human Embryonic Kidney 293 cells (HEK293) and African green monkey kidney cells (COS-7) at 50-70% confluence (24h after plating onto 6-well plates or onto glass coverslips in 12-well plates) were transiently transfected with cDNA expression constructs (1.8-3 ug/well) using Jet-PEI solution (Polyplus-transfection). The transfected cells were grown for 24-48 hours before fixation for immunocytochemistry or lysis for coimmunoprecipitation and GST pulldown. COS-7 and HEK293 cells were mainteined in Dulbecco's modified Eagle medium plus 10% fetal bovine serum and 1% penicillin/Streptomycin. The HEK293 cell line for generating lentivirus was grown in 1% G418, an aminoglycoside antibiotic.

Primary hippocampal neurons were prepared from embryonic days 18-19 rat brains (Brewer, Torricelli et al. 1993) and plated on coverslips coated with poly-D-lysine (0,25mg/ml) at 75.000/well for immunochemistry and 300.000/well for biochemistry experiments. Cultured neurons were transfected using the calcium phosphate method as described in (Lois, Hong et al. 2002). Immature neurons were transfected or infected at DIV4-11 and fixed or lysated at DIV7-19.

Lentiviruses expressing shRNAs, scrambled, full-length or C-terminal PCDH19 protein were produced using HEK293 cells as described by (Lois, Hong et al. 2002).

3.3 Culture treatments

COS-7, HEK293 cells and hippocampal mature neurons (DIV15-19) were treated after removing one-half of the culture conditioned medium (CM) and replaced with fresh medium. Reagents were added to the cultures: MG132, DAPT and DRB 10 μM for 1.30 hour; NMDA (50 μM), AP5 (100 μM) for 30 min; BIC (10 μM) and TTX (20 μM) for 1 hour (all of these compounds were from Sigma Aldrich). After treatments cells were fixed or lysed, for ICC, fractionation or immunoblotting experiments.

3.4 GST-pull down assay and Co-Immunoprecipitation

GST fusion proteins were prepared in E.coli strain BL21 and purified according to standard procedures. HEK293 cells and were lysed with a standard lysis buffer (PBS, 1% Triton X-100, 1mM EDTA, protease inhibitor cocktail, pH 7.4).

The lysates were incubated with 30µg GST fusion protein immobilized on glutathione-Sepharose 4B beads (GE Healthcare) for 3 hours at 4°C, wash 3-5 times in lysis buffer and resuspended in 25µl 3X SDS sample buffer. GST alone was used as control.

Samples were separated by SDS-PAGE followed by Western blotting with appropriate antibodies.

For immunoprecipitation experiments, HEK293 cells (homogenization buffer: 50mM TRIS-HCl, 200mM NaCl, 1 mM EDTA, 1%NP40, 1% Triton X-100, pH 7.4, protease inhibitor cocktail) were centrifuged at 16.500 g for 20 min at 4°C and supernatants were incubated at 4°C with Protein A-agarose beads (GE Healthcare) conjugated with rabbit IgG (6ug/ml SIGMA). The beads were separated by centrifugation and the supernatants were incubated at 4°C for 4 hours with protein A beads conjugated with either anti-V5 rabbit or anti-HA rabbit (6 µg/ml) or, as control, IgG (6 µg/ml). Then the beads were washed three times with lysis buffer and twice with PBS plus protease inhibitors and after resuspension in 3X sample buffer by boiling them for 5 minutes, were analyzed by SDS-PAGE.

The following antibodies and dilutions were used for immunoprecipitation: HA (1:1000 Invitrogen), V5 (1:400 Invitrogen), PCDH9 (1:400 AbCam)(all raised in rabbit) and PCDH19 (1:400, AbCam, raised in mouse). The secondary antibodies were horseradish peroxidase-conjugated anti-rabbit or anti-mouse IgG, light chain (both from 1:70000 Jackson ImmunoResearch laboratories) (RT, 1h in 5% milk). Immunoreactive bands were visualized by enhanced chemiluminescence (PerkinElmer).

3.5 Biotinylation assay

Plasma membrane proteins were biotinylated using membrane-impermeant sulfo-NHS-SS-biotin (0,3 mg/ml, Pierce) for 5 minutes at 37°C. Labeled neurons were washed with TBS supplemented with 0,1 mM CaCl2, 1mM MgCl2 and 50 mM glycine. After 3 washes with TBS supplemented with 0,1 mM CaCl2 and 1mM MgCl2 on ice, cells were lysed in extraction buffer (50 mM Tris-HCl, pH 7.4, 1 mM EDTA, 150 mM NaCl, 1% SDS, and protease inhibitors).

Lysates were boiled for 5 minutes, quantify with BCA kit (ThermoScientific) and, after kept the inputs, immunoprecipitated with streptavidin-conjugated magnetic beads (Dynabeads, Invitrogen).

The fractions obtained (input, biotinylated and intracellular components) were resuspended in 3X sample buffer, boiled for 5 minutes and analyzed by SDS-PAGE.

3.6 Isolation of crude synaptosomes

Adult mice brains were homogenized using cold homogenization buffer (0.32 M sucrose, 10 mM HEPES pH7.4, 2 mM EDTA, protease and phosphatase inhibitors) and spined at 1000g for 15 min to separate pelleted nuclear fraction (P1). The supernatant (S1) was recovered and centrifuged at 10.000g to produce a crude synaptosomal pellet (P2) and a supernatant (S2) which contains the cytosol and the light membranes. Synaptosomal pellet was resuspended in hepes buffer (50 mM Hepes pH 7.4, 2 mM EDTA, protease and phosphatase inhibitors). Samples were separated using SDS-PAGE and visualized by immunoblotting.

3.7 Subcellular fractionation of primary cell cultures (Cos-7, HEK293)

Primary culture cells were washed once with PBS and lysed in appropriate buffer (75 mM NaCl, 50 mM TrisHCl pH 7.4, 1% Np40, proteases and phosphatases inhibitors). After 1 hour of homogenization at 4°C they were centrifuged at 13.200 rpm for 10

min at 4°C. The surnatant were collected and centrifuged at 12.500 g for 10 minutes at 4°C in order to obtained the surnatant (S2) containing membrane and cytosol and pellet (P2) containing nuclear compartment. All these fractions (total homogenate, S2 and P2) were resuspended in 3X sample buffer, boiled for 5 minutes at 100°C and separated using SDS-PAGE.

3.8 Subcellular fractionation of primary neuronal cells

Two week-old high-density cultures of rat hippocampal neurons treated with NMDA and NMDA+AP5 were lysed in PBS. Subsequently were homogenate in hypotonic buffer (10 mM Hepes pH 7.5, 0.5% NP-40, 10 mM KCl, 1mM EDTA, 1mM DTT, protease and phosphatase inhibitors). After 15 min of mild agitation, cells were centrifuged at 400g for 10 min at 4°C. The supernatant was then centrifuged at 15.000g for 10 min at 4°C to clarify the extract and the supernatant (S1), representing the cytosolic/membrane enrich fraction, was collected. The pellet (P1) obtained from the 400g centrifugation was treated with an hypertonic buffer (20 mM Tris-HCl pH7.5, 0.6 M NaCl, 0.2 mM EDTA, 1.4 mM MgCl2, 25% glycerol, protease and phosphatase inhibitors) and centrifuged at 80.000g for 10 min at 4°C. The supernatant (S2) was collected and represented the soluble nuclear-enriched fraction, while the pellet (P2) was resuspended in SB3X and represented the nuclear aggregates-enriches fraction. All the fractions were separated using SDS-PAGE and visualized by immunoblotting.

3.9 SDS-PAGE, western-blot analysis and antibodies

Brain homogenization was performed in RIPA buffer (TrisHCl pH 7.4 50mM, NaCl 150 mM, EDTA 1mM, NP_{40} 1%, Triton 1% and protease inhibitors).

Cellular lysis was performed as previously indicated. Proteins were separated in 10% SDS-PAGE and electroblotted onto nitrocellulose membranes in buffer containing 0.025 M Tris-HCl, 0.192 M glycine, 20% methanol, pH 8.3 at 80 V for 120 min. Immunoblotting reactions were performed by incubating with the primary antibodies

(RT, 2-3h in 5% milk): -rabbit abs anti: GAPDH (1:2000, Santa Cruz), HA (1:1000, Invitrogen), V5 (1:1000, Invitrogen), LSD1 (1:1000, MBL) or mouse anti: α-tubulin (1:10000, SIGMA), PCDH19 (1:400, AbCam), GFP (1:2000, Roche Applied Science), PSD95 (1:20000, NeuroMab), Synaptophysin (1:1000, SIGMA).

Horseradish peroxidase-conjugated anti-rabbit or anti-mouse antibodies (1:2000 GE Healtcare) were used as secondary antibodies (RT, 1h in 5% milk). Immunoreactive bands were visualized by enhanced chemiluminescence (ECL, PerkinElmer).

Quantification analyses were performed using ImaJ software.

3.10 Total RNA extraction and RT-PCR analysis

After specific neuronal cells infections or treatments, total RNA was isolated using the Trizol reagent (Sigma-Aldrich) and the purified RNA was treated with RNase-free DNase set (Qiagen) to remove any residual DNA.

Quantitative RT-PCR analysis was performed on an iQ5 Real-Time PCR Detection System (Biorad) using the iScript™ two-step RT-PCR Kit with SYBR® Green (Biorad).

These experiments were performed in collaboration with Battaglioli's laboratory.

3.11 Immunofluorescence and antibodies

Hippocampal neurons or COS7 cells were fixed in 4% paraformaldeyde/4% sucrose for 8-10 minutes at room temperature and incubated with rabbit anti: V5 (1:400, Invitrogen), HA (1:100, Invitrogen), NOVA-1(1:400, SIGMA), GluA1 (1:1000, Chemicon), GAD 65/67 (1:400, MilliporMerck); with mouse anti: PCDH19 (1:200, AbCam) or with Guinea Pig anti: MAP2 (1:20000, Synaptic System) in GDB1X solution (2X: gelatin 2%, Triton X100 10%, 0.2 M Na2HPO4 pH 7.4, 4 M NaCl) for 2-3 hours at room temperature or over night at 4°C.

Then, cells were washed and incubated with Alexa 488 (1:400, Invitrogen), Alexa 555 (1:400, Invitrogen) or Cy5 (1:200, Jackson Immunoresearch) secondary antibodies diluted in GDB1X solution for 1 hour at room temperature.

3.12 Image acquisition and quantification

Confocal images were obtained using a Nikon 40x and 60x objectives with sequential acquisition setting at 1024x1024 pixels resolution. Each image was a 'z' series projection of approximately 7 to 12 images taken at 0.75 μm depth intervals, except that regarding nuclear compartment which are single stacks. Transfected or infected neurons were chosen randomly for quantification from two to five coverslips from three to five independent experiments. Morphometric and fluorescence intensity measurements were performed using MetaMorph images analysis software (Universal Imaging, West Chester, PA) and ImageJ. Statistical comparisons were performed with appropriate statistical test.

3.13 Statistical analysis

Data were expressed as mean ± standard error of the mean (SEM). Statistical significance was assessed using the paired and unpaired Student's t test as appropriate (for two group comparisons) or ANOVA followed by Bonferroni's post hoc tests. The level of significance was taken as: *$p < 0.05$, **$p<0.01$, ***$p<0.001$. All statistical analyses were performed using Prism 6 software (GraphPad, San Diego, CA). Each in vitro experiment was repeated at least three times. Primary neurons from three independent preparations were used.

4. RESULTS

4.1 PCDH19 is highly expressed in cortex and hippocampus and localizes at synapse

We first investigated PCDH19 localization in adult rat brain by western blotting experiments. Quantification analysis of PCDH19 levels showed that it is highly expressed in cortex and hippocampus, regions where we focused our attention, while it is less expressed in the cerebellum (*Figure 10A*).
Moreover, adult mouse brain fractionation shows the presence of PCDH19 in crude synaptosomes, together with PSD95 and synaptophysin markers (P2 fraction, *Figure 10B*).
These results suggest that PCDH19 is involved in cognitive processes, in accordance with the clinical aspects of the pathology, since PCDH19-FLE is characterized by epileptic seizures, intellectual disability and autism (Specchio, Marini et al. 2011).

Further, PCDH19 belongs to the cadherin superfamily, that is composed by cell adhesion transmembrane molecules mainly involved in intercellular interactions. Those, we performed biotinylation experiments on mature cultured hippocampal neurons (DIV19) to analyze PCDH19 cellular distribution. The results showed that PCDH19 localizes both at neuronal surface and intracellularly (*Figure 10C*). In addition, immunocytochemistry (ICC) on both COS-7 cells and hippocampal neurons overexpressing PCDH19 protein revealed that it is recruited at cell-cell contacts, suggesting a role of PCDH19 in intercellular interactions and adhesion (*Figure 10D*).

These findings indicate that PCDH19 has a potential role in cognitive processes and intercellular communications, since it is highly expressed in hippocampus, synaptic compartment and neuronal surface.

4.2 PCDH19 distributes both in developing and mature hippocampal neurons

We decided to further investigate temporal and spatial expression of PCDH19 protein in hippocampal neurons in order to go deeper into PCDH19 neuronal functions.

ICC on PCDH19 endogenous protein in developing hippocampal cells revealed that it is abundantly expressed in immature neurons (DIV4), while distributes heterogeneously in mature cells (DIV18, *Figure 11A*). Moreover, in neurons at DIV12 PCDH19 distributes along dendritic shaft, while in mature neurons it acquires punctuated pattern at synaptic level (*Figure 11B*).

Finally, we analyzed in which type of neuronal cells it is preferentially localized. ICC experiments on mature hippocampal neurons revealed that it is expressed both in inhibitory and in excitatory cells, colocalizing partially both with PSD95 and α_1-$GABA_A$ receptor subunit (*Figure 11C*).

Its presence both in immature and mature hippocampal neurons suggests a putative role for PCDH19 in neuronal development. Further, since it is expressed both in inhibitory and excitatory cells, we could hypothesized that PCDH19 has different roles according to the type of neurons it is expressed.

4.3 Proteolytic cleavage of PCDH19 protein in heterologous cells

Several recent studies reveal a new intracellular role of some cadherins besides their adhesion functions. In particular, some of these proteins, such as N-cadherin and γ-protocadherin, are cleaved by different enzymes. Usually, in the first step, the extracellular domain is released after metalloproteases action and, subsequently, a second enzyme cleaves intracellularly releasing the cytoplasmic domain of the protein in the cytosol. As a consequence, these protein's domains are able to solve intracellular signaling functions (Junghans, Haas et al. 2005).

Looking at PCDH19 protein sequence, we identified a motif in the transmembrane domain that is common among γ-secretase substrates. Moreover, by informatic tools, we found out a putative nuclear localization sequence (NLS) at the C-terminal domain that could transport the C-terminal tail of the protein in the nuclear compartment (schematic representation in *Figure 12A*).

To check whether also PCDH19 protein could undergo a proteolytic process, like other cadherins, we performed experiments on COS-7 cells and HEK293 cells transfected with PCDH19-V5 cDNA.

Firstly, we treated COS-7 cells with different compounds. We used a proteasome inhibitor (MG132) to prevent degradation of small protein fragments and be able to visualize all the cleavage products. Further we treated cells with a specific γ-secretase inhibitor (DAPT-1) to understand if this enzyme was involved in PCDH19 proteolytic process. MG132 treatment allowed the detection of a small fragment, whose molecular weight less than 60 KDa corresponds to the C-terminal domain (CTF) of PCDH19 protein. Indeed, without MG132 treatment we could not detect the band corresponding to the CTF anymore, suggesting that is rapidly degradated by proteasome. By contrast, when we treated cells with DAPT-1 and MG132, we were not more able to detect the cleaved fragment, suggesting that γ-secretase enzyme is involved in PCDH19 proteolytic process (*Figure 12B*).

These findings suggest that, at least in heterologous cells, PCDH19 can be cleaved by γ-secretase enzyme under basal conditions releasing the C-terminal tail that is rapidly degraded.

4.4 Nuclear localization of PCDH19 C-terminal domain in heterologous cells

After we established that PCDH19 can be cleaved by γ-secretase enzyme releasing the C-terminal domain, we investigated the localization of this fragment since it contains a putative NLS. Firstly we performed fractionation experiments on COS-7 cells overexpressing PCDH19 and treated with MG132. The results show an enrichment of CTF in nuclear compartment (P2 fraction, *Figure 12C*).

Further, ICC experiments on HEK293 cells transfected with either PCDH19-V5 cDNA or CTF-HA cDNA revealed that MG132 treatment lead PCDH19 distribution both in the cytoplasm and in the nucleus *(Figure 13A).* Moreover, ICC on HEK293 cells transfected with the CTF of PCDH19 showed that the C-terminal tail is able to enter in the nuclear compartment and its nuclear detection is clearer after proteasome degradation blockage *(Figure 13B)*.

All these findings indicate that PCDH19 can be cleaved and that the CTF released is able to enter the nucleus of HEK293 and COS-7 cells suggesting a nuclear role of the protein.

4.5 Activity dependent nuclear localization of PCDH19 in neuronal cells

Recent works demonstrate that soluble cytoplasmic domains of cadherins, which are released after a proteolytic process, are detected into the nucleus after neuronal activation where they regulate gene expression (Hambsch, Grinevich et al. 2005, Junghans, Haas et al. 2005).

To investigate the effects of synaptic activity on PCDH19 CTF generation, we treated rat primary hippocampal cultures infected with lentivirus of PCDH19-V5 with a set of compounds. Firstly, we acutely treated for 1.30 hours mature (DIV19) neurons with either bicuculline (BIC), which by blocking $GABA_A$ receptors promotes the excitatory transmission in neuronal network, or tetradotoxine (TTX), which blocks the voltage-gated sodium channels and decreases the neuronal network activity, and investigated protein localization by ICC experiments.

Confocal images showed that in control conditions the protein distributes in soma compartment and along dendrites, while bicuculline treatment promotes nuclear localization of PCDH19 *(Figure 14A)*. These findings are shown clearly in single stacks of nuclear compartment. Indeed, after stimulation of neuronal activity there is an increased co-localization between PCDH19 and nuclear marker DAPI (*Figures 14B*). Moreover, quantification analysis of fluorescence intensity level of PCDH19 confirmed that acute bicuculline treatment significant increases the intensity level of PCDH19 signal in nucleus, while TTX treatment decreases PCDH19 nuclear localization as control condition *(mean nucleus: NT 1,230 ± 0,128; BIC 2,013 ± 0,069; TTX 1,099 ± 0,252, One-Way ANOVA **p<0,01) (Figure 14C).*

These results indicate that PCDH19 neuronal distribution is highly dependent on neuronal activity: in particular, an acute stimulus increases PCDH19 nuclear localization suggesting that PCDH19 can transduce external stimuli to nucleus.

Next we wondered which receptor influenced PCDH19 cellular distribution. In particular we focused on NMDA receptor activity since it is involved in other cadherin cleavage and is associated to γ-secretase activity (Junghans, Haas et al. 2005).
To this purpose, we acutely treated for 30 minutes mature neurons overexpressing PCDH19-V5 with NMDA to specifically activate the NMDA receptors. Further, we used AP5 to specifically block NMDA receptors. ICC experiments revealed that thirteen minutes NMDA treatments are sufficient to change PCDH19 distribution, promoting its nuclear localization, while AP5 treatment decrease PCDH19 nuclear localization *(Figure 15A)*. Also in this case, single stack images of the nucleus clearly show the co-localization between PCDH19 protein and DAPI signal after NMDA receptors activation *(Figure 15B)*. Quantification analysis of PCDH19 fluorescence intensity levels confirmed a statistically significant increase of protein nuclear localization after NMDA acute treatment compared to control and AP5 treated neurons *(mean nucleus: CTRL 1,576 ± 0,124; NMDA 2,701 ± 0,377; NMDA+AP5 1,399 ± 0,146, One-Way ANOVA *p<0,05) (Figure 7C).*

These findings indicate that PCDH19 changes its neuronal distribution depending on NMDA receptor activity and lead us to a new question: is the cleavage of PCDH19 dependent on NMDA receptors activation?

4.6 PCDH19 cleavage is NMDA activity dependent and mediated by γ-secretase enzyme

To get insights into the molecular mechanism that mediates PCDH19 nuclear localization in response to NMDA receptors activation, we acutely treated mature hippocampal neurons with NMDA and performed different biochemical assays.

Western blotting analysis on treated neurons revealed that the endogenous full-length protein (PCDH19-FL) levels significantly decrease after NMDA receptors activation while AP5 treatment restores the control levels. Concomitantly with PCDH19-FL decrease, PCDH19-CTF significant increases *(Figure 16A, One-Way ANOVA *p<0,05).*

These findings were confirmed by western blotting experiments performed on hippocampal neurons overexpressing PCDH19-V5. Indeed, also in this case we observed a strong decrease of PCDH19-FL after NMDA treatment and an increase of CTF *(Figure 16B, One-Way ANOVA ***p<0,0001, *p<0,05).*

Moreover, we acutely stimulated AMPA receptors for 30 minutes in mature hippocampal neurons and investigated endogenous protein levels. PCDH19-FL levels after AMPA treatment are comparable to control conditions, proving the specific action of NMDA receptors on PCDH19 cleavage (*Figure 17A*).

Then, to go deeper into the mechanism of activity dependent PCDH19 processing we performed byotinilation assay on mature hippocampal neurons acutely treated with NMDA or NMDA plus AP5. The results show that neuronal activation significantly decreased PCDH19 surface levels suggesting that the protein is cleaved in an activity-dependent manner and released the C-terminal domain with a concomitant decrease in its membrane portion. Further, blocking NMDA receptors with AP5, we observed a restore of both PCDH19 membrane and CTF levels to the control condition *(CTRL 3,666 ± 0,744; NMDA 1,375 ± 0,162; NMDA+AP5 2,711 ± 0,359, One-Way ANOVA *p<0,05) (Figure 17B).*

Now we know that cadherins cleavage is mediated by γ-secretase enzyme that is activated by NMDA receptors (Junghans, Haas et al. 2005) and we showed that in heterologous cells PCDH19 is cleaved by this enzyme.
Therefore, we were wondering if this mechanism occurs also in hippocampal neuronal cells. To investigate this point, we treated mature hippocampal neurons with different compounds: in particular we used MG132 to prevent degradation of endogenous CTF; NMDA to stimulate the cleavage; and DAPT-1 to inhibit the γ-secretase enzyme. Western blot analysis revealed that, also in neuronal cells, γ-secretase is responsible for PCDH19 cleavage. Indeed, in the presence of DAPT, MG132 and NMDA both endogenous PCDH19-FL and CTF remain similar to control conditions *(Figure 18A, One-Way ANOVA *p<0,05, **p<0,01).*
Moreover, we confirmed these findings repeating the same treatments on hippocampal neuronal cells overexpressing PCDH19. In particular we stimulated cells with NMDA and blocked the γ-secretase enzyme using DAPT-1. We observed a rescue

of both PCDH19-FL and CTF levels after the treatment with DAPT-1 *(Figure 18B, One-Way ANOVA *p<0,05).*

Altogether these results indicate that NMDA receptors activation stimulates the cleavage of PCDH19 protein mediated by γ-secretase.

4.7 PCDH19 CTF translocates from cytoplasm to the nucleus in an activity-dependent manner

Our results showed that NMDA receptors activation increases nuclear localization of PCDH19 *(Figure 15)* and that, after neuronal activation, the protein is cleaved by γ-secretase enzyme releasing the soluble CTF *(Figure 16)*.

Therefore, we were asking if is the CTF released by the activity-dependent proteolytic process that translocate into the nucleus. To this aim, we performed ICC experiments on hippocampal neurons overexpressing either the PCDH19-V5 protein or the CTF-V5 alone. Single stacks of nuclear compartment showed that the protein distributes in part in the nucleus, while almost all the CTF overexpressed localizes in the nuclear compartment *(Figures 19A and 19B).*

These results indicate that PCDH19, specifically its CTF, enters the nuclear compartment suggesting a gene-expression regulatory role of the protein also in hippocampal neuronal cells.

To confirm that is the C-terminal tail of PCDH19 that localizes in the nuclear compartment, we performed fractionation experiments on mature hippocampal neuronal cells acutely treated with NMDA or with NMDA plus AP5 and observed PCDH19-FL and CTF distribution among different fractions. In basal condition PCDH19-FL is present in the total homogenate and membrane/cytoplasmic fractions (H.T., S1), while the CTF can be detected also in nuclear aggregates (P2) fraction. These findings indicate that PCDH19 cleavage occurs also in basal conditions.
However, after NMDA receptors activation there is an important enrichment of CTF in P2 fraction, as showed by quantification analysis, indicating that the cleaved fragment

obtained after neuronal activation (CTF) is targeted in to nuclear compartment (*Figure 20).*

Finally, to be sure that the CTF observed in the nucleus is transported from cytoplasm to nucleus and that is not the product of new protein synthesis, we treated neurons with NMDA to stimulate the cleavage together with an inhibitor of protein transcription (DRB). Subsequently, on these neuronal cells we performed the same fractionation experiments as before and observed that, even after DRB treatment, the CTF is still enriched in P2 fraction *(Figure 21)*.

These findings indicate that the CTF released after PCDH19 cleavage shuttles from cytoplasm to nucleus of neuronal cells suggesting that it can link external stimuli at synaptic levels and nuclear compartment.

4.8 Downregulation of PCDH19 in hippocampal neuronal cells increases NOVA1 protein and nLSD1 transcript levels

The results discussed above highlight a novel feature of PCDH19. CTF nuclear translocation after NMDA receptors activity gives rise to various questions, in particular what genes PCDH19 regulates and what are their roles in the pathogenesis of PCDH19-FLE.

In order to mimic the pathology, we down-regulated PCDH19 expression using shRNAs.

Firstly we designed three different shRNAs that specifically target the rat (sh1873, sh1240 and sh2120) and human (only sh2120) PCDH19 transcripts. To test the efficacy of these shRNAs, we analyzed PCDH19 endogenous protein level in hippocampal neurons lentivirally-infected with the three different shRNAs. All of these shRNAs efficiently reduced PCDH19 expression *(Figure 22A).*
Then we used the shRNA1873, since it efficiently reduced PCDH19 protein levels, and its scrambled sequence as control for PCDH19 silencing experiments, and the human PCDH19-V5 cDNA together with shRNA1873 to rescue PCDH19 endogenous levels. We observed that scrambled sequence is not able to silence PCDH19 protein and that

the lentiviral expression of PCDH19-V5 cDNA together with its specific shRNA1873 allows maintaining the control level of PCDH19 protein *(Figure 22B)*.

Interestingly, we observed that in hippocampal neurons infected with PCDH19 shRNA there was a significant increase of NOVA1 protein levels. These results were obtained with ICC and western blotting experiments *(Figure 22C-D, t-test *p<0,05, One-Way ANOVA *p<0,05).* NOVA1 regulates alternative splicing of various genes and it is involved in the maintenance of inhibitory/excitatory neuronal network balance. Since NOVA1 promotes LSD1 neuronal isoform (neuroLSD1) (Rusconi, Paganini et al. 2015), we investigated if also the mRNA levels of this isoform were changed after the downregulation of PCDH19. The results showed a significant increase of neuroLSD1 transcript compared to control conditions (scramble and rescue, *Figure 22E, One-Way ANOVA **p<0,01).*

These findings represent a new territory of investigation to get into the pathophysiologic basis of the disease. In particular they suggest a new mechanism by which PCDH19 loss of function in PCDH19-FL epilepsy could affect a neuro-restricted epigenetic corepressor (LSD1), which modulates circuitry excitability.

4.9 CTF proteolytic processed is able to associate with LSD1 and neuroLSD1

Since the CTF of PCDH19 protein is cleaved following NMDAR activity and that NOVA1 and neuroLSD1 are important for neuronal homeostasis, we were wondering if there is a connection between PCDH19 cleavage and NOVA1/neuroLSD1 pathways.

To this aim, we first checked the interactions. Firstly, we performed pull-down experiments and coimmunprecipitations (Co-IP) in HEK293 cells using PCDH19 protein or its CTF as show in *Figure 23A*.

In pull-down experiments we used CTF fused to GST as a bait that was incubated with lysates of HEK293 cells transfected with LSD1-HA or NOVA1-HA constructs. We found that LSD1 is able to interact with the C-terminal domain of PCDH19, while NOVA1 is not (*Figure 23B*).

Then, we transfected HEK293 cells with PCDH19-V5 together with either LSD1-HA, neuroLSD1-HA or NOVA1-HA. In all these experiments we immunoprecipitated PCDH19 and the results show that both LSD1 and neuroLSD1 can associate with PCDH19. By contrast NOVA1 cannot (*Figure 23C*).

To reduce the region of interaction of PCDH19 with neuroLSD1 and LSD1, we performed Co-IP experiments in HEK293 cells co-transfected with LSD1-HA or neuroLSD1-HA and different PCDH19 constructs. In particular we used the CTF-V5 and the PCDH19 with Δ844-1161aa (*Figure 24A*). We found that the sequence of PCDH19 protein that is involved in the interaction with LSD1 and neurLSD1 is in the CTF, in particular between aa844 and 1161 (*Figure24B-C*).

Finally, to establish whether the two common motifs of cadherin family proteins (CM1 and CM2) were involved in this interaction, we tested PCDH9 that belongs to the protocadherin family and contains CM1, CM2 and CM3 domains (*Figure 25A*). We co-transfected HEK293 cells with PCDH9-myc and either LSD1-HA or neuroLSD1-HA and immunoprecipitated for PCDH9-myc. The results showed that LSD1 and neuroLSD1 are not able to interact with PCDH9 protein, indicating that CM1 and CM2 are not sufficient to mediate the interaction and other regions between aa844 and 1161 are involved (*Figure 25B*).

Altogether these findings suggest the existence of a complex between the CTF of PCDH19 protein and two important epigenetic corepressor factors, LSD1 and its neuro-restricted isoform neuroLSD1.

4.10 NeuroLSD1splicing is regulated by NMDA activity

Previous studies revealed that, in response to epileptogenic stimuli, downregulation of NOVA1 reduces the expression of neuroLSD1 to homeostasis (Eom, Zhang et al. 2013, Rusconi, Paganini et al. 2015). We demonstrated that PCDH19 is cleaved after strong activation of NMDA receptors and releases its CTF that goes into the nucleus.

After proving that CTF can interact with LSD1 and neuroLSD1, we were asking if the same activity that stimulated PCDH19 cleavage could regulate LSD1/neuroLSD1 balance. If this is the case, we can hypothesize that PCDH19 cleavage together with

LSD1/neuroLSD1 corepressing actions might linked to each other in the same regulatory pathway of neuronal excitability.

To this purpose, we firstly treated mature hippocampal neurons with NMDA and NMDA plus AP5 and analyzed LSD1 protein levels by western blotting. The quantification showed that there is a statistically significant increase of LSD1 protein levels after NMDA receptors activation and an important decrease after AP5 treatments (*Figure 26A, One-Way ANOVA *p<0,05).*

Thus, we demonstrated that LSD1 can be regulated by the same activity pattern that stimulates PCDH19 cleavage.

To go deeper into the investigation of this mechanism, in particular to be able to discriminate between the two isoforms of LSD1, we performed also mRNA analysis on hippocampal neuronal cells treated as before. The results show that there is an important decrease in the percentage of neuroLSD1 isoform after NMDA receptors stimulation (*Figure 26B, One-Way ANOVA **p<0,01, ***p<0,0001)*

Altogether these results suggest that after a strong activation of NMDA receptors the levels of LSD1 and neuroLSD1 change in order to restore neuronal cells into a homeostasis. Further, CTF released after PCDH19 cleavage could solve a crucial role in this regulatory mechanism, through the interaction with LSD1 and neuroLSD1 elements.

5. FIGURES AND LEGENDS

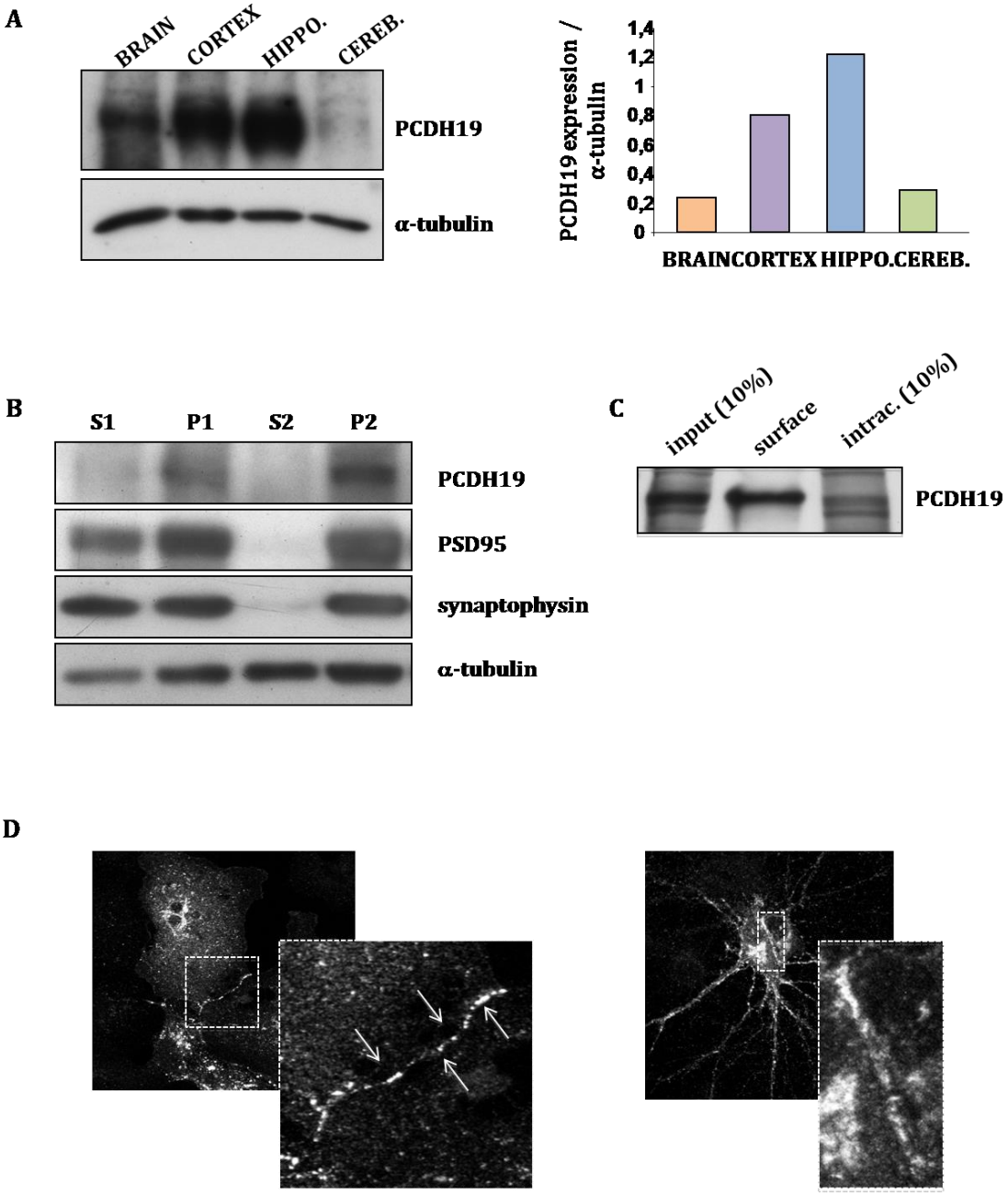

Figure 10: PCDH19 is highly expressed in cortex and hippocampus and localizes at synapse. (A) Western blot of adult rat brain homogenates using anti-PCDH19 and anti-α tubulin. Quantification analysis of PCDH19 levels (right panel) showing that PCDH19 is expressed at high level in cortex and hippocampus. (HIPPO: hippocampus; CEREB: cerebellum). (B) Adult mouse brain fractionation showing the presence of PCDH19 in crude synaptosomes (P1: nuclear fraction; S1 and S2: cytosol and light membranes; P2: crude synaptosomal pellet). (C) Biotinylation experiment on mature hippocampal neurons showing both surface and intracellular expression of PCDH19. (D) ICC performed on COS-7 cells (left) and mature hippocampal neurons (right) overexpressing PCDH19-V5 showed that PCDH19 is recruited at cell-cell contacts (zoom boxes).

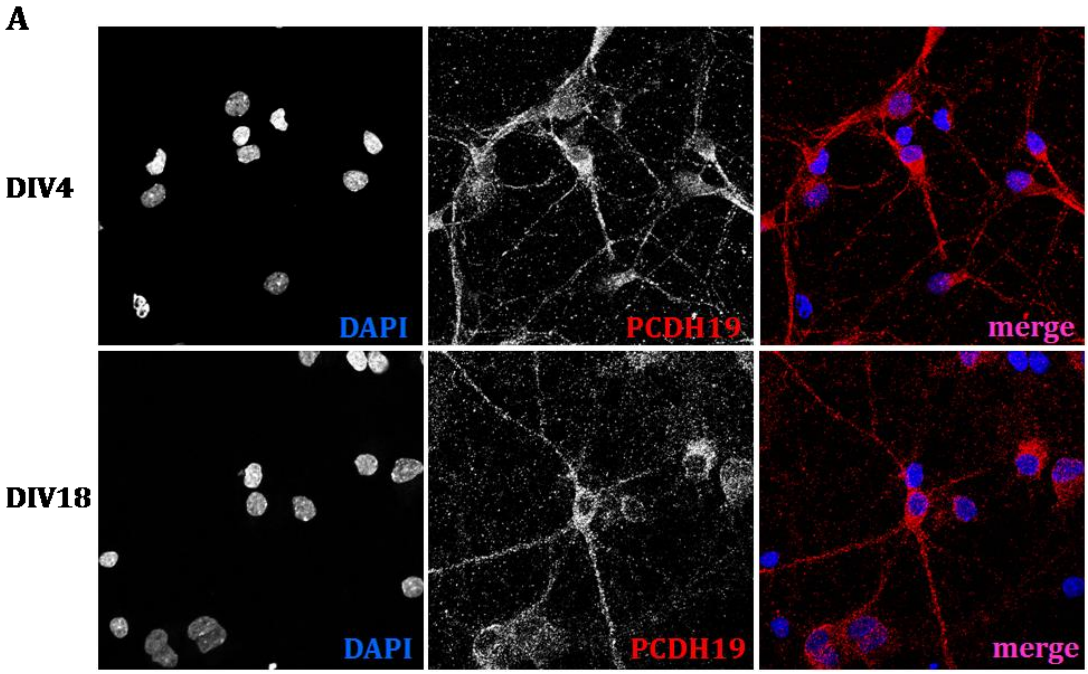
A
DIV4
DIV18
DAPI
PCDH19
merge
DAPI
PCDH19
merge

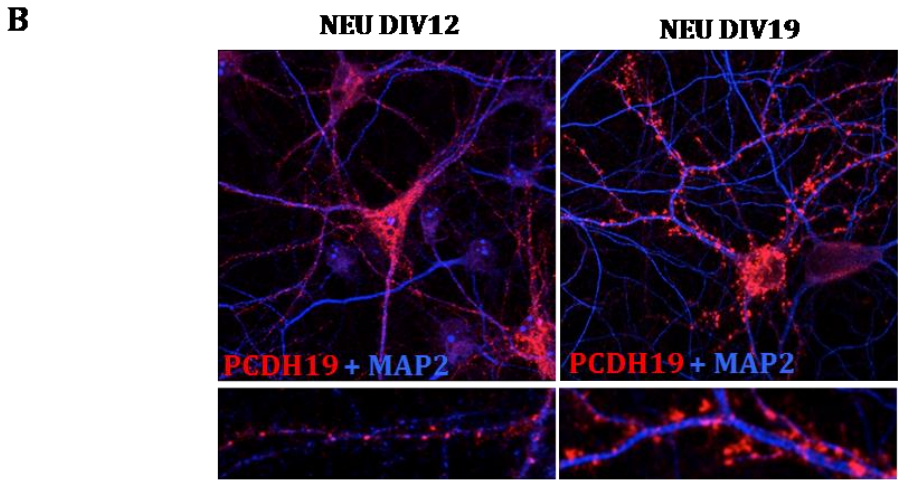
B
NEU DIV12
NEU DIV19
PCDH19 + MAP2
PCDH19 + MAP2

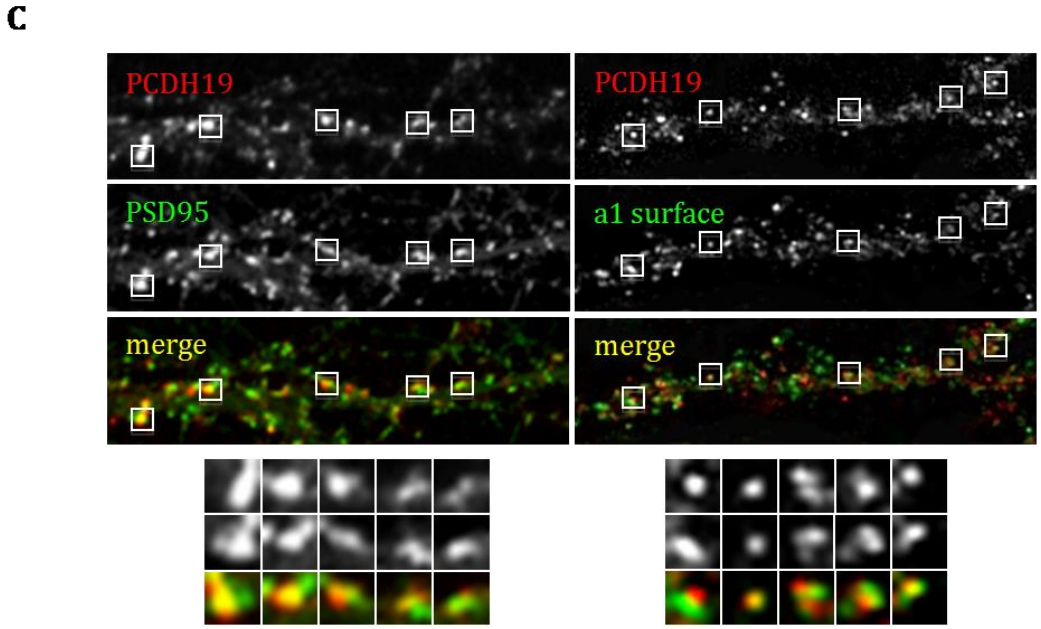
C
PCDH19
PCDH19
PSD95
a1 surface
merge
merge

Figure 11: PCDH19 distributes both in immature and mature neurons, both in inhibitory and excitatory cells. (A) Confocal images of hippocampal neuronal cells fixed at DIV4 and DIV18 and immunostained for DAPI and PCDH19 to visualize nuclei and endogenous protein respectively. PCDH19 is abundantly expressed in immature neurons, while it distributes heterogeneously in mature neuronal cells. (B) Confocal images of hippocampal neuronal cells fixed at DIV12 and DIV19 and immunostained for PCDH19 and MAP2 to visualize endogenous protein and cellular morphology respectively. PCDH19 distribution along dendritic shaft (neurons DIV12); PCDH19 punctuated pattern (neurons DIV19). (C) Confocal images of mature hippocampal neurons stained for PCDH19, PSD95 and α1 subunit of GABAA receptor. Zoom boxes showing partial co-localization between PCDH19 and both PSD95 and α1 subunit of GABAA receptor.

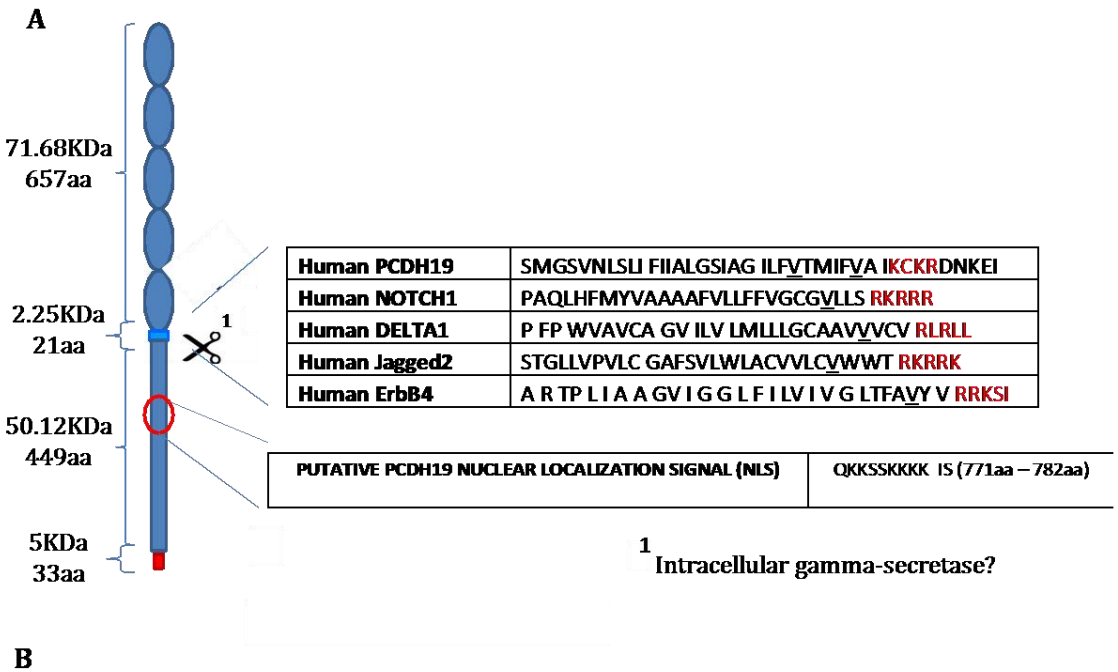
A
71.68KDa
657aa
2.25KDa
21aa
50.12KDa
449aa
5KDa
33aa
1
Human PCDH19 SMGSVNLSLI FIIALGSIAG ILFVTMIFVA IKCKRDNKEI
Human NOTCH1 PAQLHFMYVAAAAFVLLFFVGCGVLLS RKRRR
Human DELTA1 P FP WVAVCA GV ILV LMLLLGCAAVVVCV RLRLL
Human Jagged2 STGLLVPVLC GAFSVLWLACVVLCVWWT RKRRK
Human ErbB4 A R TP L I A A GV I G G L F I LV I V G LTFAVY V RRKSI
PUTATIVE PCDH19 NUCLEAR LOCALIZATION SIGNAL (NLS)
QKKSSKKKK IS (771aa – 782aa)
1 Intracellular gamma-secretase?

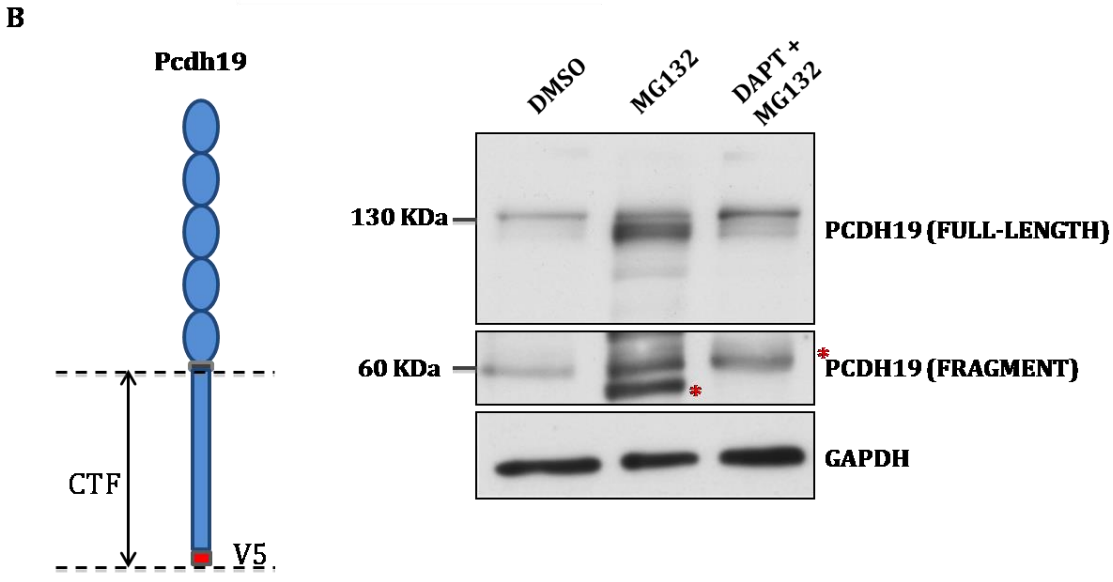
B
Pcdh19
CTF
V5
DMSO
MG132
DAPT + MG132
130 KDa
60 KDa
PCDH19 (FULL-LENGTH)
PCDH19 (FRAGMENT)
GAPDH

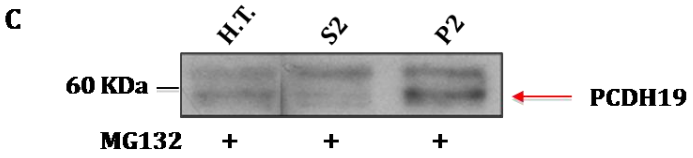
C
H.T.
S2
P2
60 KDa
PCDH19
MG132 + + +

Figure 12: proteolytic cleavage of PCdh19 in heterologous cells. (A) Schematic representation of PCDH19 protein and its putative cleavage site for γ-secretase. On the right are shown γ-secretase substrates: red amino acids represent the accommodation site for the enzyme; underlined valines represent the site of action of the enzyme. In the transmembrane domain of PCDH19 there are two valine residues (aa 683, 698) that could be the sites of action for γ-secretase. Indication of a putative nuclear localization sequence (NLS) in the C-terminal domain of PCDH19, between aa 771-782. (B) Schematic representation of CTF released after PCDH19 cleavage (left). Western blot of COS-7 cells overexpressing PCDH19 and treated with MG132 and DAPT to prevent proteasome degradation and inhibit γ-secretase action respectively (10 μM, 1.30 h, 37°C). Detection of CTF after MG132 treatment. DAPT inhibits of PCDH19 cleavage even in the presence of MG132. (C) Fractionation experiment on COS-7 cells transfected with PCDH19 and treated with MG132. CTF (indicated by red arrow) is enriched in the nuclear compartment (H.T.: total homogenate; S2: cytoplasmic compartment; P2: nuclear compartment).

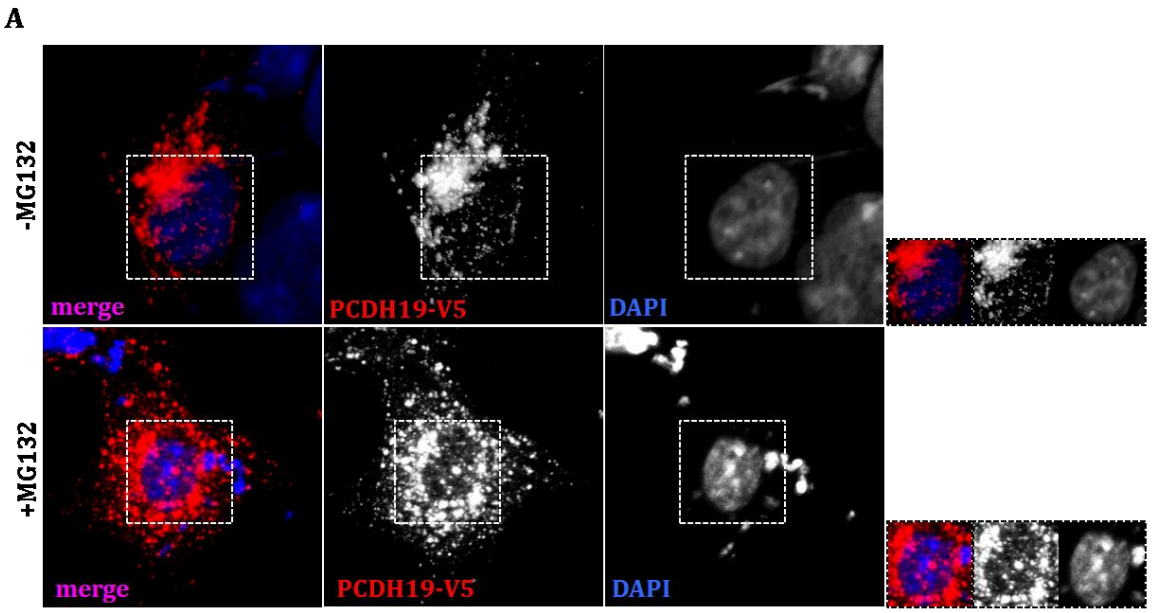
A
-MG132
+MG132
merge
PCDH19-V5
DAPI
merge
PCDH19-V5
DAPI

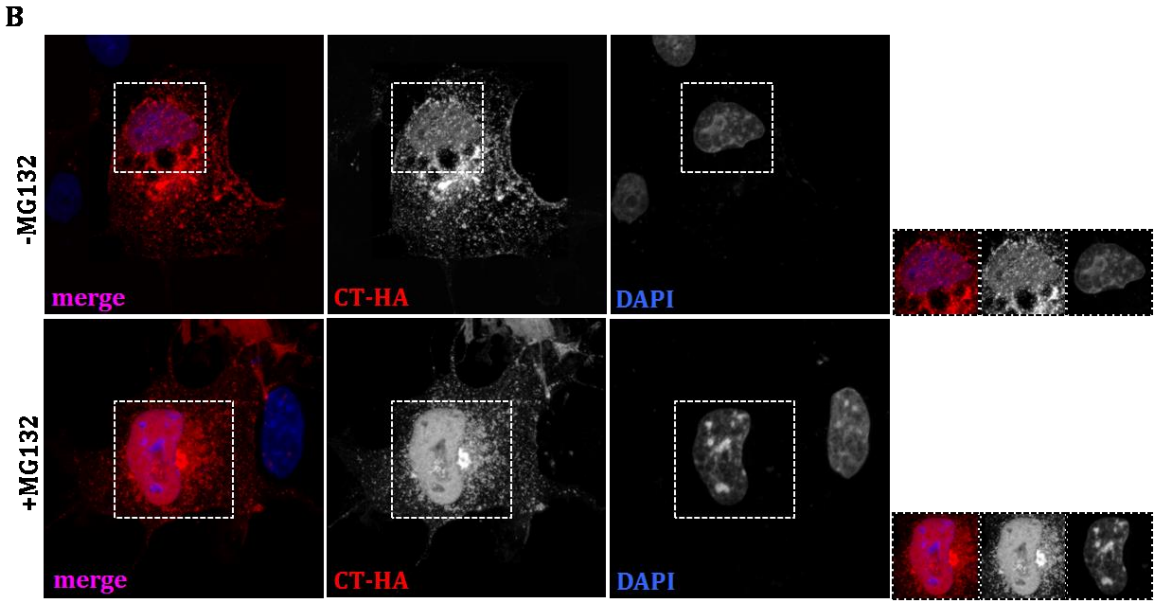
B
-MG132
+MG132
merge
CT-HA
DAPI
merge
CT-HA
DAPI

Figure 13: PCDH19 and CTF are enriched in the nucleus of heterologous cells. (A) Confocal images of HEK293 cells transfected with PCDH19-V5 and immunostained for V5 and DAPI to visualized overexpressed protein and nuclei respectively. After MG132 treatment the protein localizes also in the nuclear compartment: better shown by single stack images of the nucleus (boxes at the right). (B) Confocal images of HEK293 cells transfected with CT-HA (C-terminal domain of PCDH19) and immunostained for HA and DAPI to visualized overexpressed protein and nuclei respectively. The fragment is enriched in the nucleus and even more after MG132 treatment: better shown by single stack images of the nucleus (boxes at the right) (MG treatment: 10 μM, 1.30 h, 37°C).

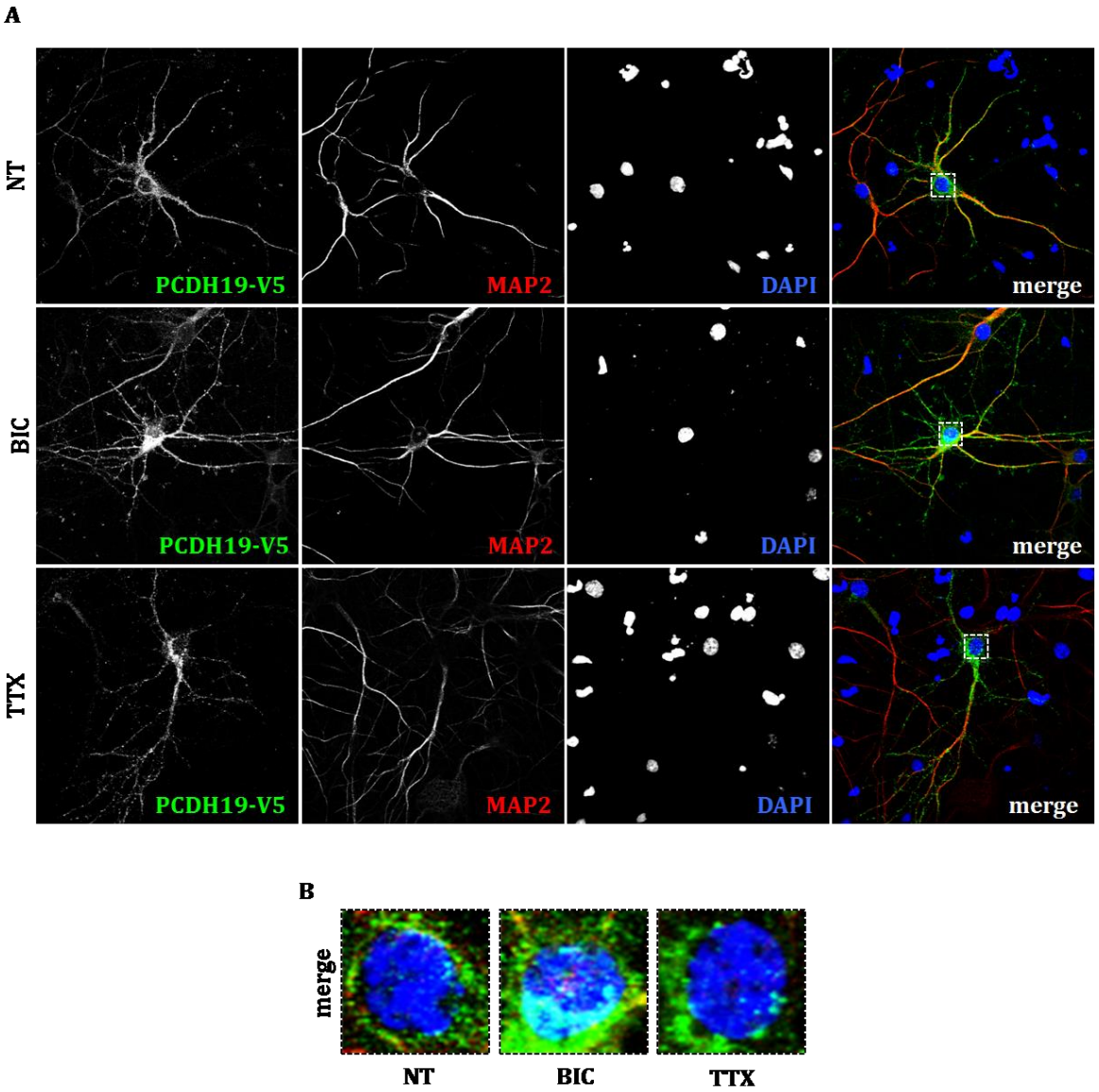
A
NT
BIC
TTX
PCDH19-V5
MAP2
DAPI
merge
B
merge
NT
BIC
TTX
C
mean nucleus
2.5
2.0
1.5
1.0
0.5
0.0
**
**
NT
BIC
TTX

Figure 14: Activity dependent nuclear localization of PCDH19 in hippocampal neurons. (A) Confocal images of hippocampal mature neurons overexpressing PCDH19, immunostained for V5, DAPI and MAP2 and acutely treated with bicuculline (BIC, 40μM, 1.30 h, 37°C) or tetradotoxine (TTX, 2μM, 1.30 h, 37°C). PCDH19 enriched in nucleus after BIC treatment. (B) Single stack of above neuronal nuclei showing better PCDH19 nuclear distribution after BIC treatment. On the other hand, TTX blocks PCDH19 enrichment in nuclear compartment. (C) Quantification analysis of PCDH19 fluorescence intensity level in nuclear compartment confirming the above observations (**p<0,01, One-Way ANOVA analysis).

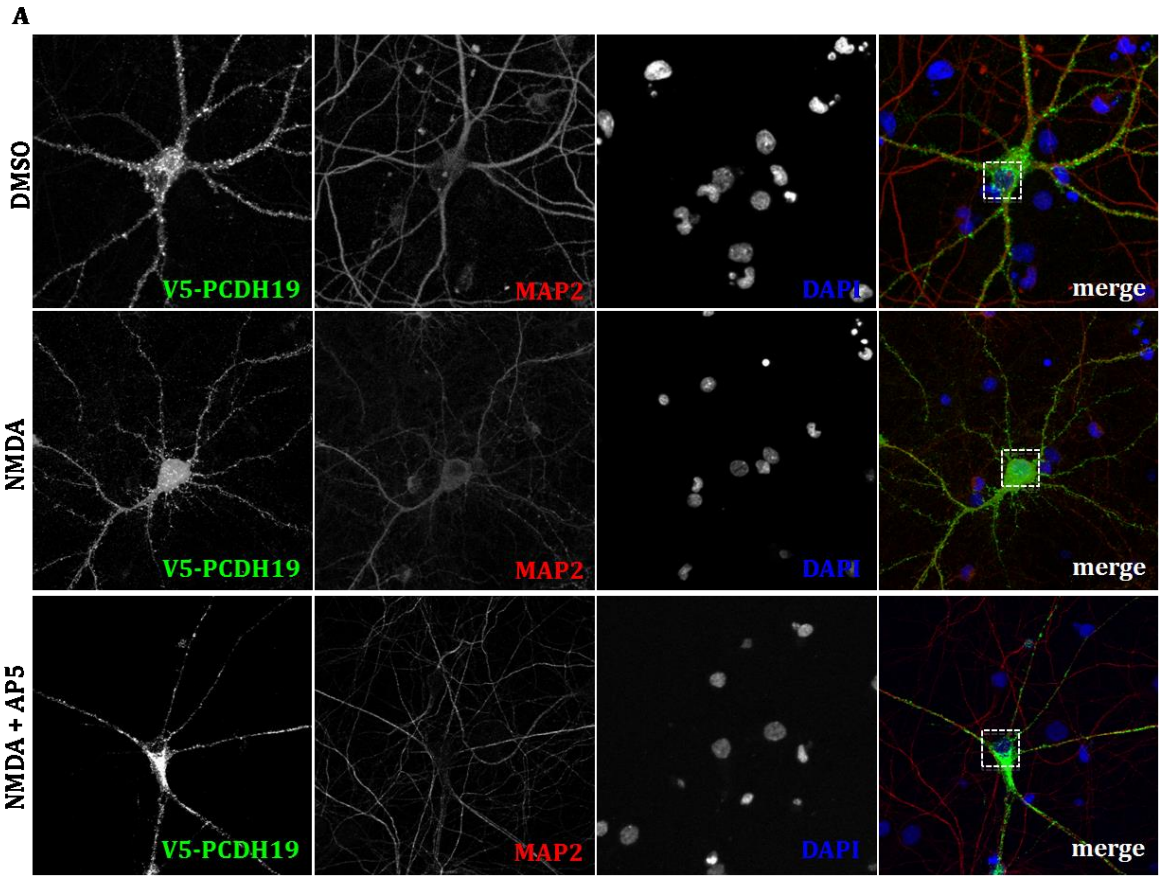
A
DMSO
NMDA
NMDA + AP5
V5-PCDH19
MAP2
DAPI
merge

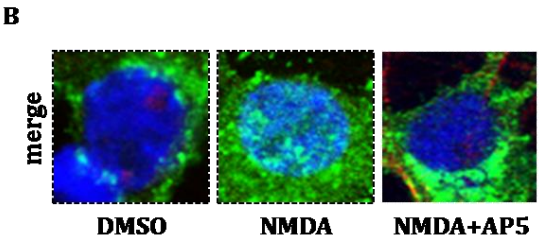
B
merge
DMSO
NMDA
NMDA+AP5

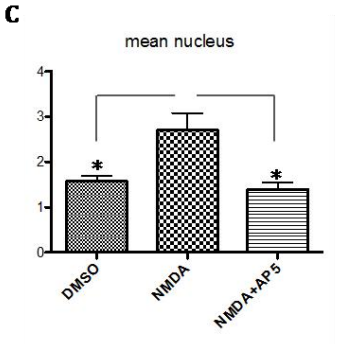
C
mean nucleus
4
3
2
1
0
*
*
DMSO
NMDA
NMDA+AP5

Figure 15: NMDA dependent nuclear localization of PCDH19 in hippocampal neurons. (A) Confocal images of hippocampal mature neurons overexpressing PCDH19, immunostained for V5, DAPI and MAP2 and acutely treated with NMDA (50μM, 30min, 37°C) or NMDA+AP5 (NMDA 50μM, AP5 100μM, 1.30 h, 37°C). PCDH19 enriched in nucleus after NMDA treatment. (B) Single stack of above neuronal nuclei showing better PCDH19 nuclear distribution after NMDA treatment. On the other hand, AP5, by blocking NMDA receptors, prevents PCDH19 enrichment in nuclear compartment. (C) Quantification analysis of PCDH19 fluorescence intensity level in nuclear compartment confirming the above observations (*p<0,05, One-Way ANOVA analysis).

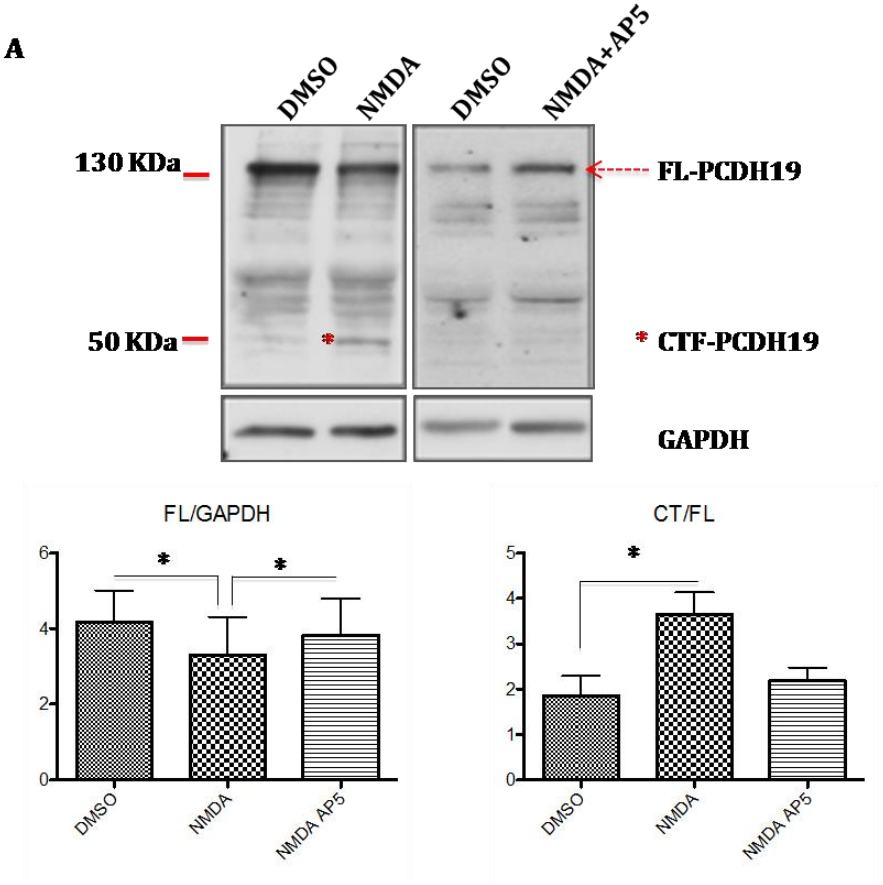
A
DMSO
NMDA
DMSO
NMDA+AP5
130 KDa
50 KDa
FL-PCDH19
* CTF-PCDH19
GAPDH
FL/GAPDH
CT/FL
DMSO
NMDA
NMDA AP5

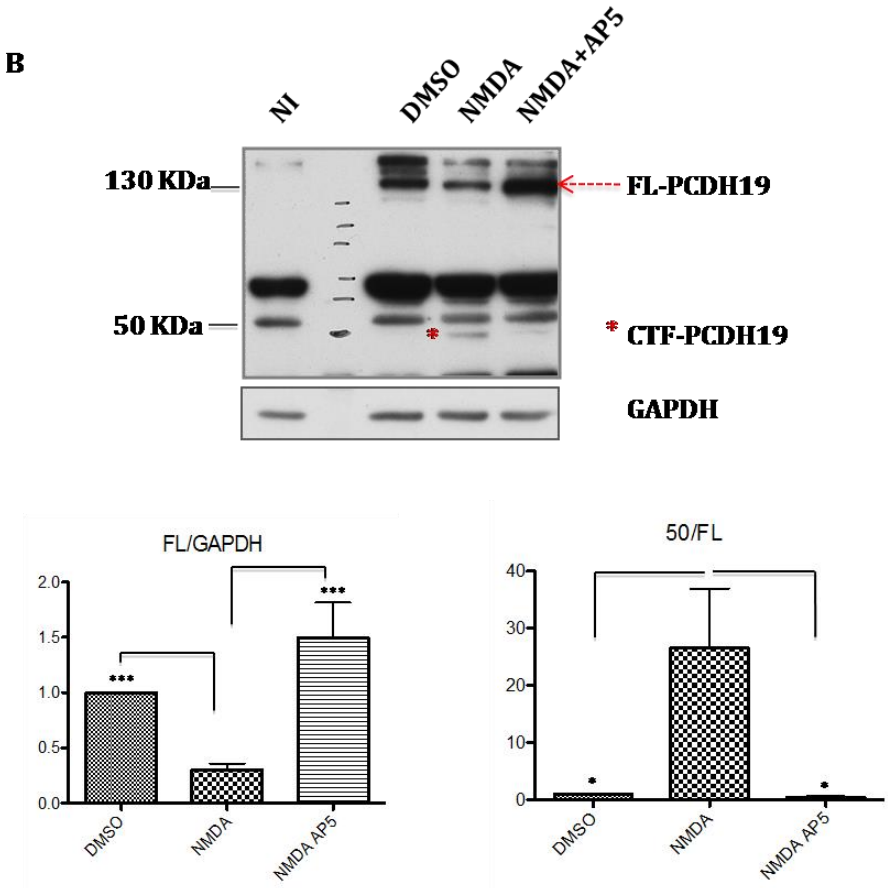
B
NI
DMSO
NMDA
NMDA+AP5
130 KDa
50 KDa
FL-PCDH19
* CTF-PCDH19
GAPDH
FL/GAPDH
50/FL
DMSO
NMDA
NMDA AP5

Figure 16: PCDH19 cleavage in hippocampal neurons is NMDA dependent. Western blot of hippocampal mature cells using antibodies against PCDH19, V5 and GAPDH to detect endogenous protein (A) or overexpressed PCDH19-V5 (B). PCDH19 full length protein is indicated by red arrow, while CTF is indicated by red asterisk. Quantification analysis (histograms below) revealed a significant decrease of PCDH19-FL and increase of CTF after NMDA treatment. PCDH19-FL and CTF levels are as control after AP5 treatments, indicating that NMDA stimulates PCDH19 cleavage and CTF release. (NMDA 50µM, 30min, 37°C; AP5 100µM, 30 min, 37°C;***p<0,0001, *p<0,05, One-Way ANOVA analysis).

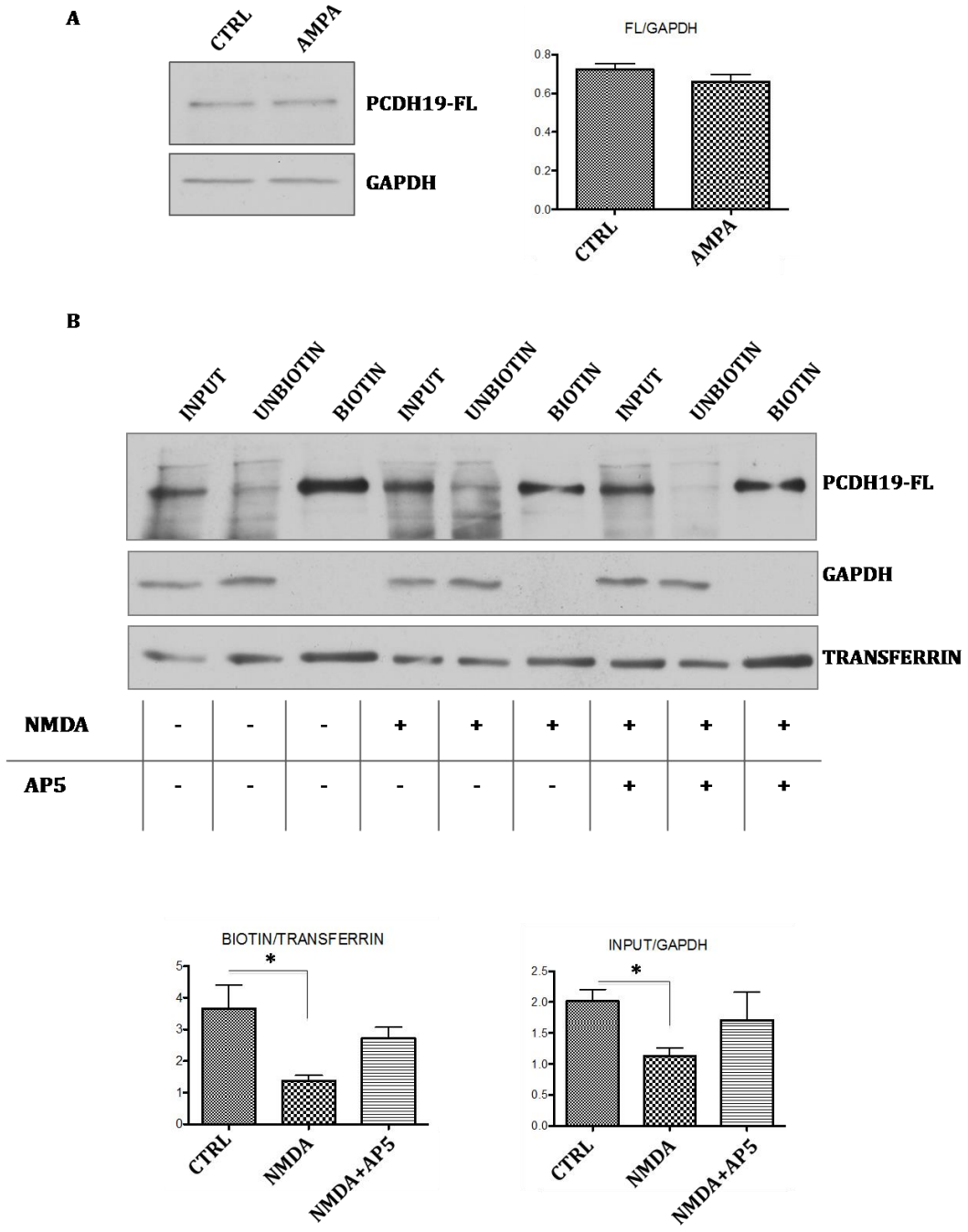
A
CTRL
AMPA
PCDH19-FL
GAPDH
FL/GAPDH
0.8
0.6
0.4
0.2
0.0
CTRL
AMPA
B
INPUT
UNBIOTIN
BIOTIN
INPUT
UNBIOTIN
BIOTIN
INPUT
UNBIOTIN
BIOTIN
PCDH19-FL
GAPDH
TRANSFERRIN
NMDA
AP5
BIOTIN/TRANSFERRIN
INPUT/GAPDH
CTRL
NMDA
NMDA+AP5

Figure 17: NMDA decreases PCDH19 neuronal surface levels. (A) Western blot of mature hippocampal neuronal cells, acutely treated with AMPA, using PCDH19 and GAPDH antibodies. Quantification analysis of PCDH19 full length protein (histogram on the right) showing that AMPA treatment doesn't reduce PCDH19-FL protein (AMPA 50μM, 30 min, 37°C). (B) Byotinilation assay on mature hippocampal neurons using anti-PCDH19 antibody, to visualize endogenous protein, anti-GAPDH and anti-transferrin to normalize input and biotinylated protein. Quantification analysis (histograms below) show a significant reduction of not only PCDH19 total protein but also PCDH19 surface levels after NMDA treatment. AP5 treatment prevents the decrease of both PCDH19 total protein and surface levels. (NMDA 50μM, AP5 100μM, 1.30 h, 37°C, *p<0,05, One-Way ANOVA analysis).

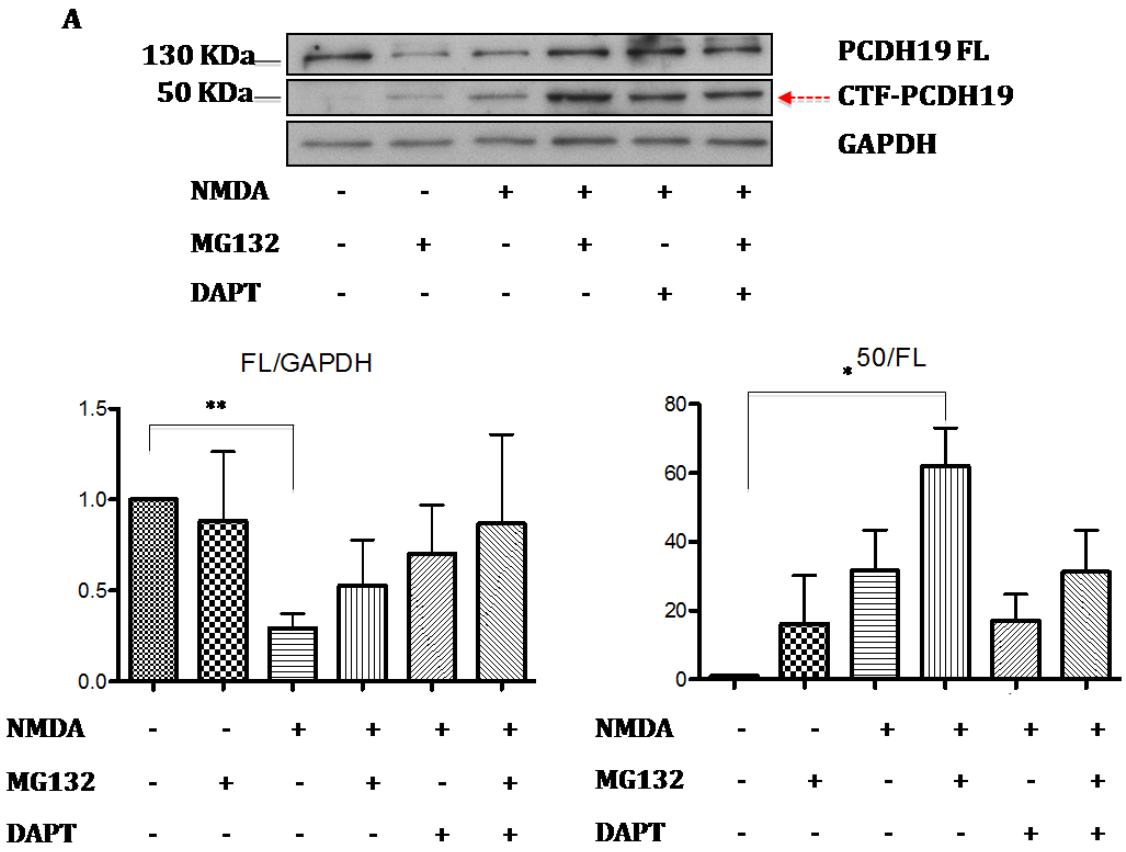
A
130 KDa
50 KDa
PCDH19 FL
CTF-PCDH19
GAPDH
NMDA - - + + + +
MG132 - + - + - +
DAPT - - - - + +
FL/GAPDH
**
1.5
1.0
0.5
0.0
50/FL
*
80
60
40
20
0
NMDA - - + + + +
MG132 - + - + - +
DAPT - - - - + +
NMDA - - + + + +
MG132 - + - + - +
DAPT - - - - + +

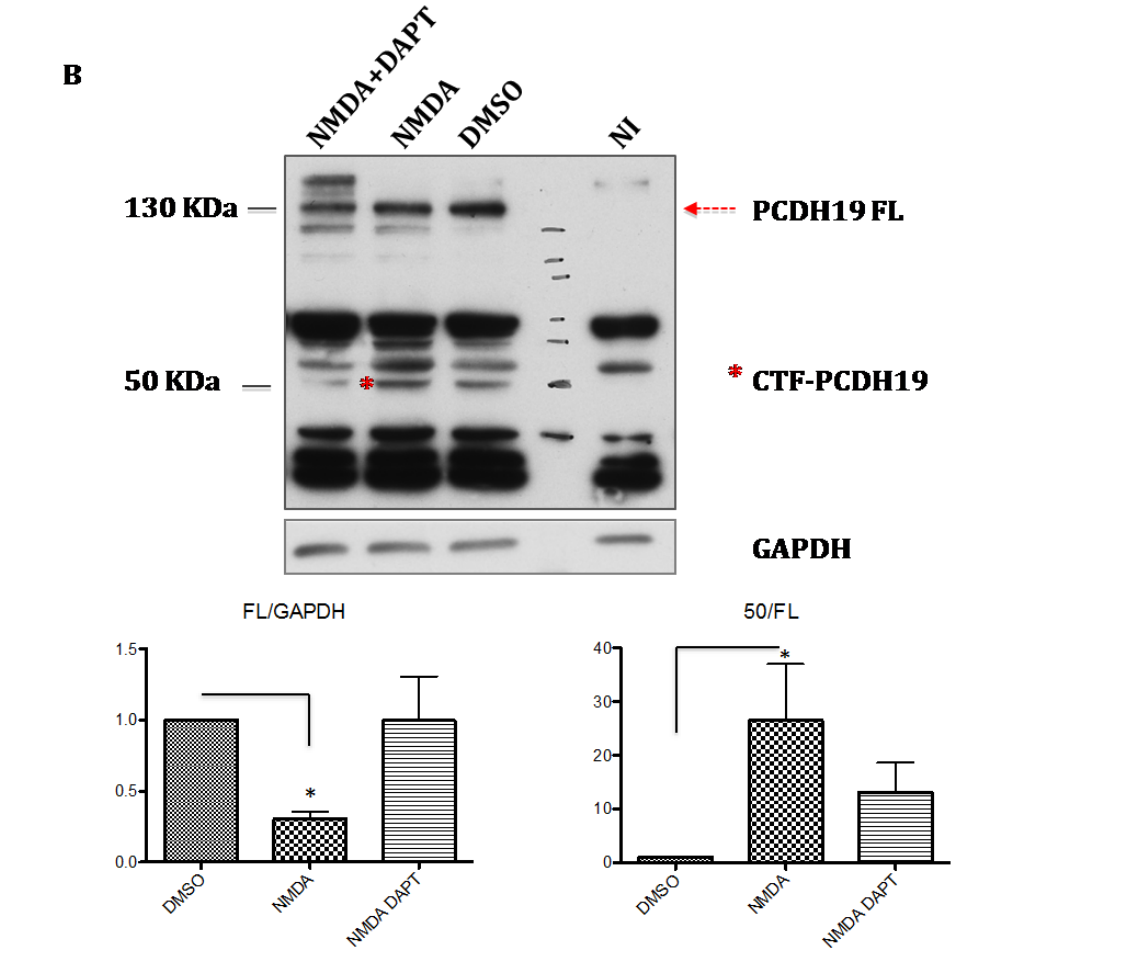
B
NMDA+DAPT
NMDA
DMSO
NI
130 KDa
50 KDa
PCDH19 FL
CTF-PCDH19
GAPDH
FL/GAPDH
1.5
1.0
0.5
0.0
*
DMSO
NMDA
NMDA DAPT
50/FL
40
30
20
10
0
*
DMSO
NMDA
NMDA DAPT

Figure 18: PCDH19 is cleaved by γ-secretase enzyme. Western blot of hippocampal mature cells using antibodies against PCDH19, V5 and GAPDH to detect endogenous protein (A) or overexpressed PCDH19-V5 (B). Cells were treated with different compound: NMDA, MG132 for endogenous protein to prevent proteasome degradation, and DAPT to inhibit γ-secretase. CTF is indicated by red arrow (A), while PCDH19-FL is indicated by red arrow and CTF by red asterisk (B). Quantification analysis (histograms below) revealed a significant decrease of PCDH19-FL and increase of CTF after NMDA treatment. PCDH19-FL and CTF levels are almost as control after DAPT treatments, indicating that γ-secretase mediates PCDH19 cleavage and CTF release. (NMDA 50µM, 30min, 37°C; MG132, DAPT 10µM, 1.30 h, 37°C;**p<0,01, *p<0,05, One-Way ANOVA analysis).

A

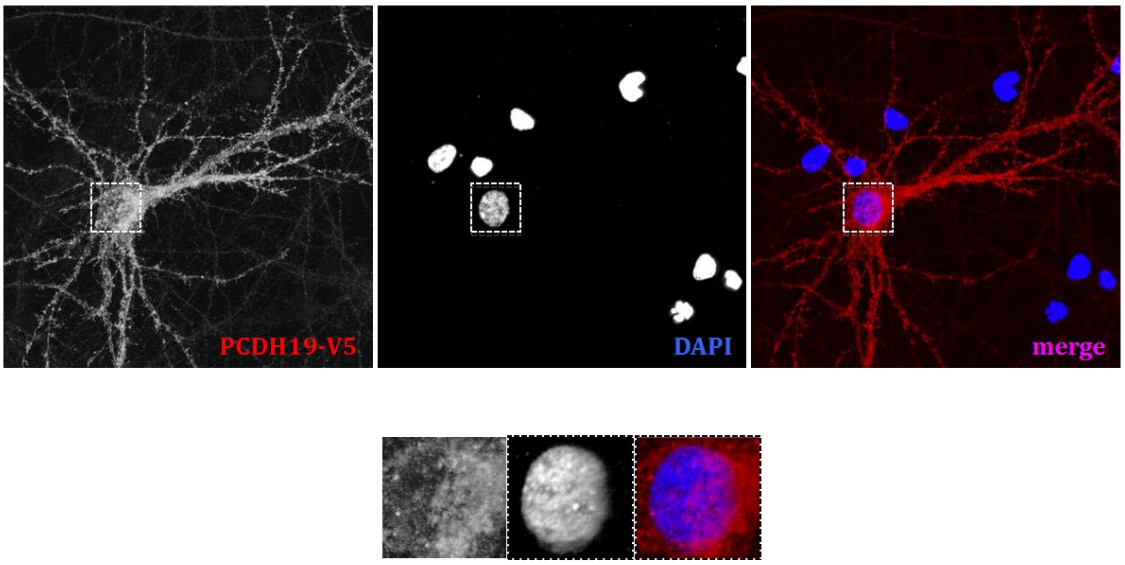

B

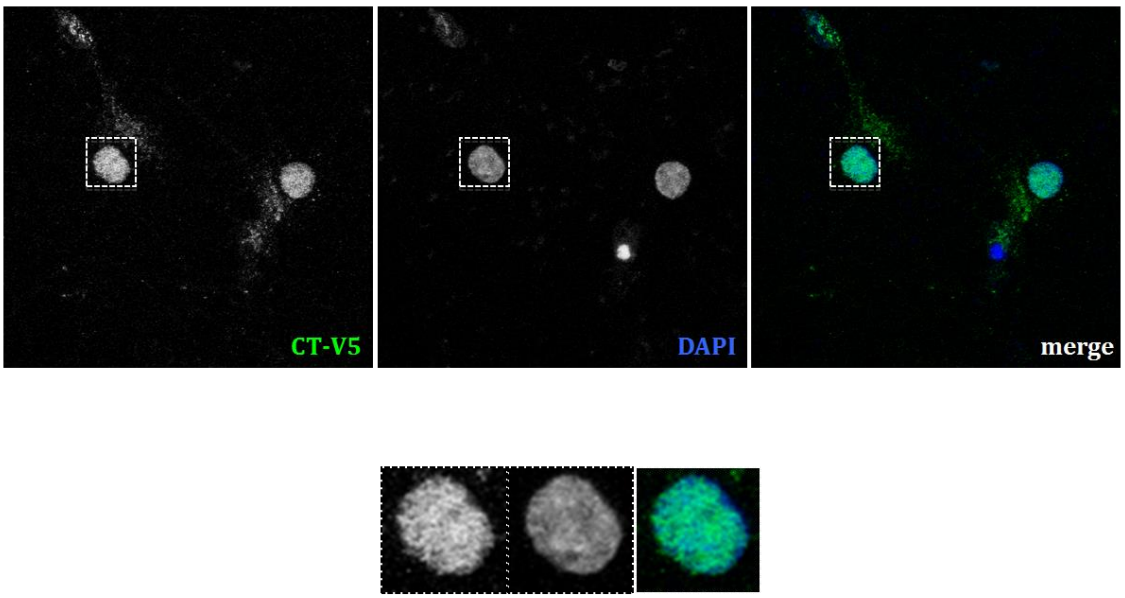

Figure 19: CTF localizes in nuclei of hippocampal neuronal cells. (A) Confocal images of hippocampal mature neurons transfected with PCDH19-V5 entire protein (A) or C terminal domain (B) and stained for V5 and DAPI. PCDH19 distributes both in cytoplasm and in nucleus (A), while CT is mainly enriched in the nucleus (B). Nuclear localizations are better shown in single stack images (boxes below confocal images). These indicates that is the C-terminal domain of PCDH19 that localizes in the nuclear compartment.

A

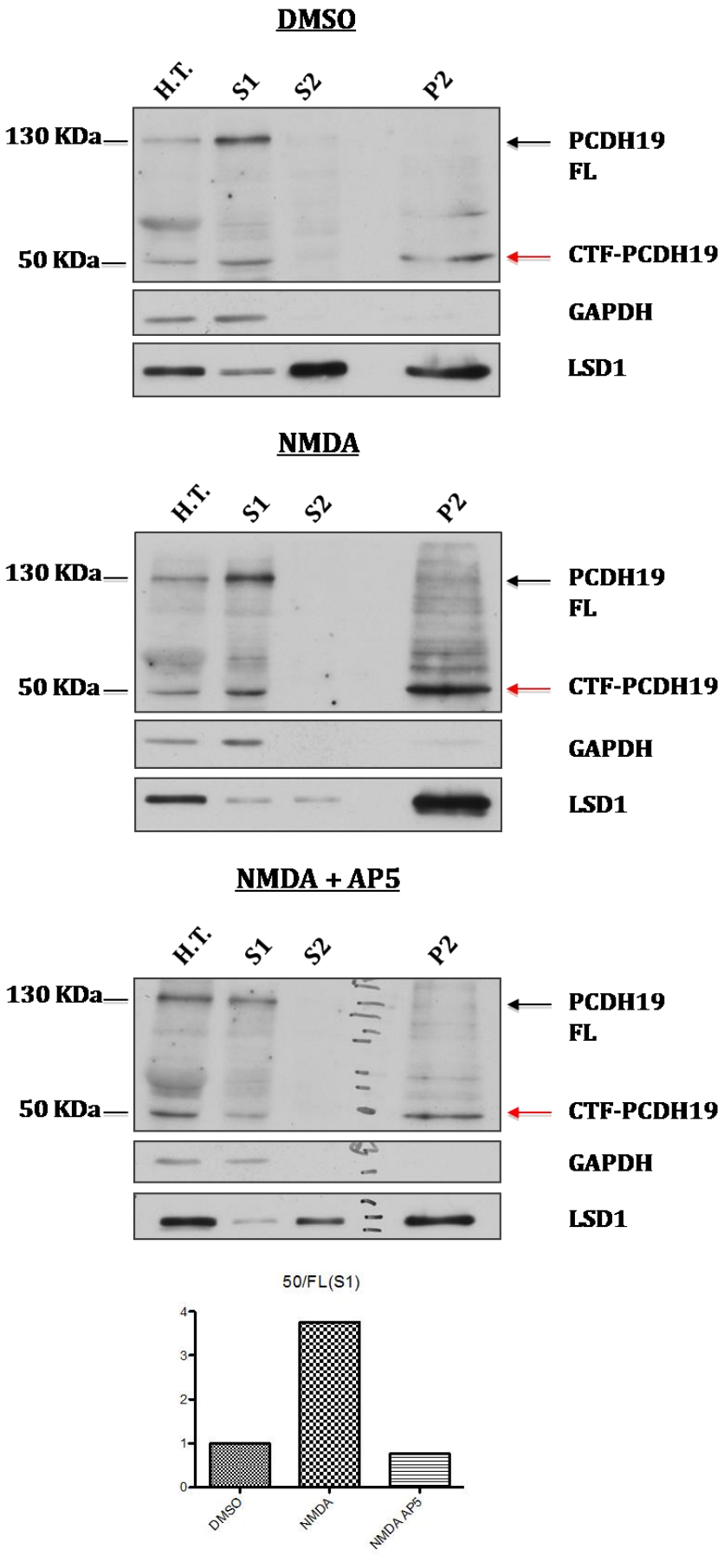
DMSO
H.T.
S1
S2
P2
130 KDa
50 KDa
PCDH19
FL
CTF-PCDH19
GAPDH
LSD1
NMDA
H.T.
S1
S2
P2
130 KDa
50 KDa
PCDH19
FL
CTF-PCDH19
GAPDH
LSD1
NMDA + AP5
H.T.
S1
S2
P2
130 KDa
50 KDa
PCDH19
FL
CTF-PCDH19
GAPDH
LSD1
50/FL(S1)
4
3
2
1
0
DMSO
NMDA
NMDA AP5

Figure 20: CTF translocates from cytoplasm to the nucleus after NMDA treatment. (A) Fractionation experiments of hippocampal neurons showing PCDH19 endogenous protein. Quantification analysis (histogram below) indicates that NMDARs activation leads to increase in CT fragment production (CT levels in P2 fraction compared PCDH19-FL in S1 fraction) that localises in P2 compartment, while AP5 treatment prevents PCDH19 cleavage. GAPDH and LSD1 are used as cytoplasmic and nuclear markers respectively. PCDH19 full-length is indicated by black arrows, while CTF is indicated by red arrows. (NMDA 50μM, AP5 100μM, 30 min, 37°C; H.T.: total homogenate; S1: membrane/cytoplasmic fraction; S2: nuclear soluble fraction; P2: nuclear insoluble fraction).

A

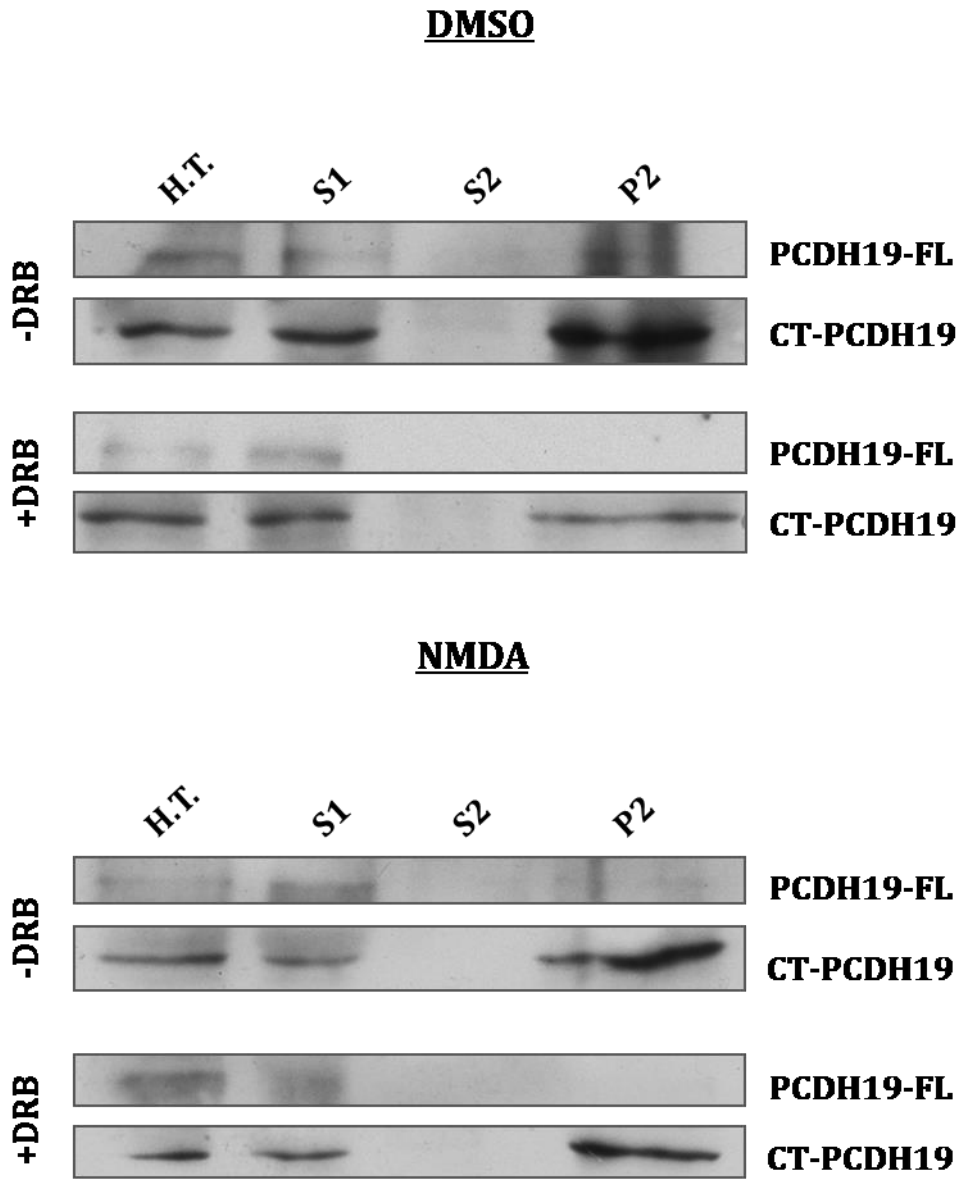
DMSO
H.T.
S1
S2
P2
-DRB
PCDH19-FL
CT-PCDH19
+DRB
PCDH19-FL
CT-PCDH19
NMDA
H.T.
S1
S2
P2
-DRB
PCDH19-FL
CT-PCDH19
+DRB
PCDH19-FL
CT-PCDH19

Figure 21: CTF produced after PCDH19 cleavage is transport from cytoplasm to nucleus. (A) Fractionation experiments of hippocampal neurons showing PCDH19 endogenous protein distributions among different fractions. Neurons were treated with NMDA to stimulate PCDH19 cleavage and with DRB to block protein transcription. Blots show that, even after DRB treatment, CTF localizes in the nuclear fraction (P2), indicating that this fragment is not a result of new protein synthesis, but, after PCDH19 cleavage, it translocates into nucleus. (DRB 10μM, 1h, 37°C, NMDA 50μM, 30 min, 37°C; H.T.: total homogenate; S1: membrane/cytoplasmic fraction; S2: nuclear soluble fraction; P2: nuclear insoluble fraction).

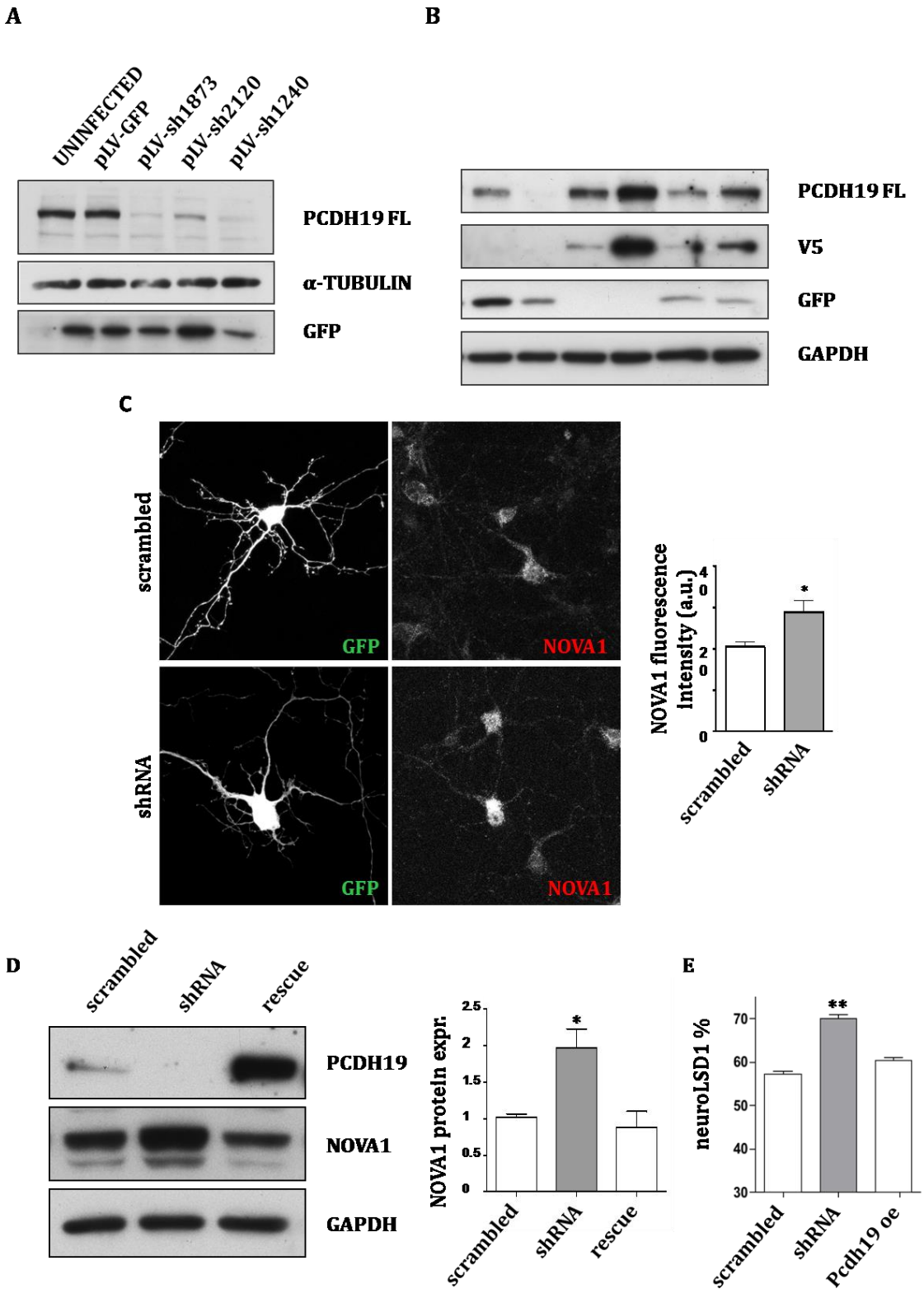
A
UNINFECTED
pLV-GFP
pLV-sh1873
pLV-sh2120
pLV-sh1240
PCDH19 FL
α-TUBULIN
GFP
B
PCDH19 FL
V5
GFP
GAPDH
C
scrambled
shRNA
GFP
NOVA1
NOVA1 fluorescence Intensity (a.u.)
scrambled
shRNA
D
scrambled
shRNA
rescue
PCDH19
NOVA1
GAPDH
NOVA1 protein expr.
scrambled
shRNA
rescue
E
neuroLSD1 %
scrambled
shRNA
Pcdh19 oe

Figure 22: Downregulation of PCDH19 in hippocampal neuronal cells increases NOVA1 and neuroLSD1 levels. Validation of PCDH19 shRNAs. Lentiviral-mediated infection of neurons with pLVTHM-GFP, pLVTHM-GFP-shRNA1873, -sh2120, -sh1240 (A) and with pLVTHM-GFP-scrambled shRNA1873, pLVTHM-GFP-shRNA1873, FuwPCDH19-V5 (B). Immunoblots refer to DIV10 cortical neurons infected at DIV3. ShRNAs downregulate PCDH19. FuwPCDH19-V5 infection rescues PCDH19 level. (C) Immunostaining of hippocampal mature neurons infected with shPCDH19 or scrambled, both expressing GFP, and marked for NOVA1 protein. The fluorescence intensity levels of NOVA1 is higher in neurons infected with shPCDH19 compared with the control expressing scrambled as shown in histogram (*p<0,05, t-test analysis). (D) These data are confirmed by western blot analyses performed on hippocampal mature neurons: there is a significant increase in NOVA1 protein levels in neurons infected with shPCDH19 compared to the two control conditions (*p<0,05, One-Way ANOVA analysis). (E) mRNA analyses of neuroLSD1 performed in hippocampal mature neurons reveal a significant increase in the ratio of neuroLSD1/LSD1 in neurons infected with shPCDH19 compared both to control condition (scrambled) and to neurons overexpressing PCDH19 (**p<0,01, One-Way ANOVA analysis).

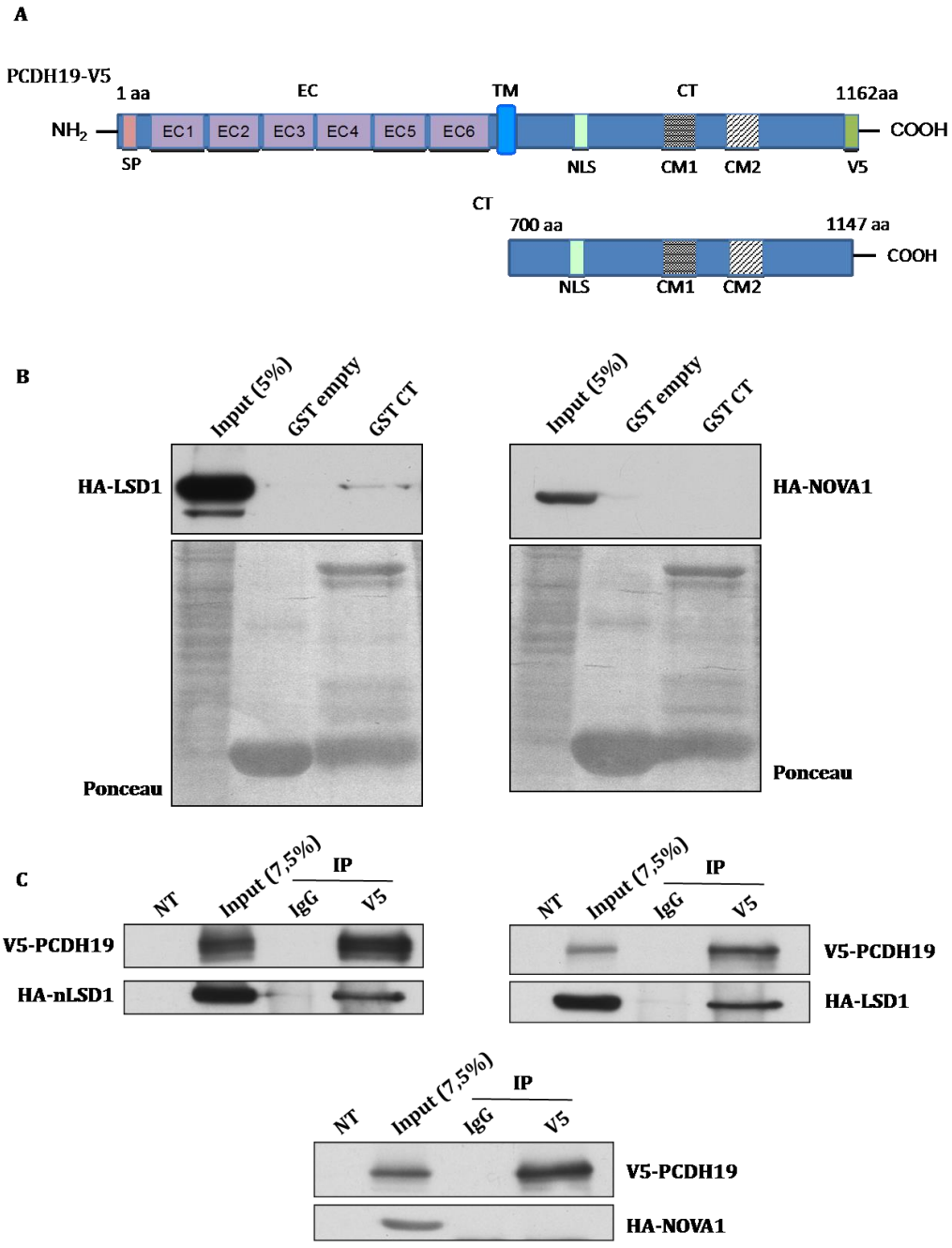
A
PCDH19-V5
1 aa
EC
TM
CT
1162aa
NH2
EC1
EC2
EC3
EC4
EC5
EC6
COOH
SP
NLS
CM1
CM2
V5
CT
700 aa
1147 aa
COOH
NLS
CM1
CM2
B
Input (5%)
GST empty
GST CT
HA-LSD1
HA-NOVA1
Ponceau
Ponceau
C
NT
Input (7,5%)
IP
IgG
V5
V5-PCDH19
HA-nLSD1
V5-PCDH19
HA-LSD1
V5-PCDH19
HA-NOVA1

Figure 23: CTF is able to interact with LSD1 and neuroLSD1 protein. (A) Schematic representation of PCDH19 used for Co-IP experiments and of C-terminal construct of PCDH19 used for Pull-down assay. (B) Pull-down assay performed in HEK293 cells transfected with LSD1-HA or NOVA1-HA. The results show that LSD1 is able to interact with the C-terminal fragment of PCDH19, while NOVA1 doesn't interact. (C) Co-immunoprecipitation experiments in HEK293 cells transfected with PCDH19-V5 and LSD1-HA, neuroLSD1-HA or NOVA1-HA. The results show that LSD1 and nLSD1 can associate with PCDH19. NOVA1 not associate with PCDH19.

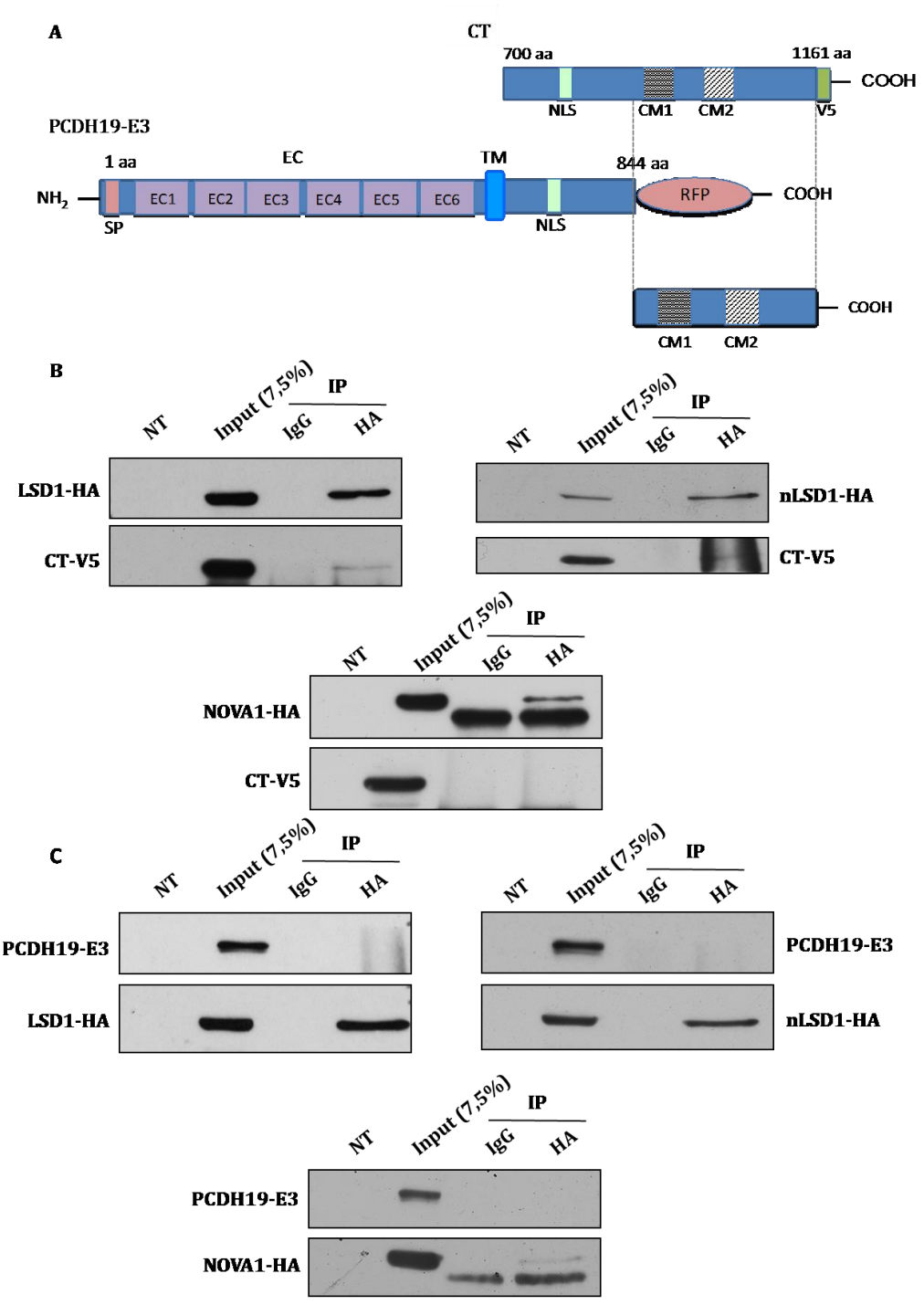
A
CT
700 aa
1161 aa
COOH
NLS
CM1
CM2
V5
PCDH19-E3
1 aa
EC
TM
844 aa
NH2
EC1
EC2
EC3
EC4
EC5
EC6
RFP
COOH
SP
NLS
COOH
CM1
CM2
B
NT
Input (7,5%)
IP
IgG
HA
LSD1-HA
CT-V5
nLSD1-HA
CT-V5
NOVA1-HA
CT-V5
C
PCDH19-E3
LSD1-HA
PCDH19-E3
nLSD1-HA
PCDH19-E3
NOVA1-HA

Figure 24: Reduction of CTF interacting portion with neuroLSD1 and LSD1. (A) Schematic representation of CTF and PCDH19Δ844-1161 (PCDH19-E3) used for Co-IP experiments and of the resulting interacting part of PCDH19. Co-immunoprecipitation experiments in HEK293 cells transfected with LSD1-HA, neuroLSD1-HA or NOVA1-HA and CT-V5 (B) or PCDH19-E3 (C). The results show that LSD1 and neuroLSD1 can associate with CT but not with PCDH19-E3 reducing the interacting part of CT.

A

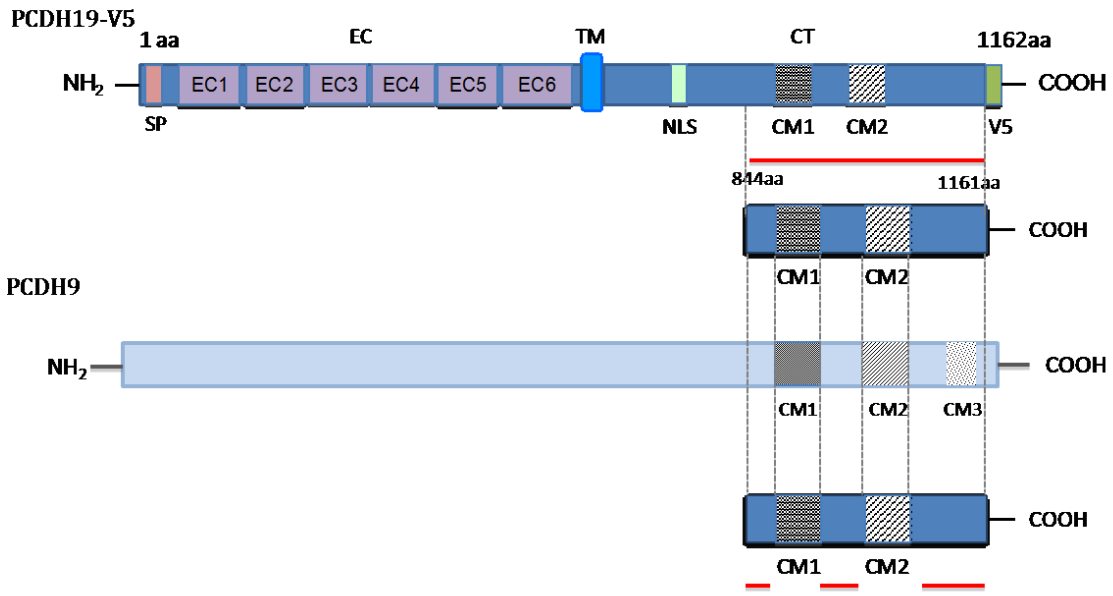
PCDH19-V5
1 aa
EC
TM
CT
1162aa
NH2
EC1
EC2
EC3
EC4
EC5
EC6
COOH
SP
NLS
CM1
CM2
V5
844aa
1161aa
COOH
CM1
CM2
PCDH9
NH2
COOH
CM1
CM2
CM3
COOH
CM1
CM2

B

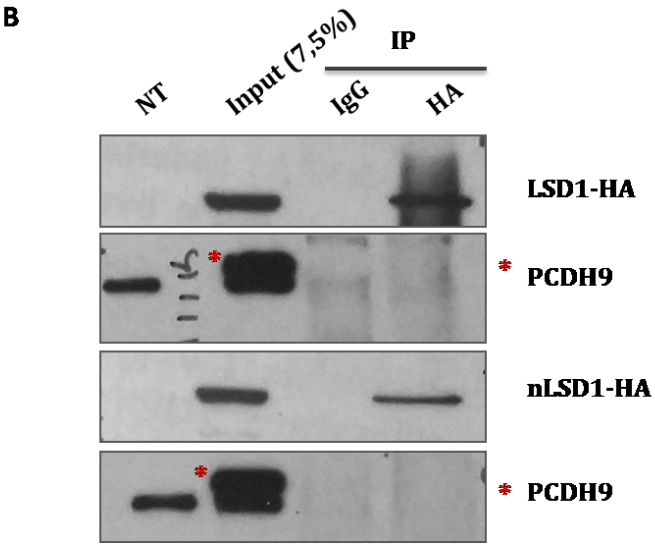
NT
Input (7,5%)
IP
IgG
HA
LSD1-HA
PCDH9
nLSD1-HA
PCDH9

Figure 25: Reduction of CTF interacting portion with neuroLSD1 and LSD1. (A) Schematic representation of PCDH9 used for Co-IP experiments and of the resulting interacting part of PCDH19. Co-immunoprecipitation experiments in HEK293 cells transfected with PCDH9 and LSD1-HA or neuroLSD1-HA. Red asterisks indicate PCDH9 specific band. The results show that LSD1 and neuroLSD1 cannot associate with PCDH9, those excluding the common motifs (CM1 and CM2) in the interaction.

A

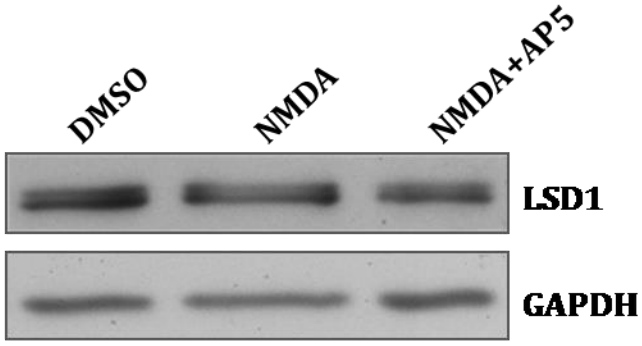
DMSO
NMDA
NMDA+AP5
LSD1
GAPDH

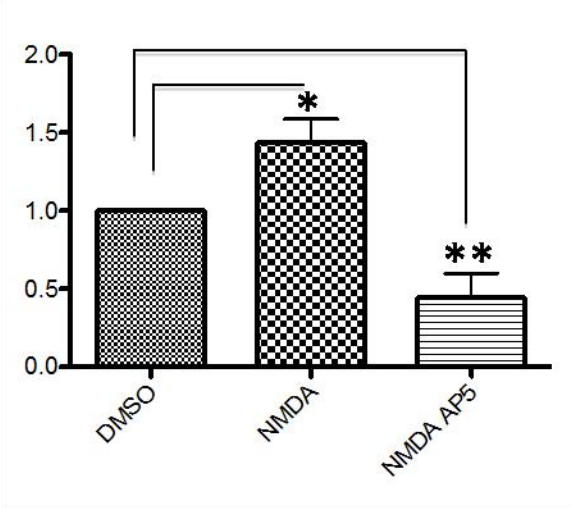
2.0
1.5
1.0
0.5
0.0
*
**
DMSO
NMDA
NMDA AP5

B

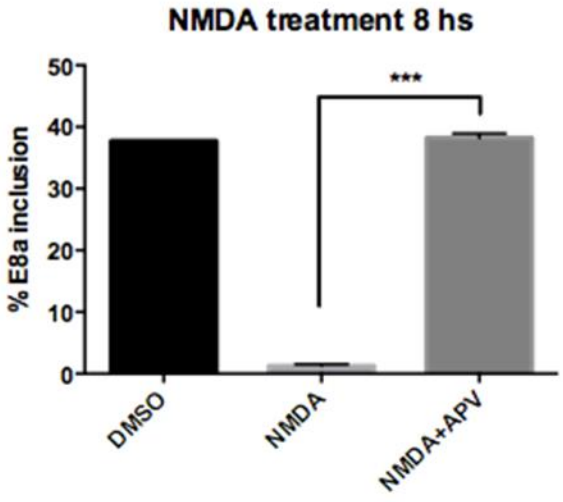
NMDA treatment 8 hs
% E8a inclusion
50
40
30
20
10
0
***
DMSO
NMDA
NMDA+APV

Figure 26: neuroLSD1 splicing is regulated by NMDA. (A) Western blot of mature hippocampal neurons treated with the compound that stimulates PCDH19 cleavage and using anti-LSD1 antibody. Histogram show that after NMDA treatment there is a significant increase in LSD1 protein levels, while AP5 prevents this increase (**p<0,01, *p<0,05, One-Way ANOVA analysis). (B) mRNA analyses of neuroLSD1 performed in hippocampal mature neurons reveal a significant decrease in the ratio of neuroLSD1/LSD1 in neurons treated with NMDA compared both to control condition and to neurons treated with AP5 (***p<0,0001, One-Way ANOVA analysis).

6. DISCUSSION

PCDH19 gene was identified in 2008 as the causative gene of PCDH19-FLE and is now considered the second gene, after the Dravet syndrome gene SCN1A, most clinically relevant in epilepsy (Dibbens, Tarpey et al. (2008)).
To date, little is known about PCDH19 biological functions and about the mechanisms that give rise to the pathology, which precludes effective therapy.

Our work is aimed to investigate PCDH19 physiological functions in order to understand the molecular pathways that are impaired in patients and highlight new therapeutic targets.

In particular, in this work we demonstrated that PCDH19 is highly expressed in cortex and hippocampus and localizes at synapses. Further, we found that it is detectable in immature and mature hippocampal neurons, both in inhibitory and excitatory cells, suggesting different roles for the protein during neuronal development and neuronal network formation as well as in synaptic function.
Importantly, we revealed through this work a new PCDH19 feature. Indeed, we demonstrated that, after neuronal activation mediated by NMDA receptors, PCDH19 is cleaved by γ-secretase and releases its C-terminal domain that is targeted to the nucleus probably to regulate gene expression.
Further, we identified two putative interactors of PCDH19-CTF, LSD1 and neuroLSD1. These two splicing isoforms of LSD1, upon their association with different complexes, solve crucial roles in the transcription regulation of several target genes mainly involved in the maintenance of homeostatic balance between neuronal inhibition and excitation Rusconi, Paganini et al. (2015).

6.1 PCDH19 protein expression and its involvement in PCDH19-FLE pathology

Since little is known about PCDH19, we firstly investigated its expression in brain and found that it is enriched in hippocampus and cortex and in crude synaptosomes of hippocampal neurons. PCDH19-FLE pathology is characterized by several clinical

features, including epilepsy, cognitive impairments, behavioral disturbances and autism that exhibits different phenotypic degrees in patients (Scheffer, Turner et al. 2008). Our findings regarding PCDH19 expression are in line with these clinical aspects, further suggesting an involvement of the protein in cognitive processes. To go deeper into neuronal functions of PCDH19, we found that it is expressed both in immature and mature neurons and in inhibitory and excitatory neuronal cells. These results suggest that the protein could be involved in several roles according to the type of neurons in which it is expressed and the developmental period. One important feature of FLE is the onset of epileptic seizures during infancy and childhood, suggesting a defect in inhibitory/excitatory circuitry caused by PCDH19 gene mutations (Scheffer, Turner et al. 2008). PCDH19 is probably involved in the maintenance of neuronal excitatory and inhibitory balance. Further, PCDH19 presence in immature neurons evoked an important role of this protein during neuronal development for circuit formation, in particular it could be fundamental for correct synaptogenesis, such as other cadherins like N-Cadherin (Frank and Kemler 2002).

One model that tries to explain the unusual manifestation pattern of PCDH19-FLE pathology is the "cellular interference", that considers the cell-cell scrambled communication due to tissue mosaicism as the principal cause of the pathology (Depienne, Bouteiller et al. 2009). In line with this model we demonstrated that PCDH19 protein is expressed on the plasma membrane, in particular at cell-cell contacts, suggesting an important role of PCDH19 in intercellular adhesion.

6.2 PCDH19 is cleaved in an activity-dependent manner by γ-secretase enzyme

PCDH19 belongs to the δ2-protocadherins subfamily. Little is known about the neuronal roles of these proteins. However, protocadherins appear to be important for circuit and synapse formation through their adhesive properties. Recent studies reveal a new intracellular role of some cadherins and protocadherins and focus their attention on intracellular signaling (Depienne, Gourfinkel-An et al. 2012). There are evidences that protocadherins, besides their cell-cell adhesion functions, play

important role at intracellular and nuclear levels. In particular, they exert this action through a proteolytic process, a mechanism that has been observed for some cadherins such as N-cadherin, E-cadherin and γ-protocadherins which are cleaved both exctracellularly and intracellularly by different enzymes (Junghans, Haas et al. 2005).

In this work we demonstrated that also PCDH19 protein is cleaved intracellularly by γ-secretase both in heterologous systems and in hippocampal neuronal cells. PCDH19 cleavage leads to the release of its C-terminal domain, which is difficult to detect since it is rapidly degradated by proteasome. Interestingly, we showed that PCDH19 proteolytic process depends on NMDA receptors activation. In line with this evidence, recent studies showed that γ-secretase complex is also located at synaptic sites and its action could be stimulated by NMDA receptors activity (Thompson, Otis et al. 2004).

These findings lead to a new territory of investigation for PCDH19 functions. Further, the observation that the cleavage depends on neuronal activity suggests that PCDH19 has a role in transducing external stimuli to intracellular responses. This was demonstrated for other cadherins, such as N-cadherin and γ-protocadherins, that, after NMDA stimuli, undergo proteolytic cleavage and release their cytoplasmic domains which could solve intracellular signaling roles (Junghans, Haas et al. 2005). We also demonstrated that NMDA activity stimulating PCDH19 cleavage leads to a decrease in the full-length form of the protein present at membrane surface, suggesting that consequence of the neuronal activity is the reduction of PCDH19-mediated adhesion. However, it is important to investigate more the extracellular domain of the protein to define its roles, analyzing the consequences of the cleavage. The proteolytic cleavage is usually characterized by two steps: the first one is mediated by metalloproteases and occurs at extracellular level; the second one is mediate by γ-secretase and occurs at intracellular level. Those it would be interesting to know which metalloproteases act on the extracellular domain of PCDH19 and if the domain is released in the extracellular space to interact with other proteins or simply degradated.

6.3 C-terminal domain of PCDH19 goes from cytoplasm to nucleus in response to neuronal activity

After we established that PCDH19 is cleaved by γ-secretase after NMDA receptors activity and, as a consequence, its C-terminal domain is released, we focused our attention on the roles of this fragment. In particular, since it contains a NLS, we investigated its nuclear localization. Firstly, we demonstrated that NMDARs activity regulates PCDH19 distribution in neuronal cells. Indeed, the protein, detected by an antibody specifically directed to PCDH19 C-terminal domain, localizes more in the nuclear compartment when neurons are stimulated by NMDA. Then, we showed that is the C-terminal domain of PCDH19 that enters the nucleus after neuronal activity and cleavage mediated by γ-secretase.

For neuronal cells it is crucial to converge and integrate in the nucleus synaptic signal to determine a genomic response able to solve proper neuronal functions such as development, plasticity and survival. Recently, it has been shown that synaptic proteins entering the nuclear compartment after neuronal activity play important role in synapse-to-nucleus communications (West, Griffith et al. 2002, Deisseroth, Mermelstein et al. 2003, Thompson, Otis et al. 2004, Greer and Greenberg 2008).

Our results revealed a completely new role of PCDH19 protein. In particular we demonstrated that PCDH19, through its C-terminal domain, is able to connect an external stimulus from synaptic compartments, where it is located, to the nucleus of the cells probably in order to regulate gene expression in response to neuronal activity. Further, we demonstrated that CTF, which accumulates in the nucleus after NMDA receptors activation, is not the product of new protein synthesis, but is likely the result of a transport from synapse to the nucleus of neuronal cells. Thus, we could speculate that PCDH19-CTF is a new protein messenger with a role in synapse-to-nucleus communication linking neuronal activity with transcriptional regulation. It is fundamental to investigate what genes it regulates in order to clarify PCDH19 functions, in particular which pathways could be impaired in PCHD19-FLE pathology.

6.4 PCDH19-CTF is part of LSD1/neuroLSD1 complex and regulates gene expression

Final experiments of this work aimed to discover nuclear functions of PCDH19. We demonstrated that downregulation of PCDH19 protein mediated by shRNA expression in neuronal cells, in order to mimic pathological conditions, increases NOVA1 protein levels and neuroLSD1 mRNA levels.

NOVA1, LSD1 and neuroLSD1 are important elements both for the correct neuronal development and for the maintenance of excitatory/inhibitory neuronal balance. NOVA1 promotes neuroLSD1 splicing isoform, which, together with different partners, regulates gene expression. In particular, by histone epigenetic modifications, it activates transcriptions of neuronal genes involved in the maintenance of excitatory/inhibitory balance. It also acts as a corepressor factor for LSD1, which repress gene transcription. High levels of neuroLSD1 result in increased neuronal excitability. In order to clarify the role of LSD1/neuroLSD1, it has been used a mouse model that completely lacks neuroLSD1 isoform expression. The authors demonstrated that these mice were protected from the onset of epileptic seizures (Rusconi, Paganini et al. 2015).

Since we demonstrated that the downregulation of PCDH19 alters NOVA1 and neuroLSD1 expression levels, we propose two hypothesis: the first one considers PCDH19 as a transcriptional regulator of genes encoding for these two elements, thus, when there is less PCDH19 there is an imbalance in NOVA1 and neuroLSD1 transcripts level; in the second hypothesis, we consider PCDH19 protein as a cofactor of neuroLSD1 that could act on regulation of gene transcription, and loss of function of PCDH19 could leads to a deficit in appropriate chromatin modifications that create, as a loop, an imbalance in neuroLSD1 transcripts level.

To investigate if these hypotheses could be both or just one true, we analyzed deeply PCDH19 protein interactions. In particular, we found that PCDH19 C-terminal domain is able to specifically interact with both LSD1 and neuroLSD1 isoform, at least in heterologous systems. These results suggest the existence of a complex with PCDH19 and LSD1/neuroLSD1, but we cannot exclude also the first hypothesis. More

experiments have to be done in order to clarify the mechanism of action that connects PCDH19-CTF with LSD1/neuroLSD1.

Further, we observed that the same neuronal activity that regulates PCDH19 cleavage (acute treatments with NMDA) is able to regulate neuroLSD1 transcript levels, drastically reducing its expression as a regulatory negative feedback: the more neuronal activity is present, the less neuroLSD1 isoform is produced in order to restore neuronal cells into a homeostatic state regarding its excitability. These findings suggest that the CTF produced after strong NMDA stimuli could solve a crucial role in this regulatory mechanism, through the interaction with LSD1 and neuroLSD1 elements.

These findings lead to hypothesize that in patients the absence of PCDH19 determines an increase in neuroLSD1 levels and, as a consequence, in neuronal excitability. Further, the same neuronal activity that stimulates PCDH19 cleavage decreases neuroLSD1 levels, acting as a regulatory negative feedback that decrease neuronal excitability. Thus the presence of PCDH19 and the release of its C-terminal domain after cleavage seem to be fundamental in the regulation of neuronal homeostasis. Neuronal cells without PCDH19 have impairment in the regulation of excitability that can lead to an excitation/inhibition imbalance in the whole neuronal network.

7. CONCLUSIONS AND FUTURE PERSPECTIVES

In this work we found a completely new role of PCDH19 protein, demonstrating that it is cleaved after NMDA receptors activity and the released C-terminal domain enters the nucleus. Thus, PCDH19-CTF becomes an important element in synapse-to-nucleus communications and probably regulates gene expression in response to neuronal activity. Further, we found a pathway in which CTF could be involved, related to LSD1/neuroLSD1 transcription factors. These findings improve the knowledge of PCDH19-FLE pathological mechanisms. Now, it is fundamental to investigate the CTF target genes, taking advantages of microarray techniques, in order to amplify the knowledge on the pathways in which PCDH19 could play a role. Once we obtain these results, it would be interesting to investigate if these pathways are impaired in pathological conditions. This information would facilitate the identification of new therapeutic targets.

8. BIBLIOGRAPHY

Adams, J. P. and S. M. Dudek (2005). "Late-phase long-term potentiation: getting to the nucleus." Nat Rev Neurosci **6**(9): 737-743.

Baki, L., P. Marambaud, S. Efthimiopoulos, A. Georgakopoulos, P. Wen, W. Cui, J. Shioi, E. Koo, M. Ozawa, V. L. Friedrich, Jr. and N. K. Robakis (2001). "Presenilin-1 binds cytoplasmic epithelial cadherin, inhibits cadherin/p120 association, and regulates stability and function of the cadherin/catenin adhesion complex." Proc Natl Acad Sci U S A **98**(5): 2381-2386.

Ballas, N., E. Battaglioli, F. Atouf, M. E. Andres, J. Chenoweth, M. E. Anderson, C. Burger, M. Moniwa, J. R. Davie, W. J. Bowers, H. J. Federoff, D. W. Rose, M. G. Rosenfeld, P. Brehm and G. Mandel (2001). "Regulation of neuronal traits by a novel transcriptional complex." Neuron **31**(3): 353-365.

Bengtson, C. P., H. E. Freitag, J. M. Weislogel and H. Bading (2010). "Nuclear calcium sensors reveal that repetition of trains of synaptic stimuli boosts nuclear calcium signaling in CA1 pyramidal neurons." Biophys J **99**(12): 4066-4077.

Biswas, S., M. R. Emond and J. D. Jontes (2010). "Protocadherin-19 and N-cadherin interact to control cell movements during anterior neurulation." J Cell Biol **191**(5): 1029-1041.

Brewer, G. J., J. R. Torricelli, E. K. Evege and P. J. Price (1993). "Optimized survival of hippocampal neurons in B27-supplemented Neurobasal, a new serum-free medium combination." J Neurosci Res **35**(5): 567-576.

Buckanovich, R. J., J. B. Posner and R. B. Darnell (1993). "Nova, the paraneoplastic Ri antigen, is homologous to an RNA-binding protein and is specifically expressed in the developing motor system." Neuron **11**(4): 657-672.

Chen, Y., Y. Yang, F. Wang, K. Wan, K. Yamane, Y. Zhang and M. Lei (2006). "Crystal structure of human histone lysine-specific demethylase 1 (LSD1)." Proc Natl Acad Sci U S A **103**(38): 13956-13961.

Cosker, K. E., S. L. Courchesne and R. A. Segal (2008). "Action in the axon: generation and transport of signaling endosomes." Curr Opin Neurobiol **18**(3): 270-275.

Dallman, J. E., J. Allopenna, A. Bassett, A. Travers and G. Mandel (2004). "A conserved role but different partners for the transcriptional corepressor CoREST in fly and mammalian nervous system formation." J Neurosci **24**(32): 7186-7193.

Dalva, M. B., A. C. McClelland and M. S. Kayser (2007). "Cell adhesion molecules: signalling functions at the synapse." Nat Rev Neurosci **8**(3): 206-220.

De Strooper, B., P. Saftig, K. Craessaerts, H. Vanderstichele, G. Guhde, W. Annaert, K. Von Figura and F. Van Leuven (1998). "Deficiency of presenilin-1 inhibits the normal cleavage of amyloid precursor protein." Nature **391**(6665): 387-390.

Deisseroth, K., P. G. Mermelstein, H. Xia and R. W. Tsien (2003). "Signaling from synapse to nucleus: the logic behind the mechanisms." Curr Opin Neurobiol **13**(3): 354-365.

Delcroix, J. D., J. S. Valletta, C. Wu, S. J. Hunt, A. S. Kowal and W. C. Mobley (2003). "NGF signaling in sensory neurons: evidence that early endosomes carry NGF retrograde signals." Neuron **39**(1): 69-84.

Depienne, C., D. Bouteiller, B. Keren, E. Cheuret, K. Poirier, O. Trouillard, B. Benyahia, C. Quelin, W. Carpentier, S. Julia, A. Afenjar, A. Gautier, F. Rivier, S. Meyer, P. Berquin, M. Helias, I. Py, S. Rivera, N. Bahi-Buisson, I. Gourfinkel-An, C. Cazeneuve, M. Ruberg, A. Brice, R. Nabbout and E. Leguern (2009). "Sporadic infantile epileptic encephalopathy caused by mutations in PCDH19 resembles Dravet syndrome but mainly affects females." PLoS Genet **5**(2): e1000381.

Depienne, C., I. Gourfinkel-An, S. Baulac and E. LeGuern (2012). Genes in infantile epileptic encephalopathies. Jasper's Basic Mechanisms of the Epilepsies. J. L. Noebels, M. Avoli, M. A. Rogawski, R. W. Olsen and A. V. Delgado-Escueta. Bethesda (MD).

Depienne, C. and E. LeGuern (2012). "PCDH19-related infantile epileptic encephalopathy: an unusual X-linked inheritance disorder." Hum Mutat **33**(4): 627-634.

Depienne, C., O. Trouillard, I. Gourfinkel-An, C. Saint-Martin, D. Bouteiller, D. Graber, M. A. Barthez-Carpentier, A. Gautier, N. Villeneuve, C. Dravet, M. O. Livet, C. Rivier-Ringenbach, C. Adam, S. Dupont, S. Baulac, D. Heron, R. Nabbout and E. Leguern (2010). "Mechanisms for variable expressivity of inherited SCN1A mutations causing Dravet syndrome." J Med Genet **47**(6): 404-410.

Dibbens, L. M., P. S. Tarpey, K. Hynes, M. A. Bayly, I. E. Scheffer, R. Smith, J. Bomar, E. Sutton, L. Vandeleur, C. Shoubridge, S. Edkins, S. J. Turner, C. Stevens, S. O'Meara, C. Tofts, S. Barthorpe, G. Buck, J. Cole, K. Halliday, D. Jones, R. Lee, M. Madison, T. Mironenko, J. Varian, S. West, S. Widaa, P. Wray, J. Teague, E. Dicks, A. Butler, A. Menzies, A. Jenkinson, R. Shepherd, J. F. Gusella, Z. Afawi, A. Mazarib, M. Y. Neufeld, S. Kivity, D. Lev, T. Lerman-Sagie, A. D. Korczyn, C. P. Derry, G. R. Sutherland, K. Friend, M. Shaw, M. Corbett, H. G. Kim, D. H. Geschwind, P. Thomas, E. Haan, S. Ryan, S. McKee, S. F. Berkovic, P. A. Futreal, M. R. Stratton, J. C. Mulley and J. Gecz (2008). "X-linked protocadherin 19 mutations cause female-limited epilepsy and cognitive impairment." Nat Genet **40**(6): 776-781.

Dieterich, D. C., A. Karpova, M. Mikhaylova, I. Zdobnova, I. Konig, M. Landwehr, M. Kreutz, K. H. Smalla, K. Richter, P. Landgraf, C. Reissner, T. M. Boeckers, W. Zuschratter, C. Spilker, C. I. Seidenbecher, C. C. Garner, E. D. Gundelfinger and M. R. Kreutz (2008). "Caldendrin-Jacob: a protein liaison that couples NMDA receptor signalling to the nucleus." PLoS Biol **6**(2): e34.

Dimova, P. S., A. Kirov, A. Todorova, T. Todorov and V. Mitev (2012). "A novel PCDH19 mutation inherited from an unaffected mother." Pediatr Neurol **46**(6): 397-400.

Duszyc, K., I. Terczynska and D. Hoffman-Zacharska (2015). "Epilepsy and mental retardation restricted to females: X-linked epileptic infantile encephalopathy of unusual inheritance." J Appl Genet **56**(1): 49-56.

Emond, M. R., S. Biswas, C. J. Blevins and J. D. Jontes (2011). "A complex of Protocadherin-19 and N-cadherin mediates a novel mechanism of cell adhesion." J Cell Biol **195**(7): 1115-1121.

Eom, T., C. Zhang, H. Wang, K. Lay, J. Fak, J. L. Noebels and R. B. Darnell (2013). "NOVA-dependent regulation of cryptic NMD exons controls synaptic protein levels after seizure." Elife **2**: e00178.

Forneris, F., C. Binda, E. Battaglioli and A. Mattevi (2008). "LSD1: oxidative chemistry for multifaceted functions in chromatin regulation." Trends Biochem Sci **33**(4): 181-189.

Frank, M. and R. Kemler (2002). "Protocadherins." Curr Opin Cell Biol **14**(5): 557-562.

Fuentes, P., J. Canovas, F. A. Berndt, S. C. Noctor and M. Kukuljan (2012). "CoREST/LSD1 control the development of pyramidal cortical neurons." Cereb Cortex **22**(6): 1431-1441.

Gaitan, Y. and M. Bouchard (2006). "Expression of the delta-protocadherin gene Pcdh19 in the developing mouse embryo." Gene Expr Patterns **6**(8): 893-899.

Gayet, O., V. Labella, C. E. Henderson and S. Kallenbach (2004). "The b1 isoform of protocadherin-gamma (Pcdhgamma) interacts with the microtubule-destabilizing protein SCG10." FEBS Lett **578**(1-2): 175-179.

Georgakopoulos, A., P. Marambaud, S. Efthimiopoulos, J. Shioi, W. Cui, H. C. Li, M. Schutte, R. Gordon, G. R. Holstein, G. Martinelli, P. Mehta, V. L. Friedrich, Jr. and N. K. Robakis (1999). "Presenilin-1 forms complexes with the cadherin/catenin cell-cell adhesion system and is recruited to intercellular and synaptic contacts." Mol Cell **4**(6): 893-902.

Georgakopoulos, A., P. Marambaud, V. L. Friedrich, Jr., J. Shioi, S. Efthimiopoulos and N. K. Robakis (2000). "Presenilin-1: a component of synaptic and endothelial adherens junctions." Ann N Y Acad Sci **920**: 209-214.

Golde, T. E., Y. Ran and K. M. Felsenstein (2012). "Shifting a complex debate on gamma-secretase cleavage and Alzheimer's disease." EMBO J **31**(10): 2237-2239.

Greer, P. L. and M. E. Greenberg (2008). "From synapse to nucleus: calcium-dependent gene transcription in the control of synapse development and function." Neuron **59**(6): 846-860.

Gu, Y., H. Misonou, T. Sato, N. Dohmae, K. Takio and Y. Ihara (2001). "Distinct intramembrane cleavage of the beta-amyloid precursor protein family resembling gamma-secretase-like cleavage of Notch." J Biol Chem **276**(38): 35235-35238.

Guy, J., B. Hendrich, M. Holmes, J. E. Martin and A. Bird (2001). "A mouse Mecp2-null mutation causes neurological symptoms that mimic Rett syndrome." Nat Genet **27**(3): 322-326.

Hambsch, B., V. Grinevich, P. H. Seeburg and M. K. Schwarz (2005). "{gamma}-Protocadherins, presenilin-mediated release of C-terminal fragment promotes locus expression." J Biol Chem **280**(16): 15888-15897.

Hardingham, G. E. and H. Bading (2010). "Synaptic versus extrasynaptic NMDA receptor signalling: implications for neurodegenerative disorders." Nat Rev Neurosci **11**(10): 682-696.

Howe, C. L. (2005). "Modeling the signaling endosome hypothesis: why a drive to the nucleus is better than a (random) walk." Theor Biol Med Model **2**: 43.

Husi, H., M. A. Ward, J. S. Choudhary, W. P. Blackstock and S. G. Grant (2000). "Proteomic analysis of NMDA receptor-adhesion protein signaling complexes." Nat Neurosci **3**(7): 661-669.

Hynes, C. A., V. E. Stone and L. A. Kelso (2011). "Social and emotional competence in traumatic brain injury: new and established assessment tools." Soc Neurosci **6**(5-6): 599-614.

Jamal, S. M., R. K. Basran, S. Newton, Z. Wang and J. M. Milunsky (2010). "Novel de novo PCDH19 mutations in three unrelated females with epilepsy female restricted mental retardation syndrome." Am J Med Genet A **152A**(10): 2475-2481.

Jeffrey, R. A., T. H. Ch'ng, T. J. O'Dell and K. C. Martin (2009). "Activity-dependent anchoring of importin alpha at the synapse involves regulated binding to the cytoplasmic tail of the NR1-1a subunit of the NMDA receptor." J Neurosci **29**(50): 15613-15620.

Jordan, B. A., B. D. Fernholz, M. Boussac, C. Xu, G. Grigorean, E. B. Ziff and T. A. Neubert (2004). "Identification and verification of novel rodent postsynaptic density proteins." Mol Cell Proteomics **3**(9): 857-871.

Jordan, B. A., B. D. Fernholz, L. Khatri and E. B. Ziff (2007). "Activity-dependent AIDA-1 nuclear signaling regulates nucleolar numbers and protein synthesis in neurons." Nat Neurosci **10**(4): 427-435.

Jordan, B. A. and M. R. Kreutz (2009). "Nucleocytoplasmic protein shuttling: the direct route in synapse-to-nucleus signaling." Trends Neurosci **32**(7): 392-401.

Junghans, D., I. G. Haas and R. Kemler (2005). "Mammalian cadherins and protocadherins: about cell death, synapses and processing." Curr Opin Cell Biol **17**(5): 446-452.

Kaether, C., C. Haass and H. Steiner (2006). "Assembly, trafficking and function of gamma-secretase." Neurodegener Dis **3**(4-5): 275-283.

Kholodenko, B. N., J. F. Hancock and W. Kolch (2010). "Signalling ballet in space and time." Nat Rev Mol Cell Biol **11**(6): 414-426.

Kim, S. Y., J. W. Mo, S. Han, S. Y. Choi, S. B. Han, B. H. Moon, I. J. Rhyu, W. Sun and H. Kim (2010). "The expression of non-clustered protocadherins in adult rat hippocampal formation and the connecting brain regions." Neuroscience **170**(1): 189-199.

Kohmura, N., K. Senzaki, S. Hamada, N. Kai, R. Yasuda, M. Watanabe, H. Ishii, M. Yasuda, M. Mishina and T. Yagi (1998). "Diversity revealed by a novel family of cadherins expressed in neurons at a synaptic complex." Neuron **20**(6): 1137-1151.

Lai, K. O., Y. Zhao, T. H. Ch'ng and K. C. Martin (2008). "Importin-mediated retrograde transport of CREB2 from distal processes to the nucleus in neurons." Proc Natl Acad Sci U S A **105**(44): 17175-17180.

Lakowski, B., I. Roelens and S. Jacob (2006). "CoREST-like complexes regulate chromatin modification and neuronal gene expression." J Mol Neurosci **29**(3): 227-239.

Laurent, B., L. Ruitu, J. Murn, K. Hempel, R. Ferrao, Y. Xiang, S. Liu, B. A. Garcia, H. Wu, F. Wu, H. Steen and Y. Shi (2015). "A specific LSD1/KDM1A isoform regulates neuronal differentiation through H3K9 demethylation." Mol Cell **57**(6): 957-970.

Lois, C., E. J. Hong, S. Pease, E. J. Brown and D. Baltimore (2002). "Germline transmission and tissue-specific expression of transgenes delivered by lentiviral vectors." Science **295**(5556): 868-872.

Magg, T., D. Schreiner, G. P. Solis, E. G. Bade and H. W. Hofer (2005). "Processing of the human protocadherin Fat1 and translocation of its cytoplasmic domain to the nucleus." Exp Cell Res **307**(1): 100-108.

Marambaud, P., J. Shioi, G. Serban, A. Georgakopoulos, S. Sarner, V. Nagy, L. Baki, P. Wen, S. Efthimiopoulos, Z. Shao, T. Wisniewski and N. K. Robakis (2002). "A presenilin-1/gamma-secretase cleavage releases the E-cadherin intracellular domain and regulates disassembly of adherens junctions." EMBO J **21**(8): 1948-1956.

Marambaud, P., P. H. Wen, A. Dutt, J. Shioi, A. Takashima, R. Siman and N. K. Robakis (2003). "A CBP binding transcriptional repressor produced by the PS1/epsilon-cleavage of N-cadherin is inhibited by PS1 FAD mutations." Cell **114**(5): 635-645.

Marini, C., D. Mei, L. Parmeggiani, V. Norci, E. Calado, A. Ferrari, A. Moreira, T. Pisano, N. Specchio, F. Vigevano, D. Battaglia and R. Guerrini (2010). "Protocadherin 19 mutations in girls with infantile-onset epilepsy." Neurology **75**(7): 646-653.

Martin, C. and Y. Zhang (2005). "The diverse functions of histone lysine methylation." Nat Rev Mol Cell Biol **6**(11): 838-849.

McCarthy, J. V., C. Twomey and P. Wujek (2009). "Presenilin-dependent regulated intramembrane proteolysis and gamma-secretase activity." Cell Mol Life Sci **66**(9): 1534-1555.

Mosammaparast, N. and Y. Shi (2010). "Reversal of histone methylation: biochemical and molecular mechanisms of histone demethylases." Annu Rev Biochem **79**: 155-179.

Nan, X. and A. Bird (2001). "The biological functions of the methyl-CpG-binding protein MeCP2 and its implication in Rett syndrome." Brain Dev **23 Suppl 1**: S32-37.

Nollet, F., P. Kools and F. van Roy (2000). "Phylogenetic analysis of the cadherin superfamily allows identification of six major subfamilies besides several solitary members." J Mol Biol **299**(3): 551-572.

Nottke, A., M. P. Colaiacovo and Y. Shi (2009). "Developmental roles of the histone lysine demethylases." Development **136**(6): 879-889.

Okamoto, I., Y. Kawano, D. Murakami, T. Sasayama, N. Araki, T. Miki, A. J. Wong and H. Saya (2001). "Proteolytic release of CD44 intracellular domain and its role in the CD44 signaling pathway." J Cell Biol **155**(5): 755-762.

Pocklington, A. J., M. Cumiskey, J. D. Armstrong and S. G. Grant (2006). "The proteomes of neurotransmitter receptor complexes form modular networks with distributed functionality underlying plasticity and behaviour." Mol Syst Biol **2**: 2006 0023.

Proepper, C., S. Johannsen, S. Liebau, J. Dahl, B. Vaida, J. Bockmann, M. R. Kreutz, E. D. Gundelfinger and T. M. Boeckers (2007). "Abelson interacting protein 1 (Abi-1) is essential for dendrite morphogenesis and synapse formation." EMBO J **26**(5): 1397-1409.

Redies, C., K. Vanhalst and F. Roy (2005). "delta-Protocadherins: unique structures and functions." Cell Mol Life Sci **62**(23): 2840-2852.

Reiss, K., T. Maretzky, I. G. Haas, M. Schulte, A. Ludwig, M. Frank and P. Saftig (2006). "Regulated ADAM10-dependent ectodomain shedding of gamma-protocadherin C3 modulates cell-cell adhesion." J Biol Chem **281**(31): 21735-21744.

Restituito, S., L. Khatri, I. Ninan, P. M. Mathews, X. Liu, R. J. Weinberg and E. B. Ziff (2011). "Synaptic autoregulation by metalloproteases and gamma-secretase." J Neurosci **31**(34): 12083-12093.

Rubinson, D. A., C. P. Dillon, A. V. Kwiatkowski, C. Sievers, L. Yang, J. Kopinja, D. L. Rooney, M. Zhang, M. M. Ihrig, M. T. McManus, F. B. Gertler, M. L. Scott and L. Van Parijs (2003). "A lentivirus-based system to functionally silence genes in primary mammalian cells, stem cells and transgenic mice by RNA interference." Nat Genet **33**(3): 401-406.

Rusconi, F., L. Paganini, D. Braida, L. Ponzoni, E. Toffolo, A. Maroli, N. Landsberger, F. Bedogni, E. Turco, L. Pattini, F. Altruda, S. De Biasi, M. Sala and E. Battaglioli (2015). "LSD1 Neurospecific Alternative Splicing Controls Neuronal Excitability in Mouse Models of Epilepsy." Cereb Cortex **25**(9): 2729-2740.

Ryan, S. G., P. F. Chance, C. H. Zou, N. B. Spinner, J. A. Golden and S. Smietana (1997). "Epilepsy and mental retardation limited to females: an X-linked dominant disorder with male sparing." Nat Genet **17**(1): 92-95.

Saleque, S., J. Kim, H. M. Rooke and S. H. Orkin (2007). "Epigenetic regulation of hematopoietic differentiation by Gfi-1 and Gfi-1b is mediated by the cofactors CoREST and LSD1." Mol Cell **27**(4): 562-572.

Scheffer, I. E., S. J. Turner, L. M. Dibbens, M. A. Bayly, K. Friend, B. Hodgson, L. Burrows, M. Shaw, C. Wei, R. Ullmann, H. H. Ropers, P. Szepetowski, E. Haan, A. Mazarib, Z. Afawi, M. Y. Neufeld, P. I. Andrews, G. Wallace, S. Kivity, D. Lev, T. Lerman-Sagie, C. P. Derry, A. D. Korczyn,

J. Gecz, J. C. Mulley and S. F. Berkovic (2008). "Epilepsy and mental retardation limited to females: an under-recognized disorder." Brain **131**(Pt 4): 918-927.

Schroeter, E. H., J. A. Kisslinger and R. Kopan (1998). "Notch-1 signalling requires ligand-induced proteolytic release of intracellular domain." Nature **393**(6683): 382-386.

Shi, Y. J., C. Matson, F. Lan, S. Iwase, T. Baba and Y. Shi (2005). "Regulation of LSD1 histone demethylase activity by its associated factors." Mol Cell **19**(6): 857-864.

Smalley, K. S., P. Brafford, N. K. Haass, J. M. Brandner, E. Brown and M. Herlyn (2005). "Up-regulated expression of zonula occludens protein-1 in human melanoma associates with N-cadherin and contributes to invasion and adhesion." Am J Pathol **166**(5): 1541-1554.

Specchio, N., C. Marini, A. Terracciano, D. Mei, M. Trivisano, F. Sicca, L. Fusco, R. Cusmai, F. Darra, B. D. Bernardina, E. Bertini, R. Guerrini and F. Vigevano (2011). "Spectrum of phenotypes in female patients with epilepsy due to protocadherin 19 mutations." Epilepsia **52**(7): 1251-1257.

Stavropoulos, P., G. Blobel and A. Hoelz (2006). "Crystal structure and mechanism of human lysine-specific demethylase-1." Nat Struct Mol Biol **13**(7): 626-632.

Sun, G., K. Alzayady, R. Stewart, P. Ye, S. Yang, W. Li and Y. Shi (2010). "Histone demethylase LSD1 regulates neural stem cell proliferation." Mol Cell Biol **30**(8): 1997-2005.

Sun, G., P. Ye, K. Murai, M. F. Lang, S. Li, H. Zhang, W. Li, C. Fu, J. Yin, A. Wang, X. Ma and Y. Shi (2011). "miR-137 forms a regulatory loop with nuclear receptor TLX and LSD1 in neural stem cells." Nat Commun **2**: 529.

Thompson, K. R., K. O. Otis, D. Y. Chen, Y. Zhao, T. J. O'Dell and K. C. Martin (2004). "Synapse to nucleus signaling during long-term synaptic plasticity; a role for the classical active nuclear import pathway." Neuron **44**(6): 997-1009.

Uemura, K., T. Kihara, A. Kuzuya, K. Okawa, T. Nishimoto, H. Bito, H. Ninomiya, H. Sugimoto, A. Kinoshita and S. Shimohama (2006). "Activity-dependent regulation of beta-catenin via epsilon-cleavage of N-cadherin." Biochem Biophys Res Commun **345**(3): 951-958.

van Harssel, J. J., S. Weckhuysen, M. J. van Kempen, K. Hardies, N. E. Verbeek, C. G. de Kovel, W. B. Gunning, E. van Daalen, M. V. de Jonge, A. C. Jansen, R. J. Vermeulen, W. F. Arts, H. Verhelst, A. Fogarasi, J. F. de Rijk-van Andel, A. Kelemen, D. Lindhout, P. De Jonghe, B. P. Koeleman, A. Suls and E. H. Brilstra (2013). "Clinical and genetic aspects of PCDH19-related epilepsy syndromes and the possible role of PCDH19 mutations in males with autism spectrum disorders." Neurogenetics **14**(1): 23-34.

Vanhalst, K., P. Kools, K. Staes, F. van Roy and C. Redies (2005). "delta-Protocadherins: a gene family expressed differentially in the mouse brain." Cell Mol Life Sci **62**(11): 1247-1259.

Wang, J., S. Hevi, J. K. Kurash, H. Lei, F. Gay, J. Bajko, H. Su, W. Sun, H. Chang, G. Xu, F. Gaudet, E. Li and T. Chen (2009). "The lysine demethylase LSD1 (KDM1) is required for maintenance of global DNA methylation." Nat Genet **41**(1): 125-129.

Wang, J., K. Scully, X. Zhu, L. Cai, J. Zhang, G. G. Prefontaine, A. Krones, K. A. Ohgi, P. Zhu, I. Garcia-Bassets, F. Liu, H. Taylor, J. Lozach, F. L. Jayes, K. S. Korach, C. K. Glass, X. D. Fu and M. G. Rosenfeld (2007). "Opposing LSD1 complexes function in developmental gene activation and repression programmes." Nature **446**(7138): 882-887.

West, A. E., E. C. Griffith and M. E. Greenberg (2002). "Regulation of transcription factors by neuronal activity." Nat Rev Neurosci **3**(12): 921-931.

Wolverton, T. and M. Lalande (2001). "Identification and characterization of three members of a novel subclass of protocadherins." Genomics **76**(1-3): 66-72.

Wu, Q., T. Zhang, J. F. Cheng, Y. Kim, J. Grimwood, J. Schmutz, M. Dickson, J. P. Noonan, M. Q. Zhang, R. M. Myers and T. Maniatis (2001). "Comparative DNA sequence analysis of mouse and human protocadherin gene clusters." Genome Res **11**(3): 389-404.

Yang, Y. Y., G. L. Yin and R. B. Darnell (1998). "The neuronal RNA-binding protein Nova-2 is implicated as the autoantigen targeted in POMA patients with dementia." Proc Natl Acad Sci U S A **95**(22): 13254-13259.

Ye, H., R. Kuruvilla, L. S. Zweifel and D. D. Ginty (2003). "Evidence in support of signaling endosome-based retrograde survival of sympathetic neurons." Neuron **39**(1): 57-68.

Zibetti, C., A. Adamo, C. Binda, F. Forneris, E. Toffolo, C. Verpelli, E. Ginelli, A. Mattevi, C. Sala and E. Battaglioli (2010). "Alternative splicing of the histone demethylase LSD1/KDM1 contributes to the modulation of neurite morphogenesis in the mammalian nervous system." J Neurosci **30**(7): 2521-2532.